Light dark matter searches with the NEWS-G experiment

Ioannis Katsioulas
Universite Paris-Saclay
CEA Saclay

University of Warwick, June 28, 2018

ioannis.katsioulas@cea.fr

The dark matter conundrum

Observations of Zwicky 85 years ago

Die Rotverschiebung von extragalaktischen Nebeln
von F. Zwicky.
(16. II. 33.)

"The Redshift of Extragalactic Nebulae", published in German in Helvetica Physica Acta in 1933

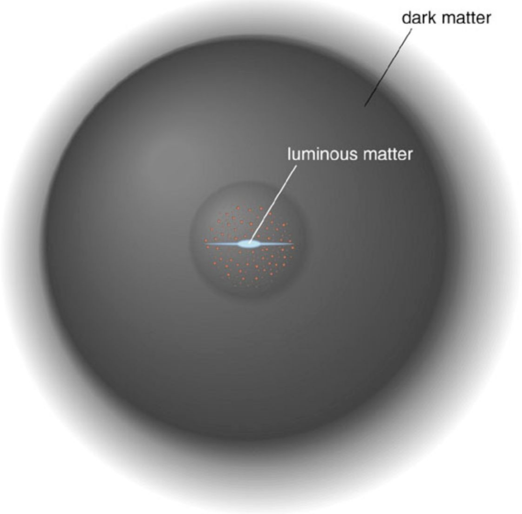

“In a spiral galaxy, the ratio of dark-to-light matter is about a factor of ten. That's probably a good number for the ratio of our ignorance-to-knowledge. We're out of kindergarten, but only in about third grade.”

Vera Rubin

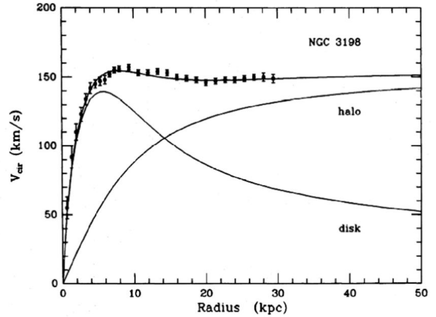

-What should it be from astrophysical constraints:

- Mostly “Cold”
- Non-Baryonic
- “Weakly” interacting
- $\underline{\Omega_X h^2 = 0.1186\pm0.002}$
- Stable or $\tau_X >> \tau_U$

No Standard Model particle matches the criteria

Dark matter detection

PHYSICAL REVIEW D VOLUME 31, NUMBER 12 15 JUNE 1985

Detectability of certain dark-matter candidates

Mark W. Goodman and Edward Witten
Joseph Henry Laboratories, Princeton University, Princeton, New Jersey 08544

(Received 7 January 1985)

We consider the possibility that the neutral-current neutrino detector recently proposed by Drukier and Stodolsky could be used to detect some possible candidates for the dark matter in galactic halos. This may be feasible if the galactic halos are made of particles with coherent weak interactions and masses $1-10^6$ GeV; particles with spin-dependent interactions of typical weak strength and masses $1-10^2$ GeV; or strongly interacting particles of masses $1-10^{13}$ GeV.

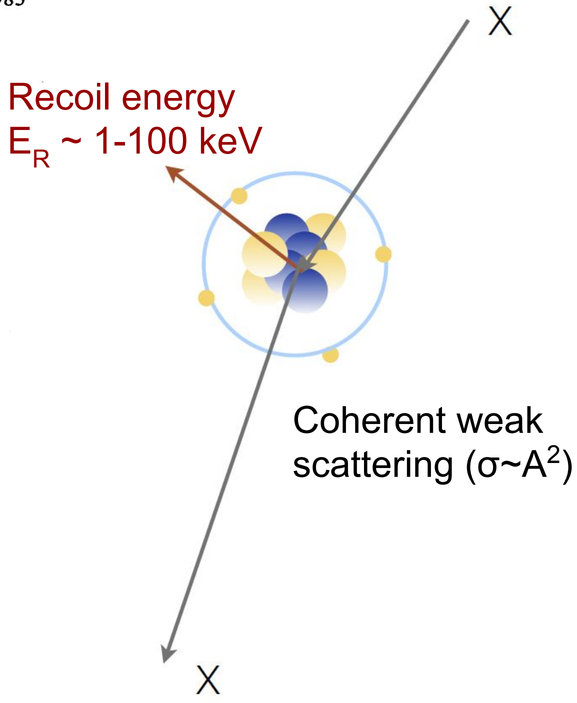

“WIMP miracle” ⇒ Relic abundance explained by a massive particle (10 GeV/c^2 - few TeV/c^2) interacting through weak scale interaction with baryonic matter

State of the art for dark matter detectors

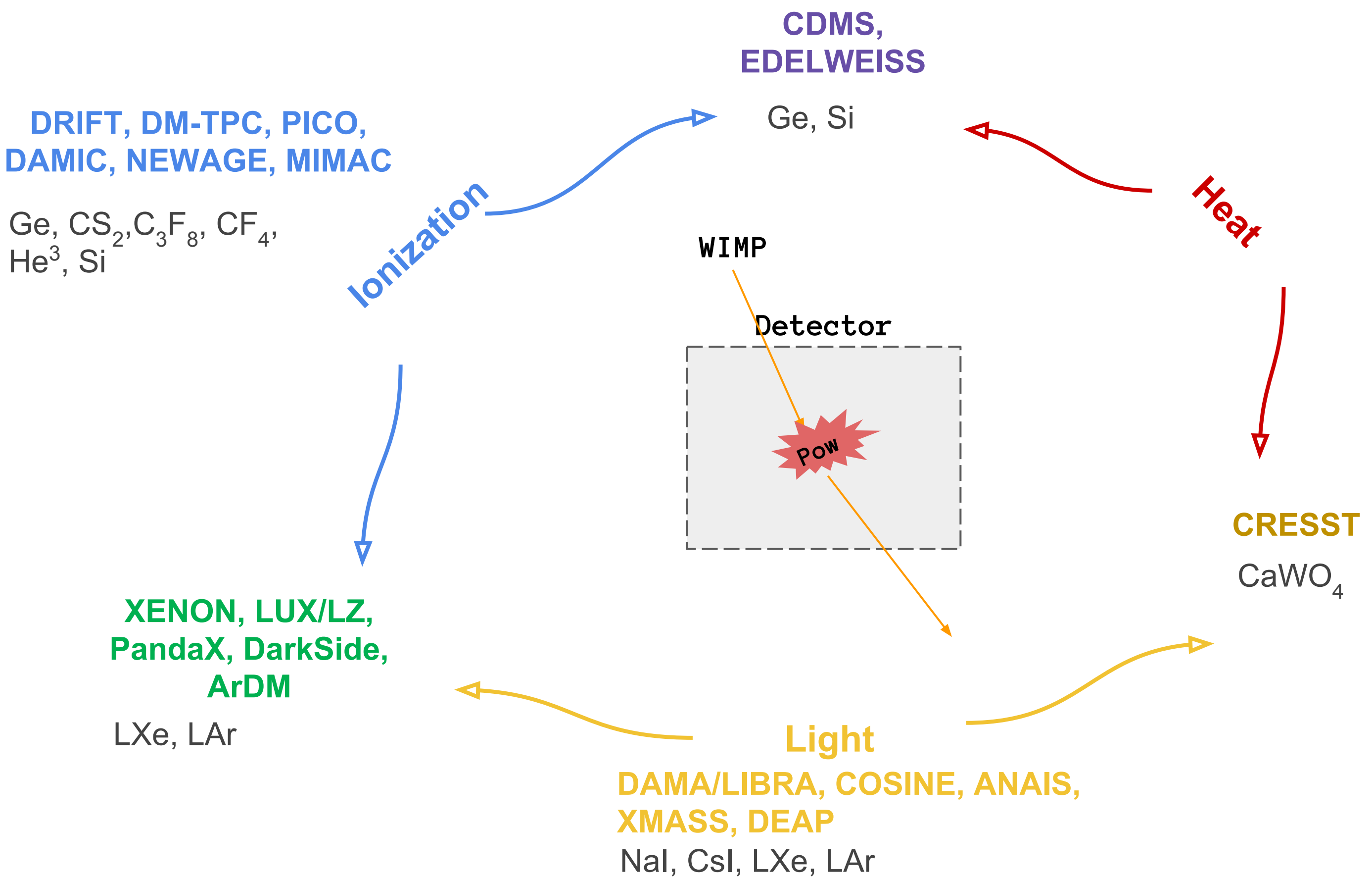

Status of dark matter searches

Detectors with a lower threshold

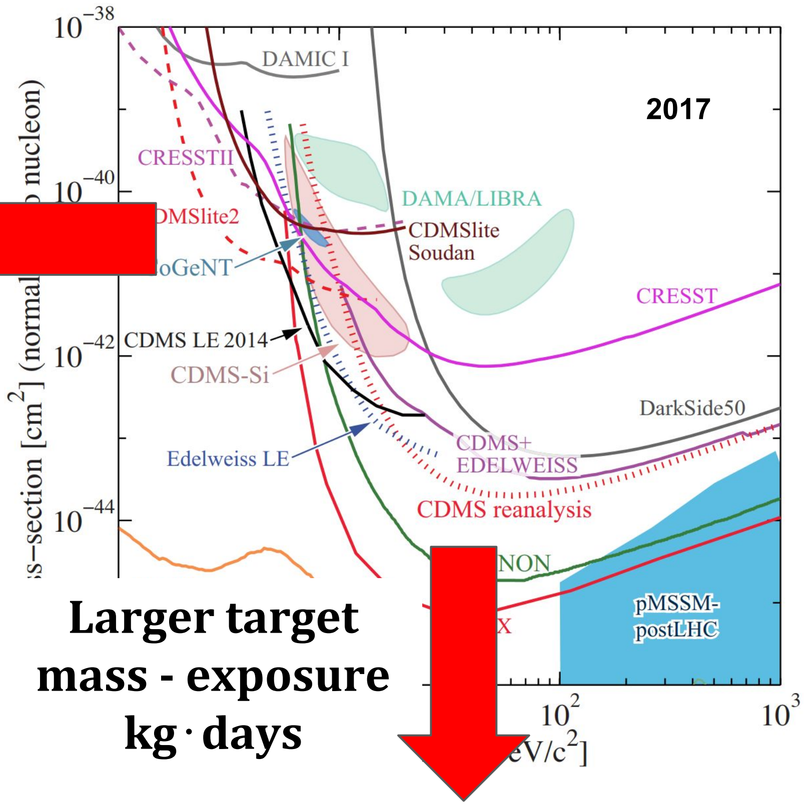

Larger target mass - exposure kg · days

[J. Feng and J. Kumar, “The WIMPless Miracle: Dark Matter Particles without Weak-scale Masses or Weak Interactions."](#)

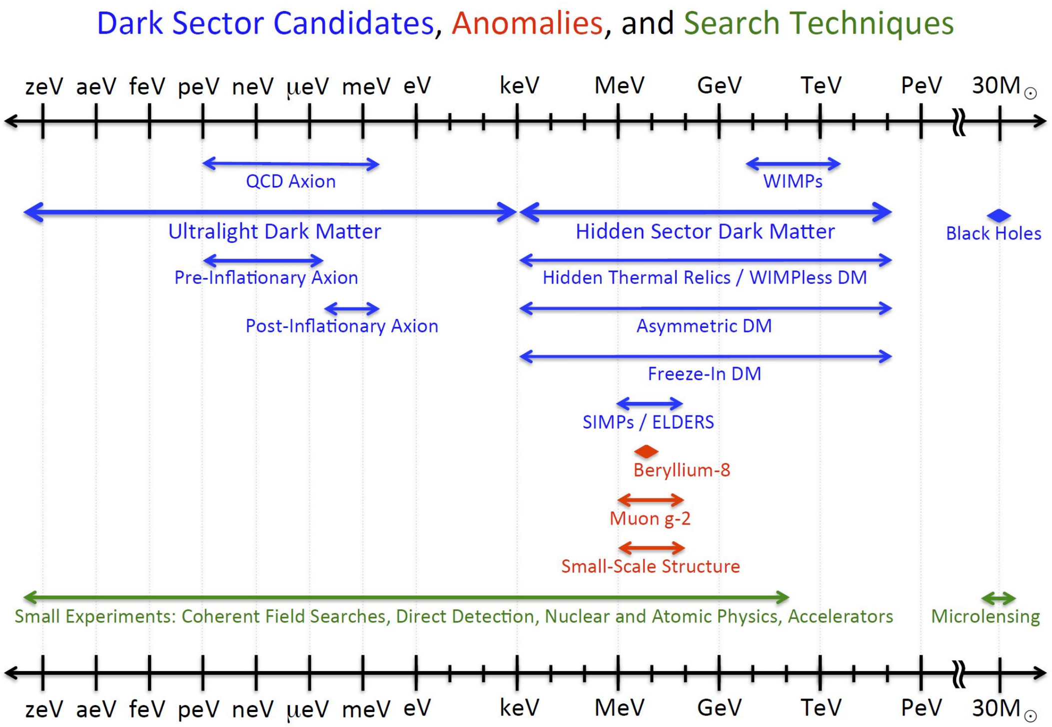

Cosmic visions 2017

Direct detection of light dark matter

Detection through ionization - An example

Light Dark Matter (LDM) Mass range
0.1GeV/c^2- few GeV/c^2

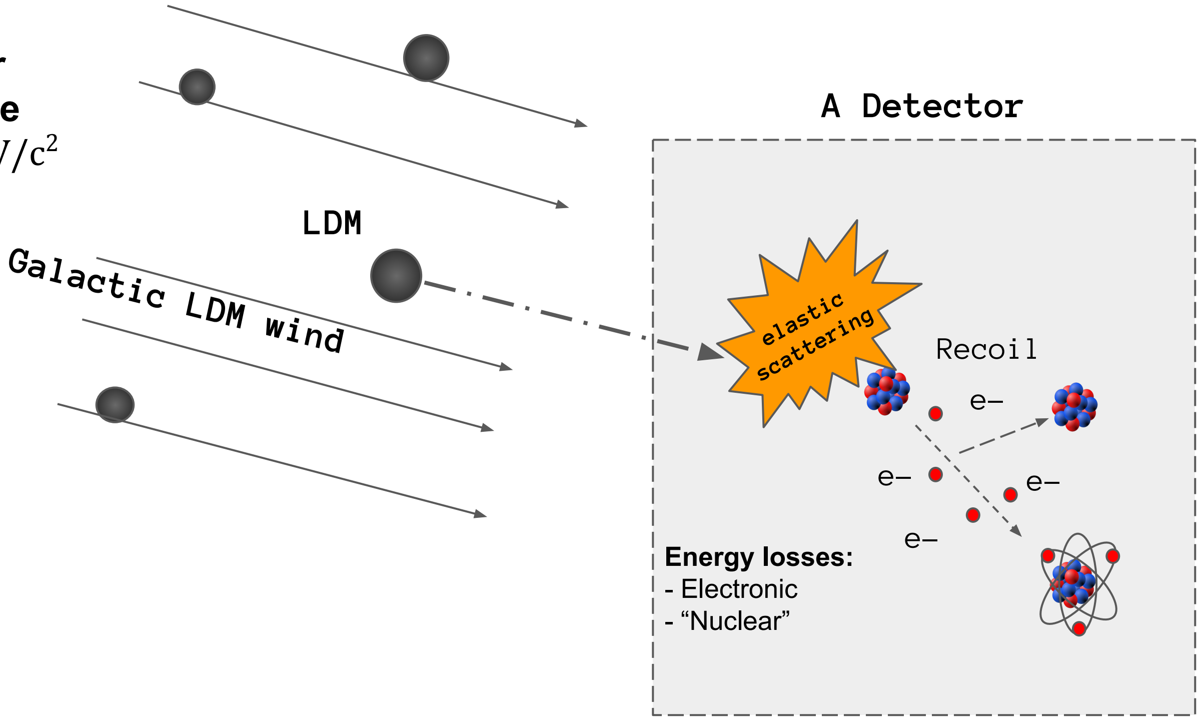

Comparison between heavy and light targets - A

Kinematics

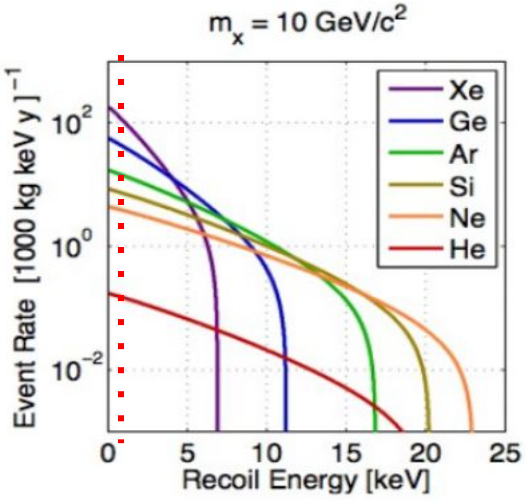

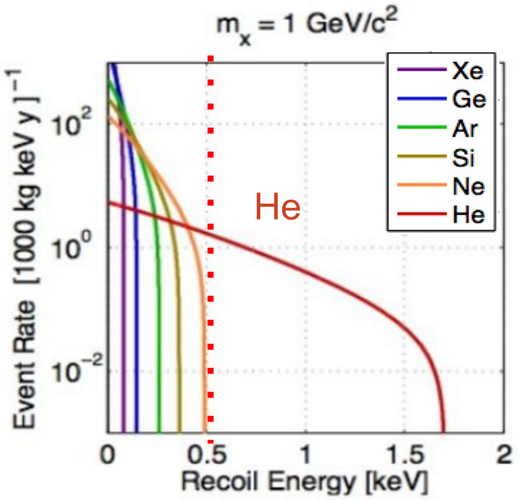

- If we have E_R= 500 eV recoil induced by LDM particle of M_χ=1 GeV/c^2

$$u_{min} = \sqrt{\frac{2 \cdot E_R}{r \cdot M_\chi}}$$

Minimum relative WIMP velocity to produce a recoil of E_R

E_R = → u_{min} { 1790 km/s for Xe target; 1340 km/s for Ge target; 1000 km/s for Ar target

WIMP escape velocity ~540 km/s

500 eV · · · · · · · · · · ·

Light Projectile + light target ⇒ Better kinematical match

Comparison between heavy and light targets - B

Ionization quenching

Quenching factor (q_f.) is defined as the fraction of the kinetic energy of an ion that is dissipated in a medium in the form of ionization electrons and excitation of the atomic and quasi-molecular states.

10 keV $^{+}$Ar in Ar

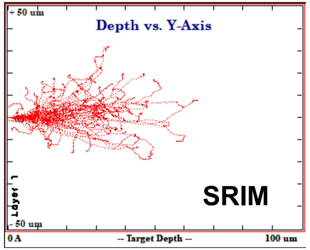

Detection energy threshold required due to quenching

Target	Threshold (eV)
Xe	50
Ge	58
Ar	74
He	105

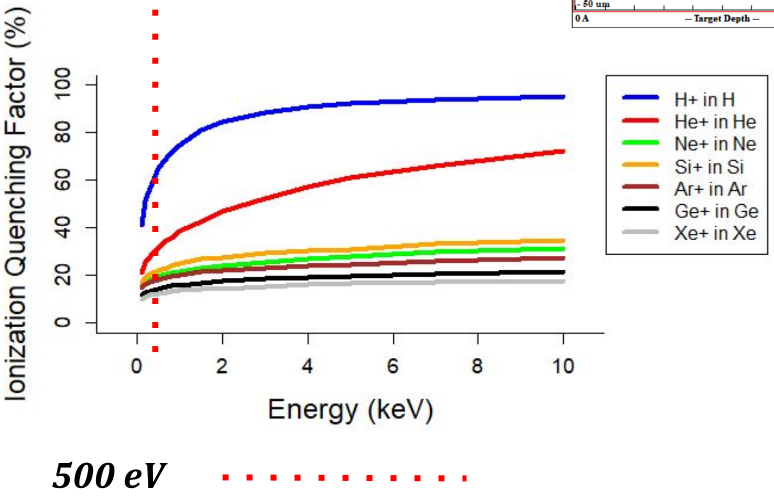

Light Projectile + light target ⇒ Less demanding detector threshold

Direct detection of light dark matter

No searches available in this region

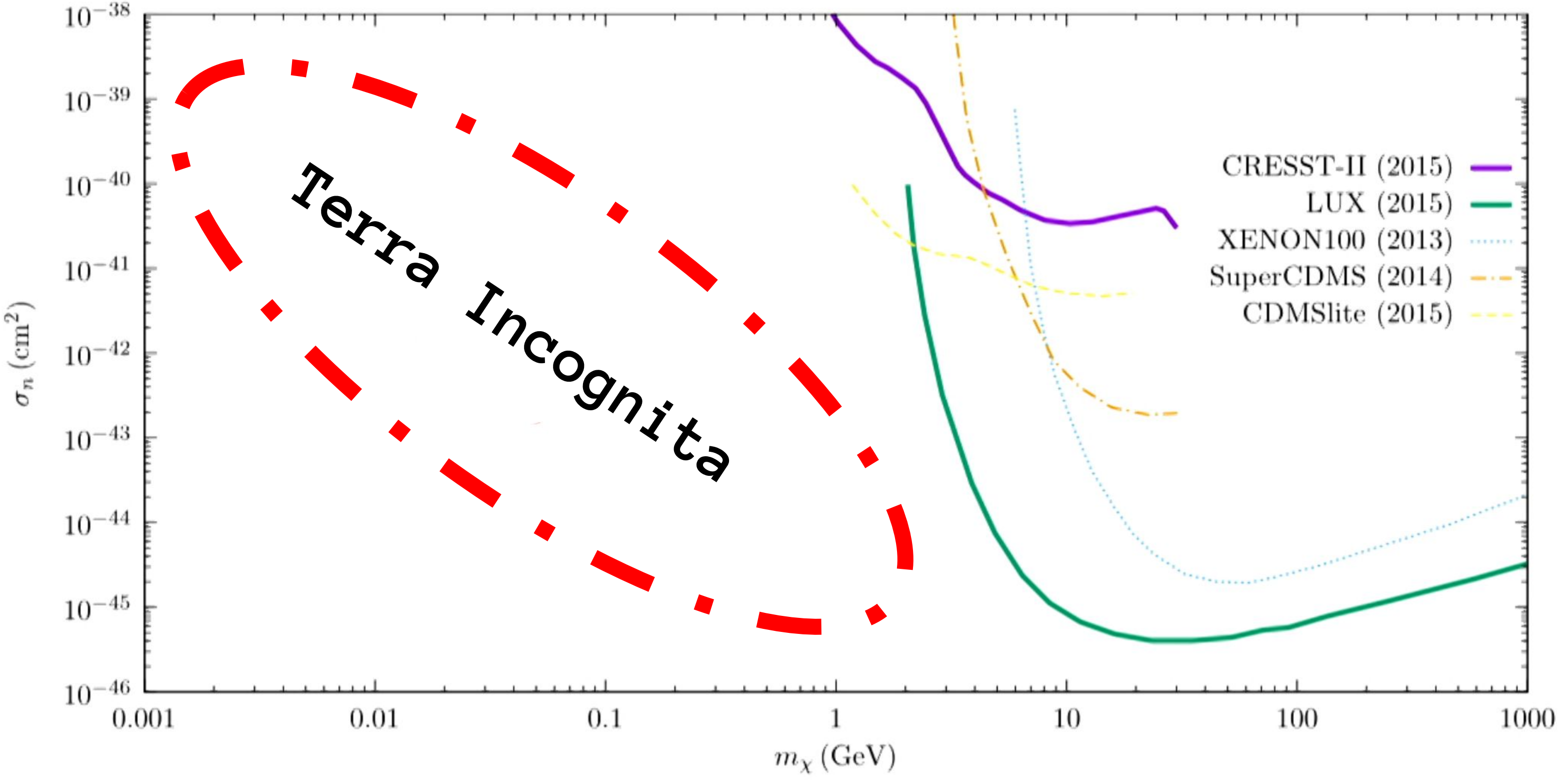

Use light targets for dark matter searches?

Hydrogen, Helium ⇒ Gases (NTP) ⇒ **Gaseous detector ???**

Spherical Proportional Counter (SPC)

Fun fact

Old LEP RF cavities

Spherical gaseous detectors

In the picture:
I.Giomataris, G.Charpak

The structure of the SPC

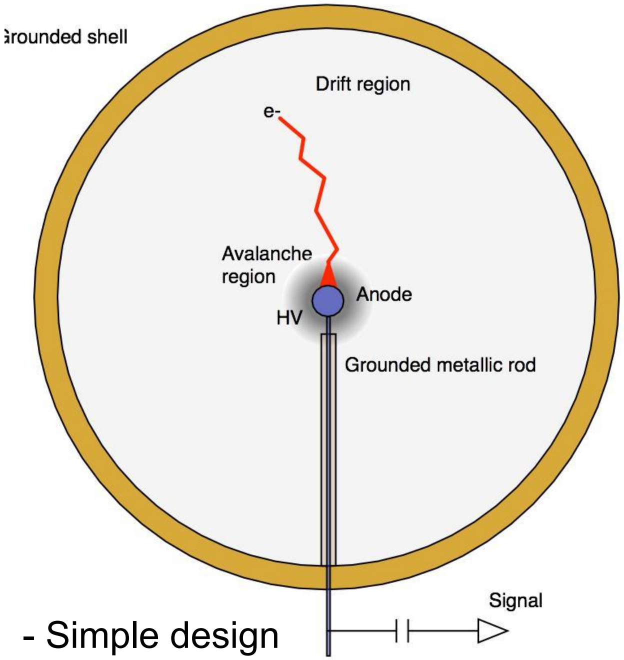

- Simple design
- Single readout

I.Giomataris et al ,JINST,2008, P09007

Electric field

Strong dependence on the radius

$$E(r) = \frac{V_0}{r^2}\frac{r_A r_C}{r_C - r_A} \approx \frac{V_0}{r^2} r_A$$

r_A = anode radius
r_C = cathode radius

Natural division of the volume in two
- *Drift volume*
- *Multiplication volume*

The "Sensor"

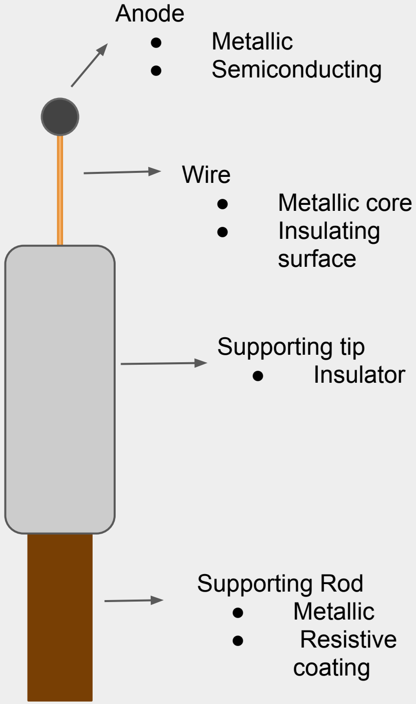

Advantage of spherical geometry - A

C~Electronic noise

↑Electronic noise ↑Threshold

Capacities for a 1 m^3 detector in different geometries

Parallel Plate

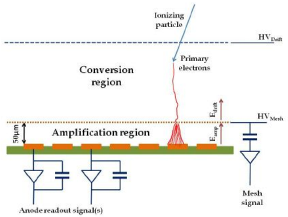

$$C = \varepsilon_0 \frac{S}{d} \approx 3500 \text{ pF}$$

Cylindrical

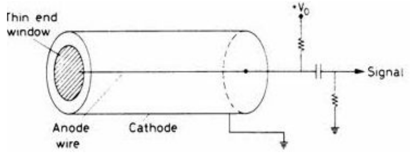

$$C = 2\pi\varepsilon_0 \frac{L}{ln(b/a)} \approx 115 \text{ pF}$$

Spherical

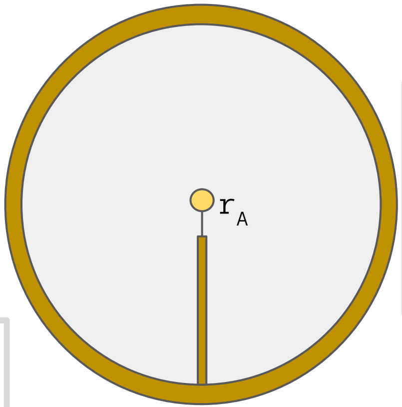

$$C \approx 4\pi\varepsilon r_A \approx 1.5 \text{ pF}$$

Advantage of spherical geometry - B

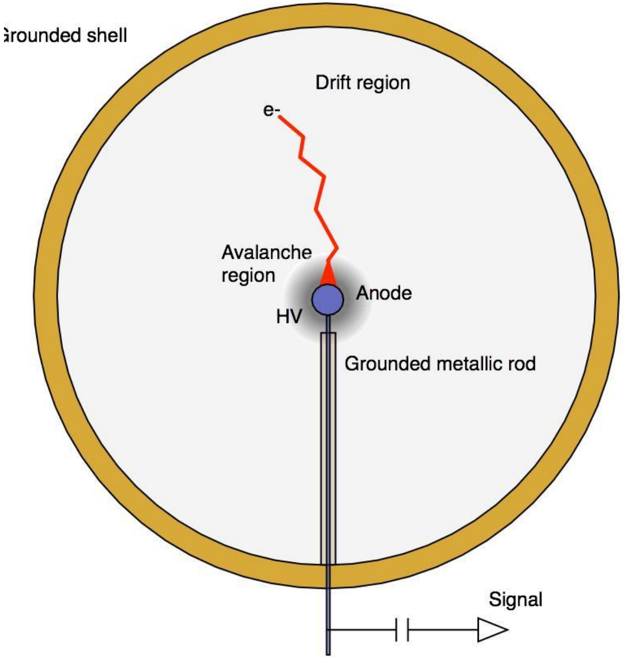

Advantages of the spherical geometry

- Lowest surface to volume ratio
- Sustains higher pressure
- Robustness (anode Ø 1 mm - 6.3 mm)

Built solely by radiopure materials

- Vessel made of Cu (~tens of kg)
- Rod made of Cu (~hundreds of gr)
- **All the rest less than weigh < 1 g**

Pulse production

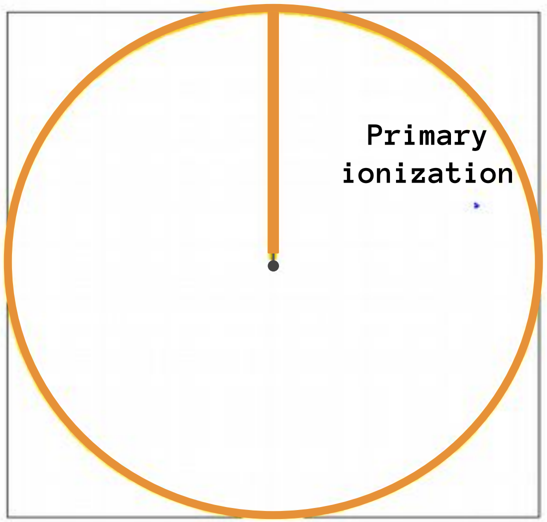

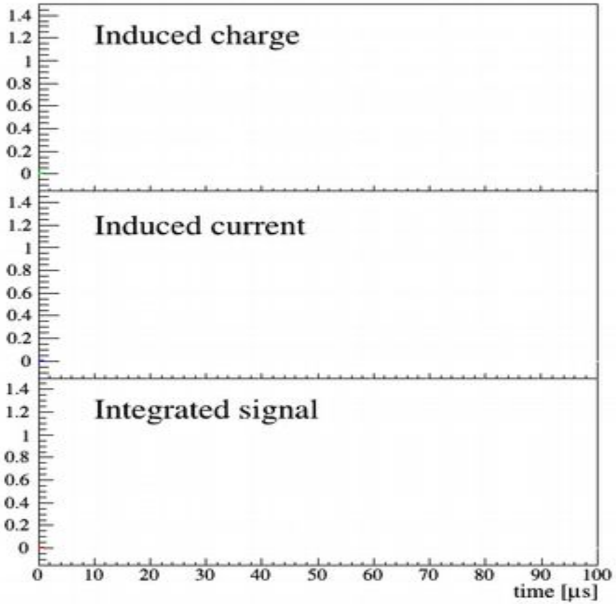

Pulse production

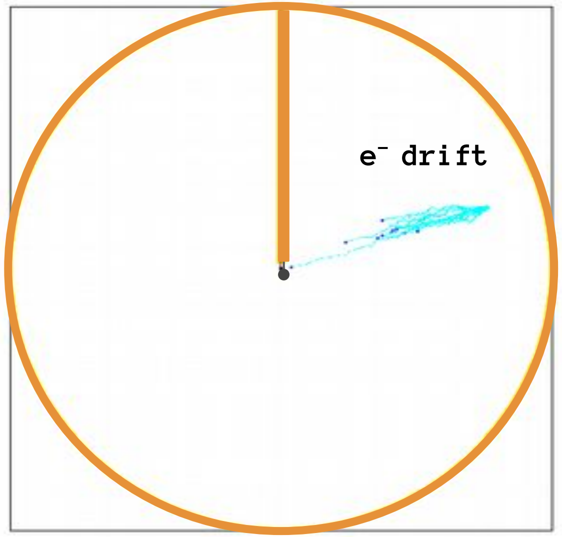

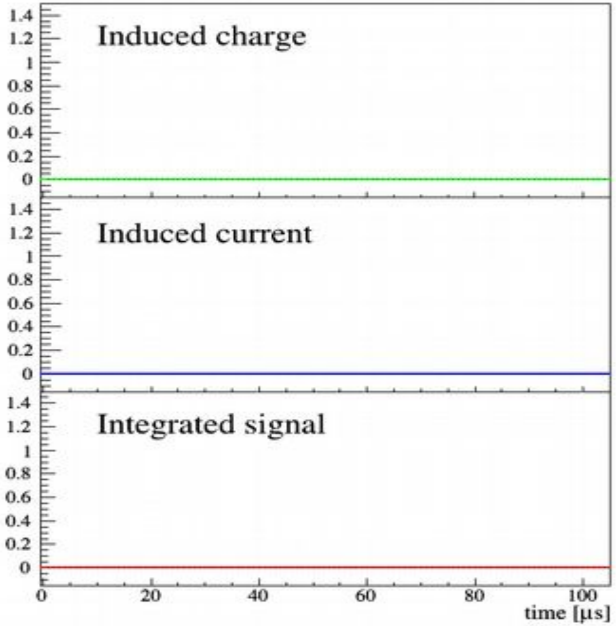

Pulse production

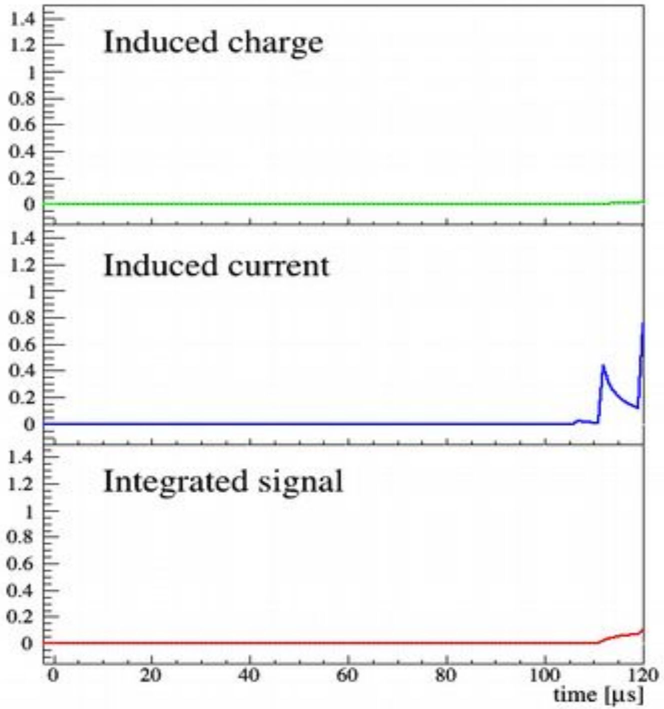

Pulse production

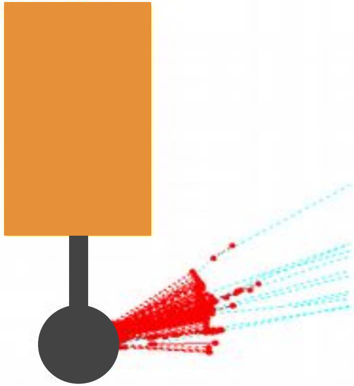

Drift of slow moving ions

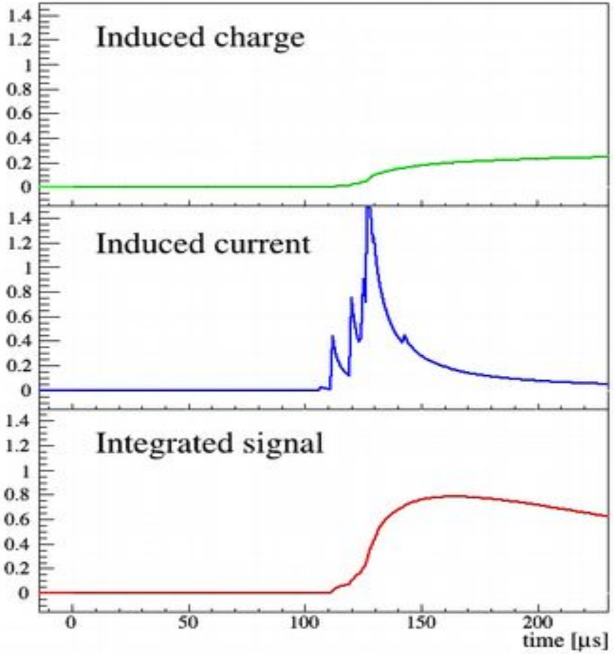

Pulse creation

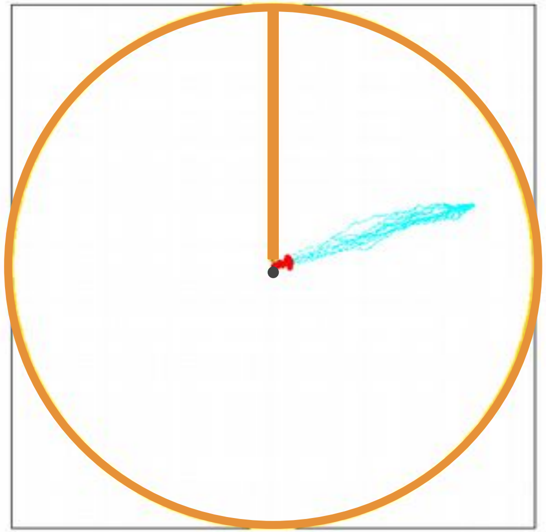

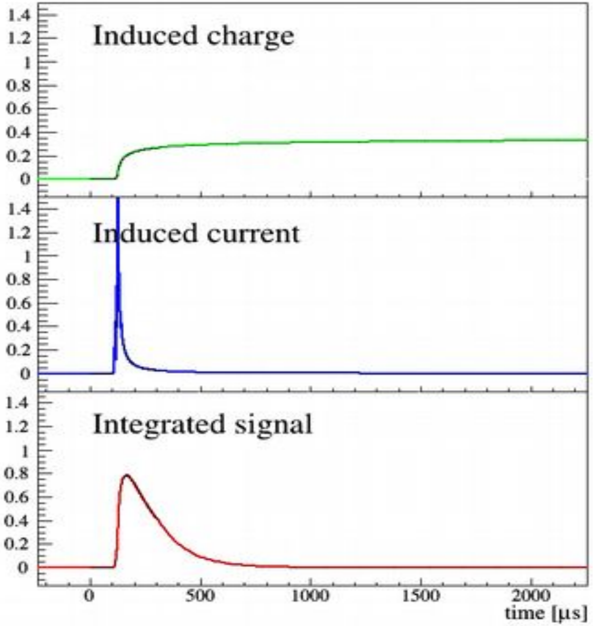

Induced Pulses

Pulse Shape Analysis (PSA) parameters

Long Tail Pulse

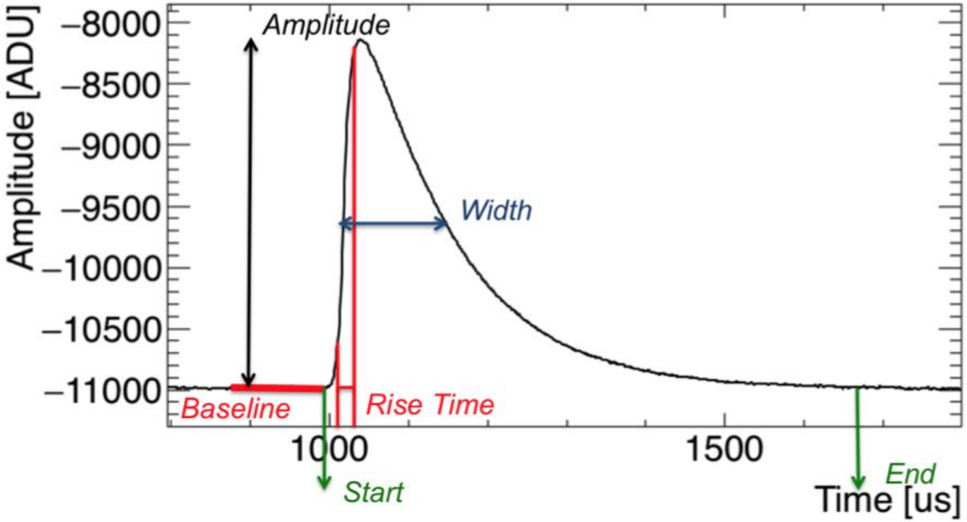

Rise time & Width ∝ Drift time dispersion

Basic Parameters

- Baseline
- Noise
- Amplitude (Pulse Height)
- Rise time
- Width
- Integral
- Number of peaks

A lot of information hiding in the pulse shape

Background rejection capabilities-A

Fiducialization

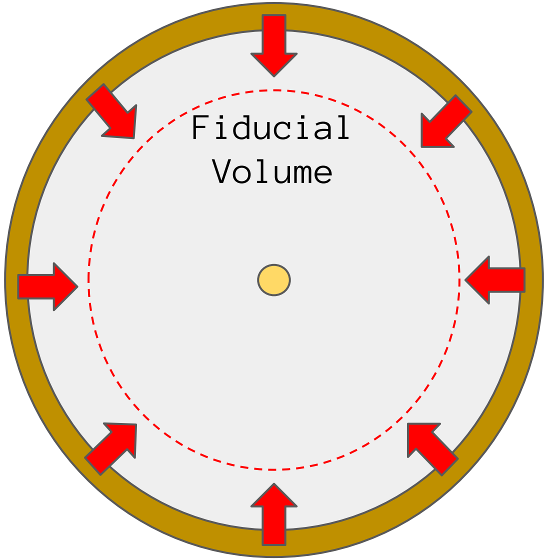

Background comes from the materials of the vessel

Surface

Primary e- drift time dispersion

$$\sigma(r) \propto (r/r_{sphere})^3$$

5.9 keV X-rays line

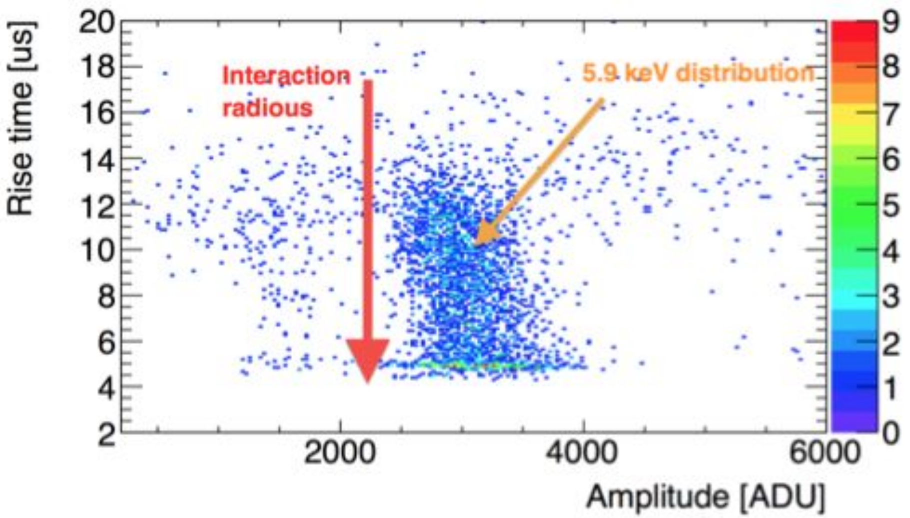

Rise time → Δt between 90% - 10% of pulse height

Background rejection capabilities-B

Event discrimination

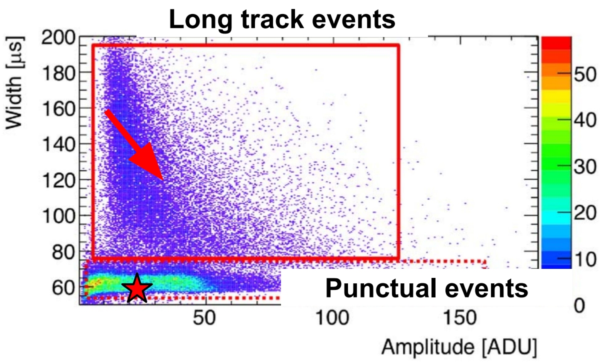

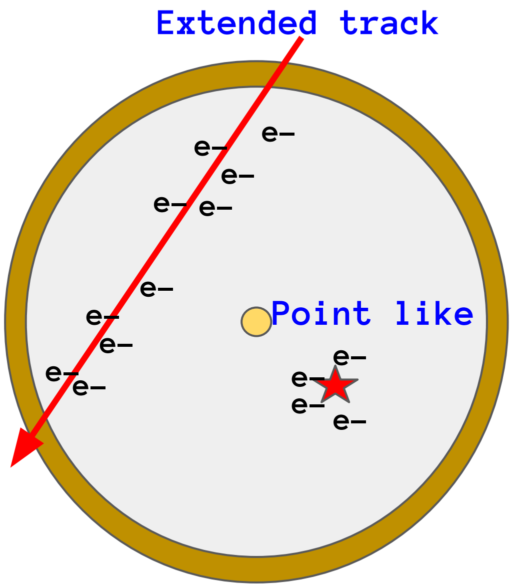

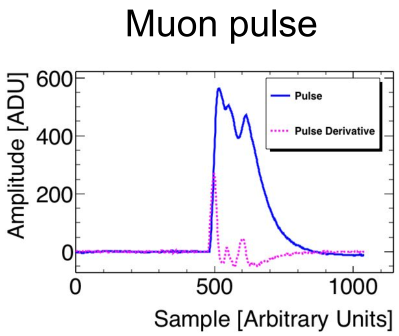

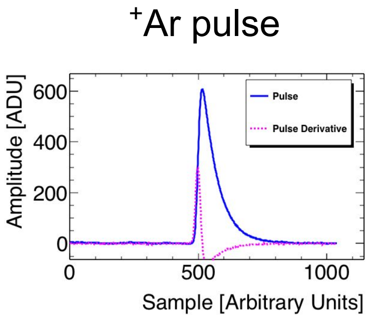

Muon pulse		$^{+}$Ar pulse	
Amplitude	= 575 ADU	Amplitude	= 606 ADU
Width (FWHM)	**= 155.5 µs**	**Width (FWHM)**	**= 63.4 µs**
Rise time	= 18.2 µs	Rise time	= 16.3 µs

Illustration of the basic analysis principle

^{109}Cd source
Irradiation through 200µm Al window
P = 100 mb, Ar-CH4 (2%)

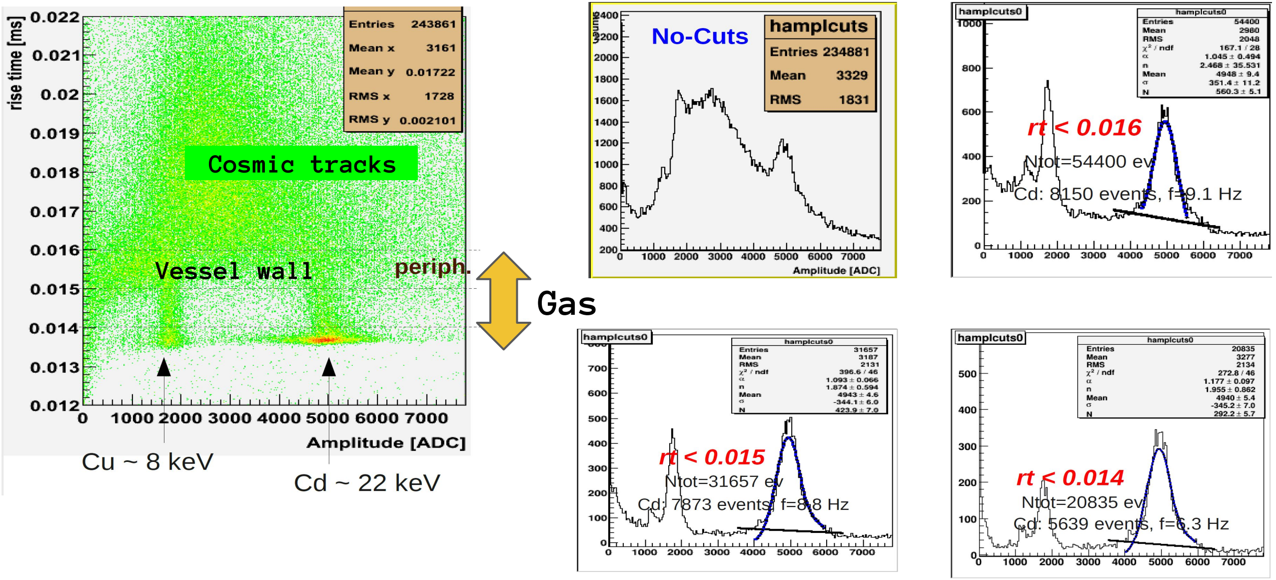

Efficiency of the cut in rt → ~ 70% signal (Cd line)
Significant background reduction

Low energy detection capabilities of a large volume SPC

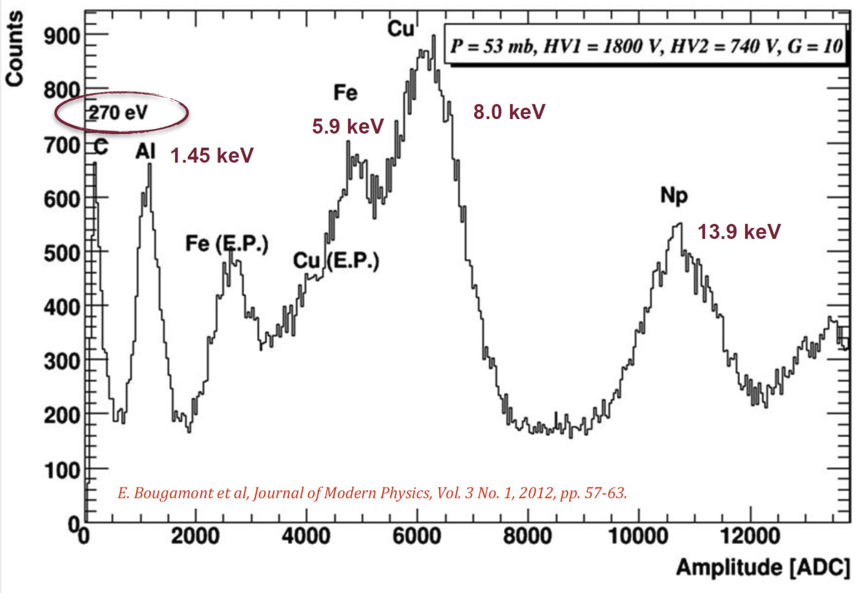

SPC Ø 130 cm

Gas: Ar+2%CH_4

Detection of fluorescence X-rays

^{241}Am -> ^{237}Np+^{4}He+ 5.6 MeV

Lines

Al -> 1.45 keV

Cu -> 13.93 keV

^{237}Np -> 13.93 keV(L_α 17.60 keV(L_β)

-Energy threshold at the single electron level

The spherical detector around the globe

LSM, Modane

CEA Saclay

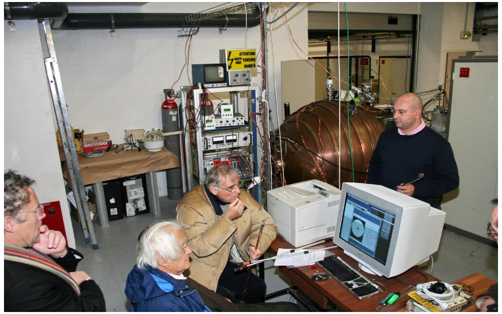

University of Saragoza

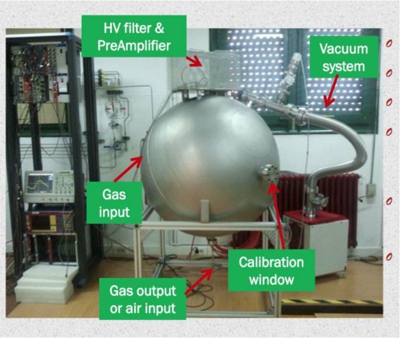

University of Thessaloniki

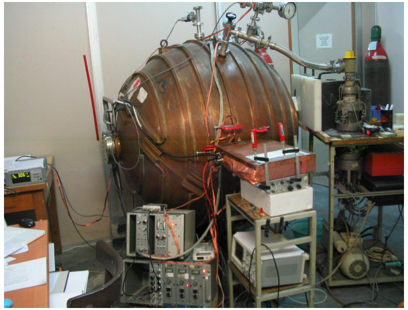

Queen's University

University of Tsinghua

Also joining University of Bordeaux and very soon University of Birmingham

The SEDINE detector at LSM - A

One of the deepest and “quietest” laboratories in the world

Laboratoire **S**outerrain de **M**odane

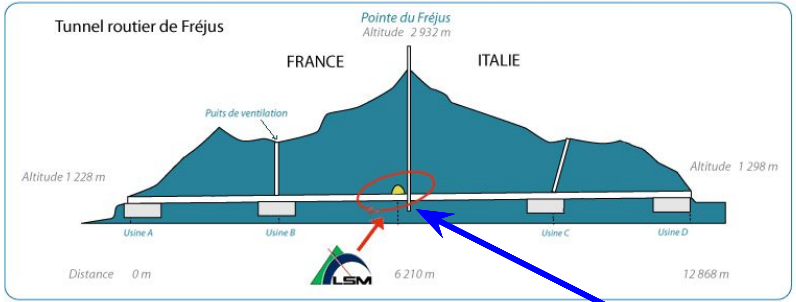

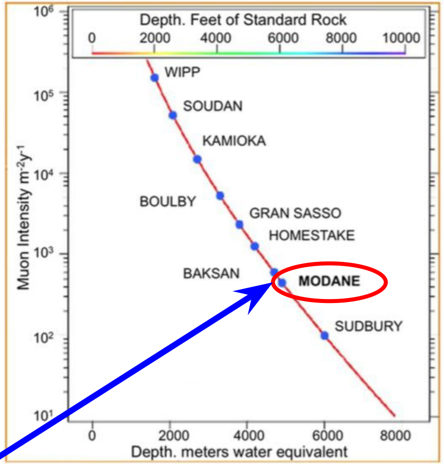

4800 wme
5 μ/m^2/day

The SEDINE detector at LSM - B

A competitive detector and a testing ground for NEWS-G / SNO

Vessel
Ø 60cm copper

Sensor
Ø 6.3mm Si

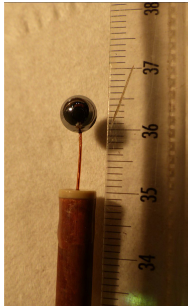

Shielding

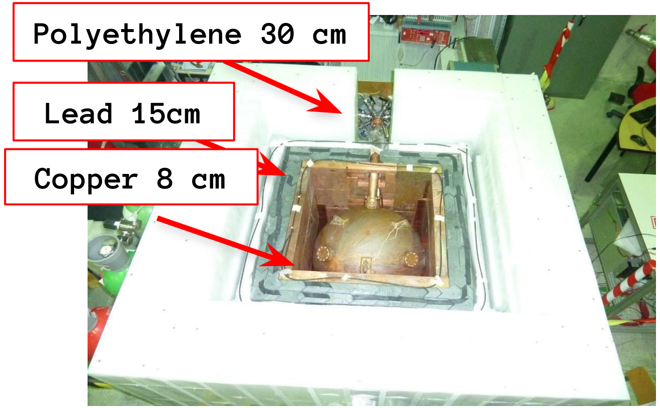

- Copper vessel (Ø 60 cm)
- Equipped with a 6.3 mm Ø sensor
- Chemically cleaned several times for Radon deposit removal

Main background sources for LSM detector

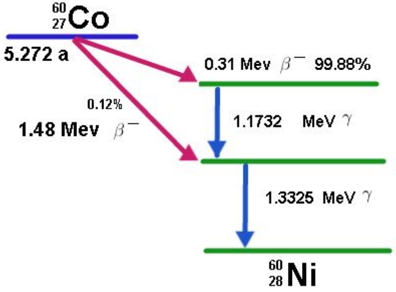

^{60}Co Contamination of 1 mBq/kg

BG Rate = 0.3-0.5 keV^{-1}kg^{-1}day^{-1}

Solution: Limit time exposure on ground for pure copper.

^{210}Pb, ^{210}Bi Contamination of 1 nBq/kg

BG Rate = 0.1 keV^{-1}kg^{-1}day^{-1}

Competitive BG levels

Solution: Chemical cleaning

Effect of cleaning:

- High energy events 180 mHz => ~2 mHz
- Low energy events 400 mHz => ~20 mHz

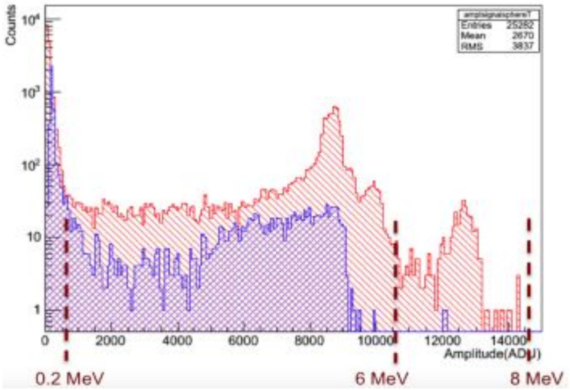

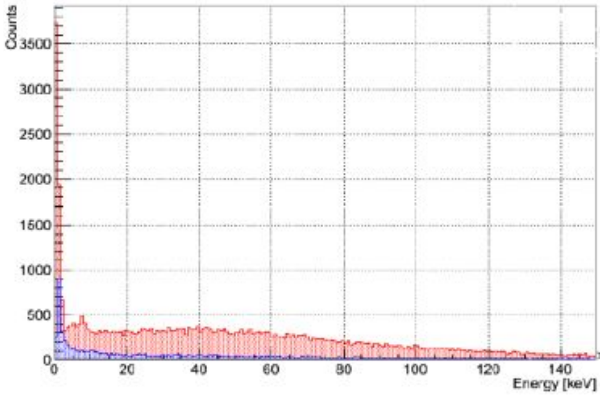

WIMP search run data

Target: Ne+0.7%CH_4 at 3.1 bar
→ 280 gr target mass

Duration: 42 days in sealed mode

Dead time: 20.1%

Exposure: 9.6 kg*days (34.1 live-days x 0.28 kg)

Trigger threshold: 35 eVee (~100% efficient at 150 eVee)

Analysis threshold: 150 eVee(~720 eVnr)

Calibration: ^{37}Ar gaseous source, 8 keV Cu fluorescence, AmBe neutron source

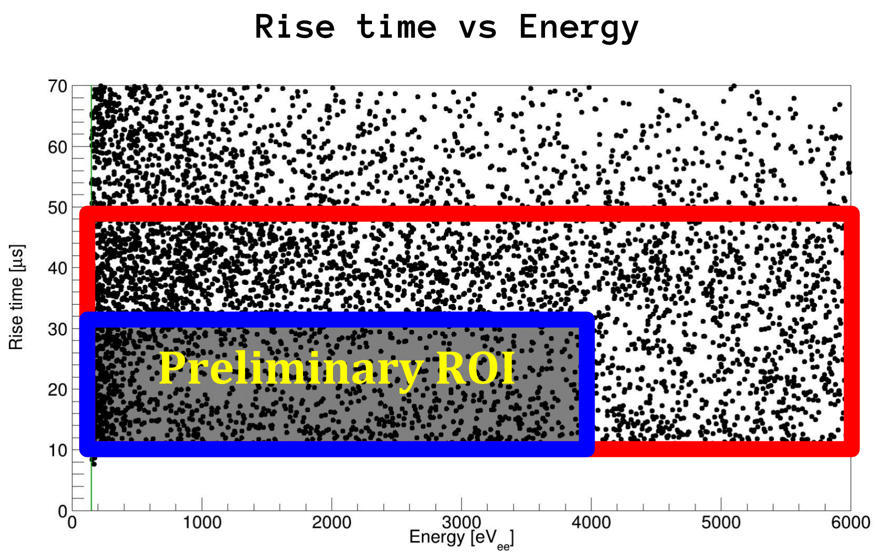

Sideband region used together with simulations to determine the number and distribution of expected events in preliminary ROI

Simulating the detector response

Modeling the rise time vs energy response

Electric field

- Field map from COMSOL

Drift of primary electrons

- Magboltz drift parameters

Quenching factor

- Parametrization derived from SRIM

Avalanche

- Polya distribution estimation using Garfield++

Simulated pulses

- Ion induced current preamplifier response
- Noise templates taken from the pretraces of real pulses

Same trigger algorithm and processing as used for real pulses

Validation

^{37}Ar gaseous source

2.82 keV and 270 eV X-rays (K and L shells)

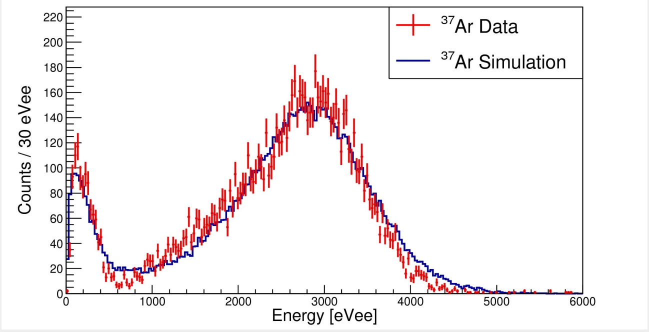

^{241}Am–^{9}Be neutron source

Nuclear recoils homogeneously distributed in the volume

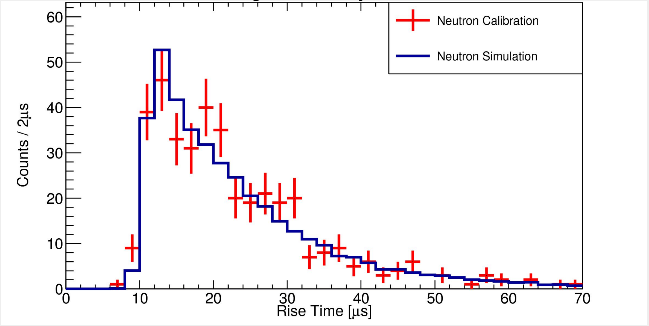

Analysis of the WIMP run data

Analysis methodology - BDT

Background modeling

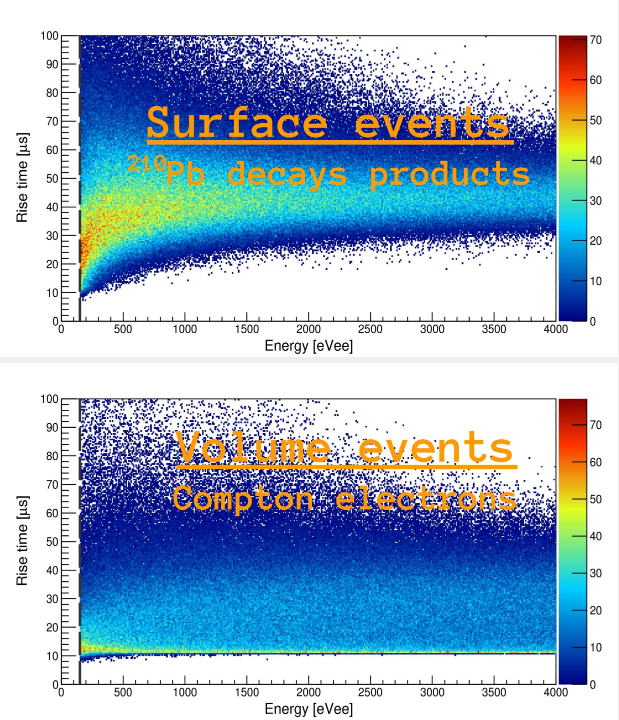

Trained with simulated WIMP and background events

BDT

Mass dependent selection for 8 WIMP masses

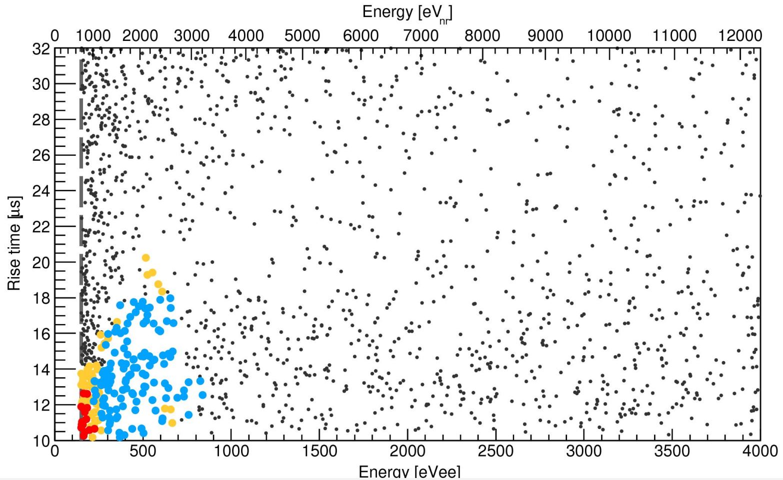

1620 events recorded in the preliminary ROI

- **Failed any of the BDT cuts**
- **pass the BDT cut for 0.5 GeV/c^2 : 15 events**
- **pass the BDT cut for 16 GeV/c^2 : 123 events**
- **pass the BDT cut for other masses**

First results of NEWS-G with SEDINE

NEWS-G collaboration, Astropart. Phys. 97, 54 (2018), doi: 10.1016/j.astropartphys.2017.10.009

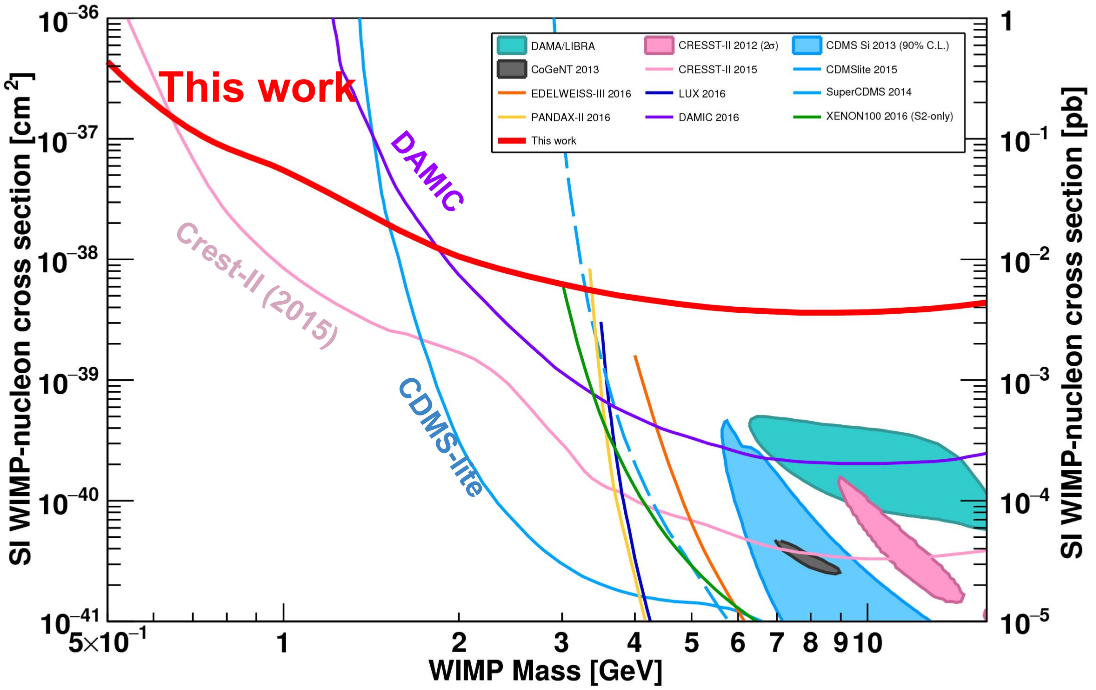

Exclusion at 90% confidence level (C.L.) of cross-sections above $4.4 \cdot 10^{-37}$ cm^2 for a 0.5 GeV/c^2 WIMP

Limit set on spin independent WIMP coupling with standard assumptions on WIMP velocities, escape velocity and with quenching factor of Neon nuclear recoils in Neon calculated from SRIM

NEWS-G current status & developments

Preparing the He physics run

Gas quality

Testing gas mixtures of He/CH_4

- High pressure operation (Penning)

-Hydrogen rich target

Upgrading gas system

- Tightness

- Filtering

- Gas recirculation

- Residual Gas Analyzer monitoring

Quenching factor measurements

- Ion / electron beam (LPSC, France)

- Neutron beam (TUNL, USA)

Study of the detector response

Solid state laser (213 nm)

- drift time measurements

- parametrization of the avalanche process

Sensor developments

Aims

- High pressure operation

- High gain

- Increased stability

- Low radioactivity

Techniques

- Resistive technologies

- 3D printing technologies

- FEM simulations

Major Issues

Reduced drift velocity

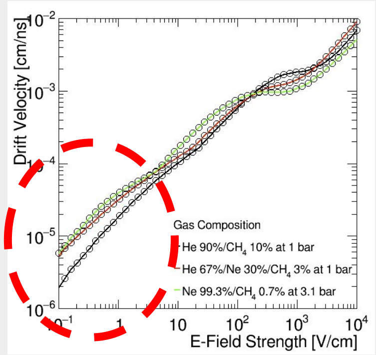

High probability of attachment

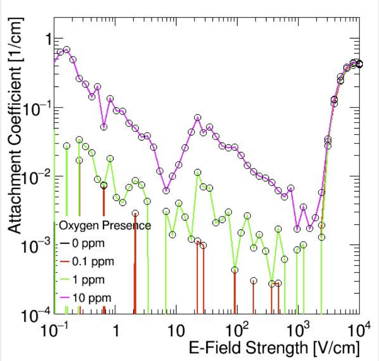

Gas quality

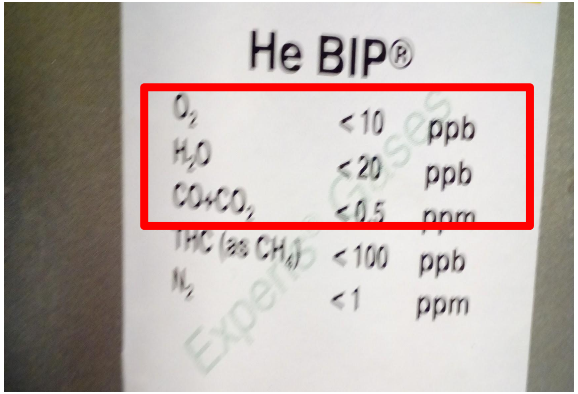
He BIP®
O_2 < 10 ppb
H_2O < 20 ppb
$CO+CO_2$ < 0.5 ppm
THC (as CH_4) < 100 ppb
N_2 < 1 ppm
Experts Gases

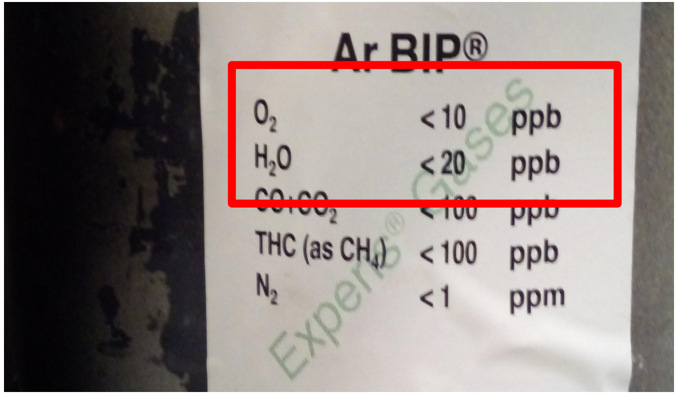
Ar BIP®
O_2 < 10 ppb
H_2O < 20 ppb
THC (as CH_4) < 100 ppb
N_2 < 1 ppm
Experts® Gases

Gas quality

Gas filtering

Rise time vs Amplitude 2D Histo

Amplitude 1D Histo

He/CH4 (90/10)
600 mbar
HV1=1820 V
HV2=+225 V
Ball Φ2 mm
No OXISORB

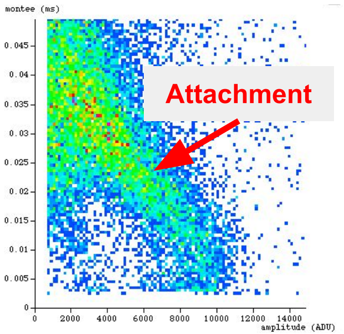

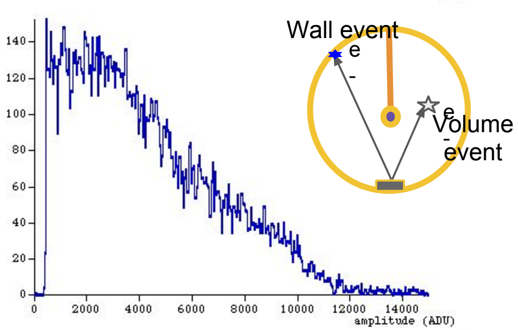

He/CH4 (90/10)
600 mbar
HV1=1840 V
HV2=+300 V
Ball Φ2 mm
OXISORB

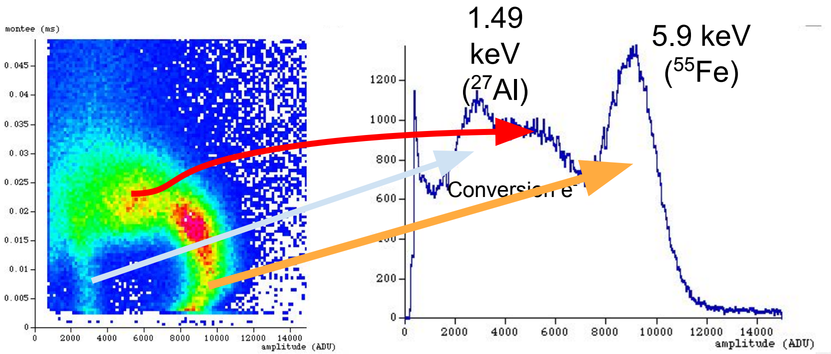

Improvements

<u>Vacuum conditions</u>

1.E-4 mbar→1.E-5 mbar→1.E-6 mbar

Leak Rate ≈ 1.4E-6 mbar*L/s

⇒ Not a dramatic effect

<u>Gas quality</u>

Contaminants ~ppm
↓
Oxisorb ~100 ppb

⇒ **Big improvement**

Increased drift velocity results in less attachment

Gas quality

Removing sources of outgassing

Rise time vs Amplitude 2D Histo

Amplitude 1D Histo

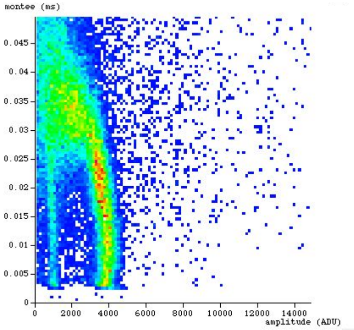

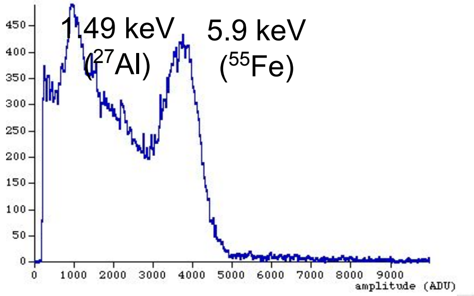

<u>No cuts</u>

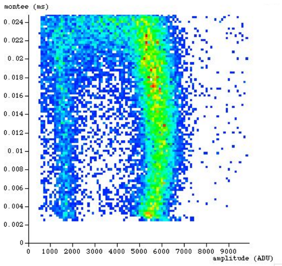

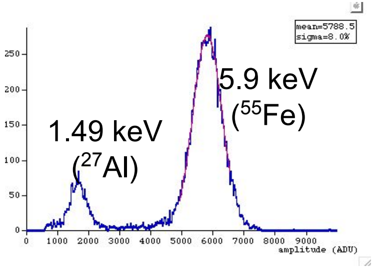

<u>After Cuts</u>
Risetime [2,25]µs

P = 600 mbar, Oxisorb used, sensor Φ 2 mm, HV1= 1750 V, HV2= +200 V

<u>Result</u>

- The whole signal is < 25 µs (before <35 µs)
- Resolution at 6 keV (σ) ~ 8% (instead ~10%)
- Resolution at 1.49 keV (σ) ~ 17.2% (instead ~22%)
- Clear separation between conversion e- events and volume events

Drift velocity increment

Addition of a third noble gas

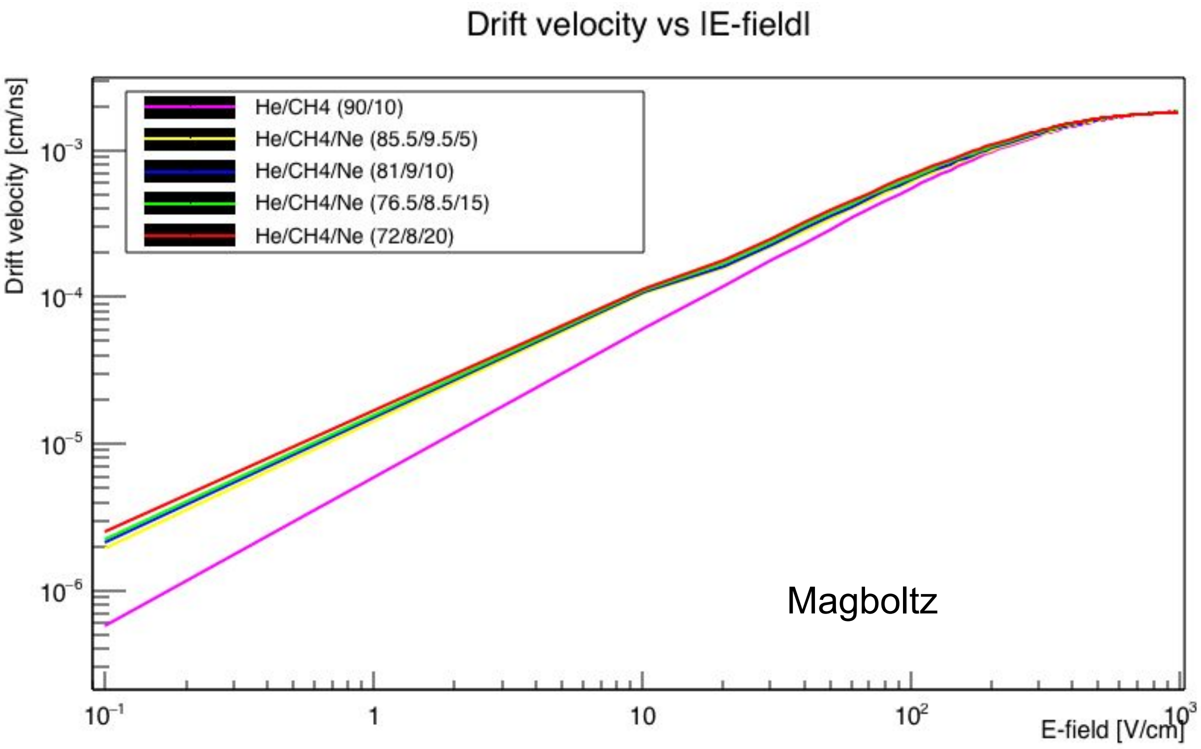

Sensor influence on the E-field

Electric field magnitude dependence on the azimuthal angle (φ) - Inhomogenous response

The ideal case

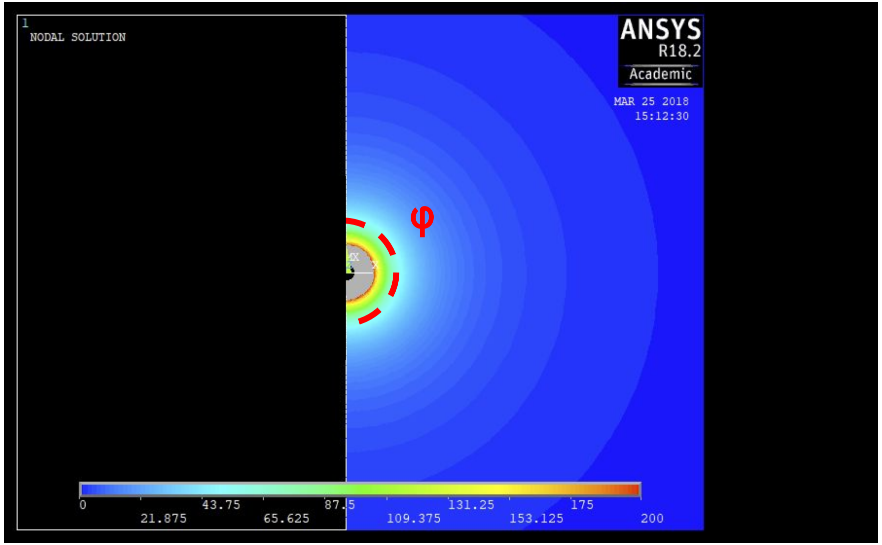

- A floating ball with a HV applied on its surface

The reality

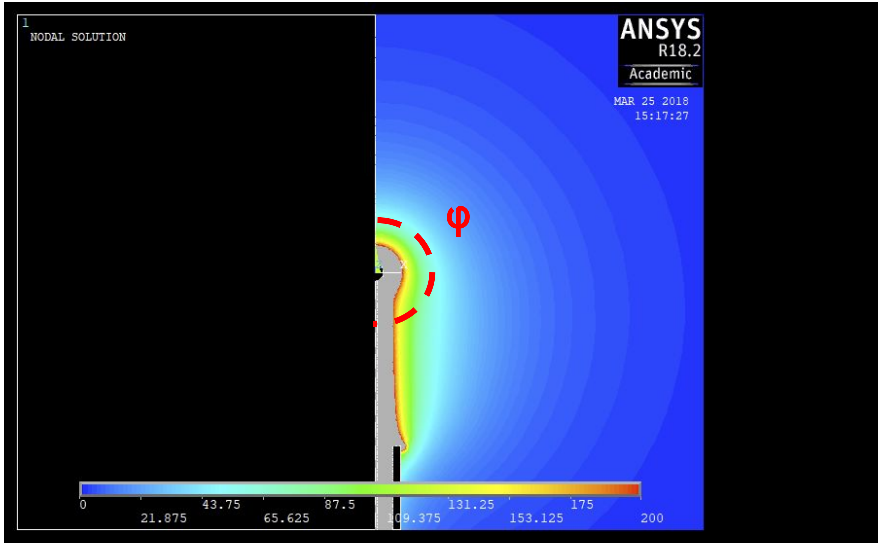

- A ball connected to a wire through which the HV is applied on the ball.
- The wire - ball structure is supported by a grounded rod.

Patrick Knights PhD, University of Birmingham & University Paris-Saclay

The umbrella

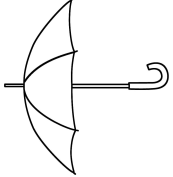

Material used: Copper, Brass, Steel, Iron, PE, PEEK, Teflon, Kapton, Plexiglass, Si, Araldite

Introduction of a secondary correction electrode

Goals:

- Homogeneous field
- Limited discharges
- Operation in high pressure
- Stability

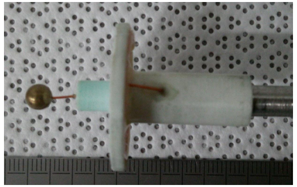

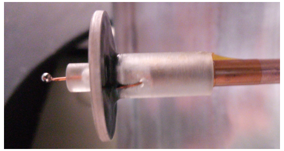

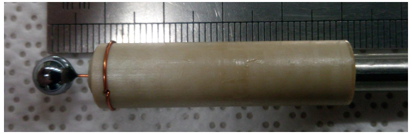

Possible issues

Inhomogeneous response

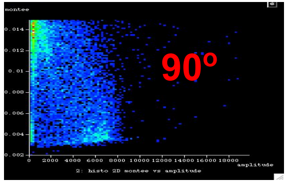

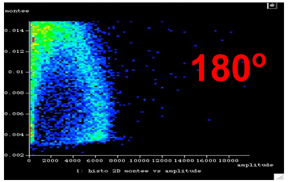

Instability

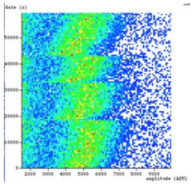

Sensor Design: Umbrella Voltage

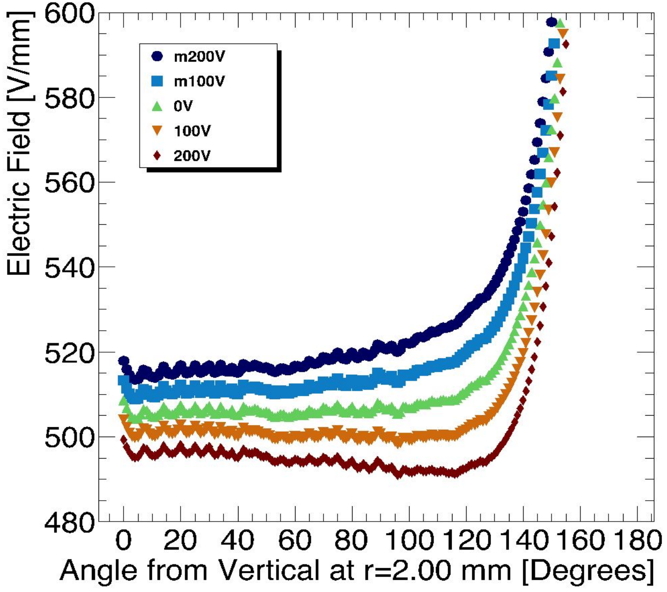

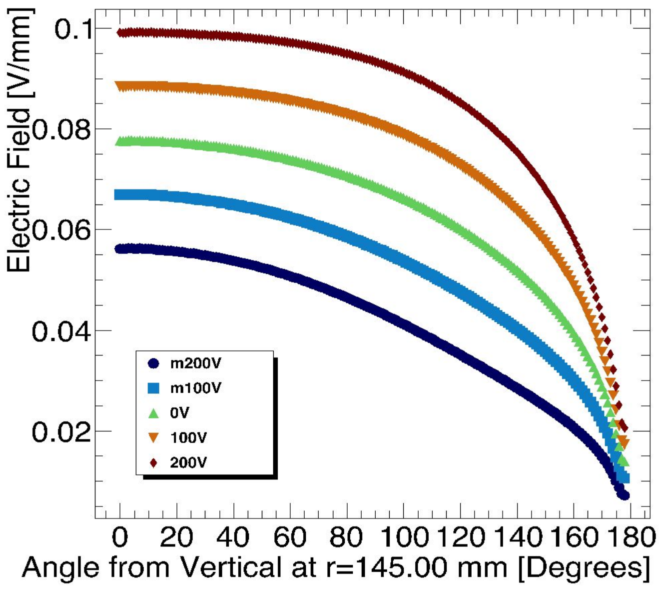

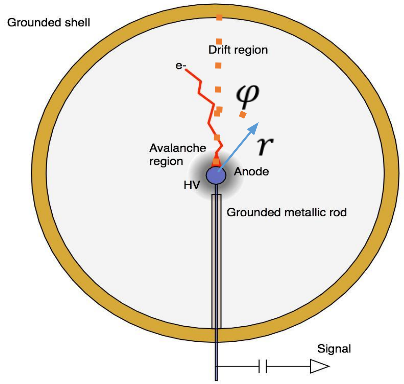

r_A = 1 mm
r_C = 150 mm
V_A = 2000 V
Separation = 3.5 mm

Sensor Design: Anode-Umbrella Separation

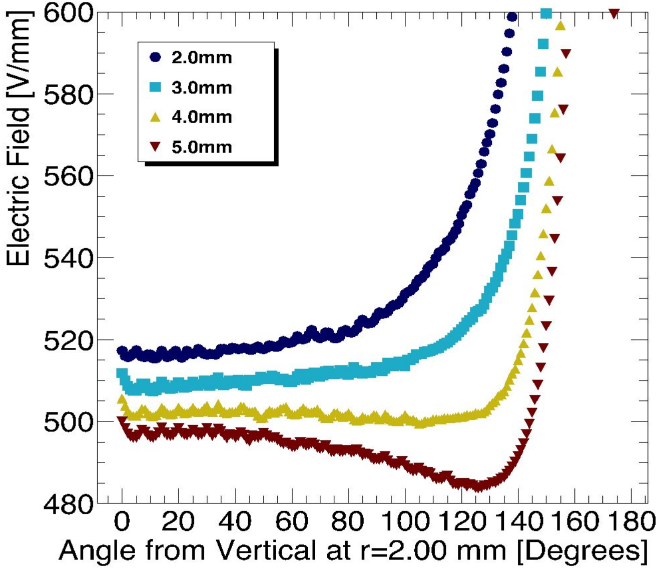

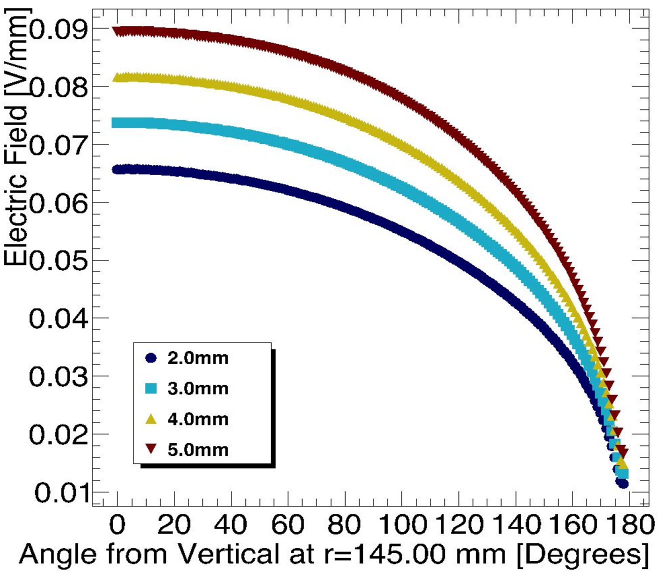

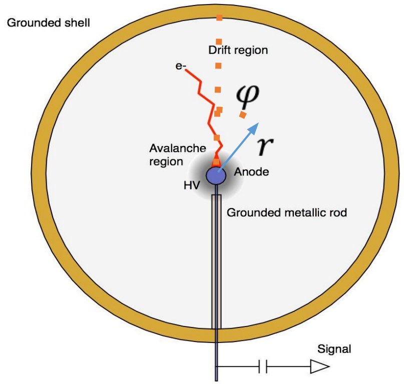

$r_A = 1$ mm

$r_C = 150$ mm

$V_A = 2000$ V

$V_U = 0$ V

Sensor Design: Measurements

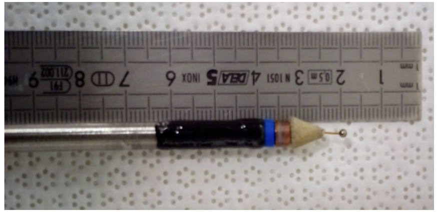

- Fe55 Source – 5.9 keV x rays
- 30 cm diameter test sphere operating at 600 mbar of He + 10% CH_4
- Anode Diameter = 2 mm, Separation = 3.5 mm

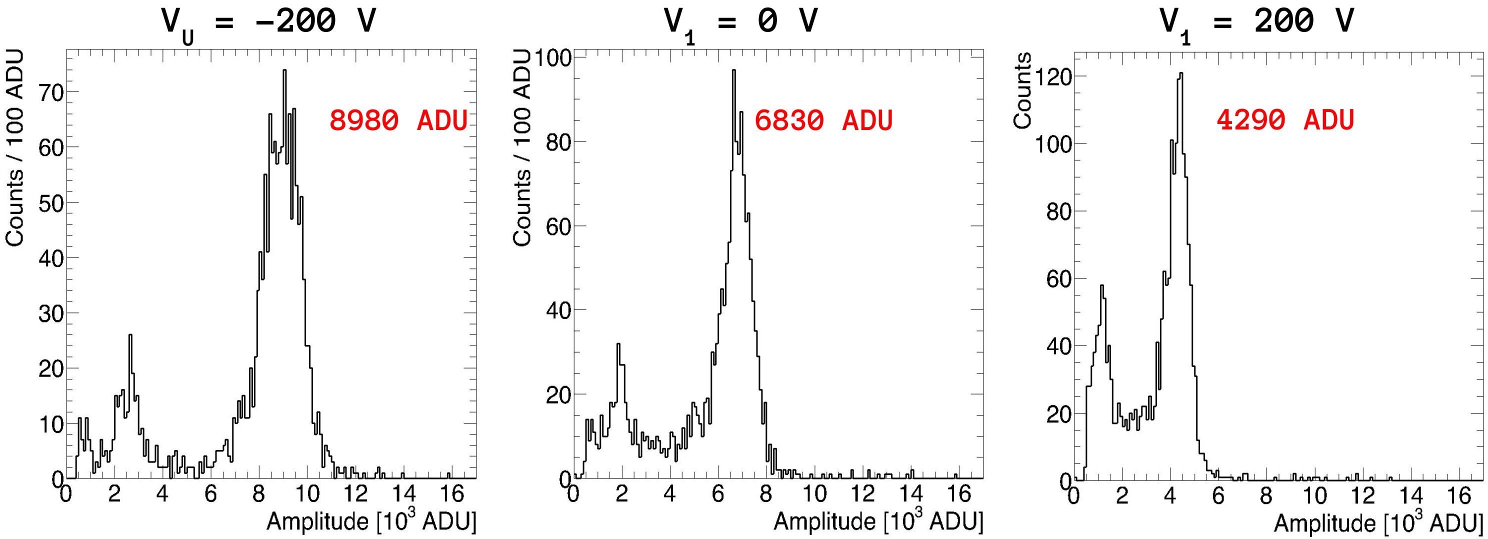

Gain reduced by presence of positive voltage on umbrella - electric field near anode reduced

The resistive umbrella

Bakelite Prototypes

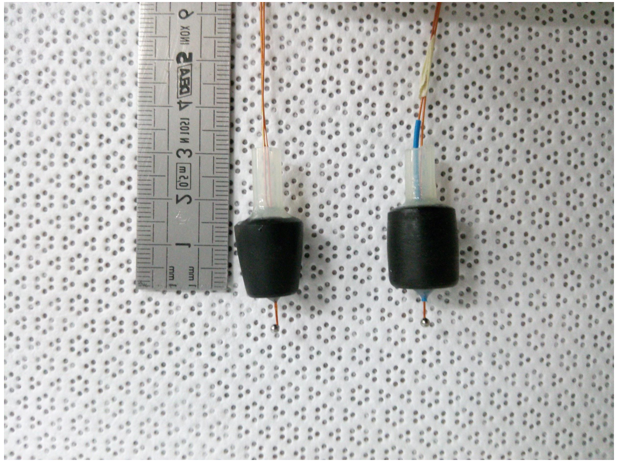

Glass Prototype

Advantages:

- Volume Resistivity $10^{10}\ \Omega\cdot cm$ - $10^{12}\ \Omega\cdot cm$
- Compact and homogeneous material
- Minimized insulating surface

Bakelite
Chemical Formula:
$(C_6-H_6-O.C-H_2-O)x$

Soda - lime glass
Chemical composition*:
70% SiO_2 (glass) +
15% Na_2O (soda) +
9% CaO (lime) +
Other
*there are a lot different compounds

Performance of the resistives umbrellas - A

Homogeneous response

$He+9\%CH_4+7\%Ar$
730 mbar
Anode Φ 2 mm

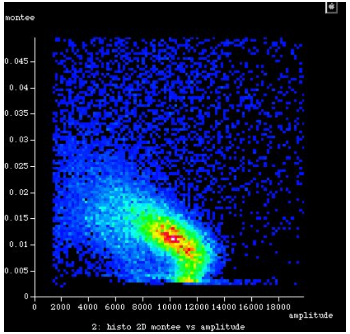

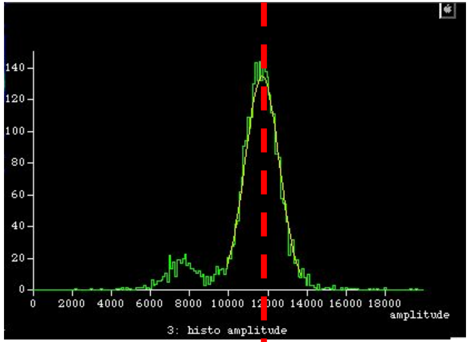

180º

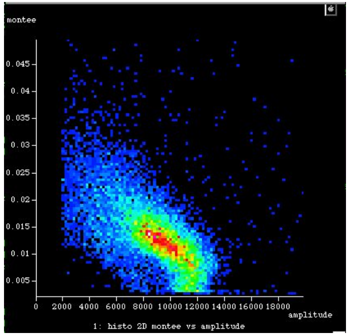

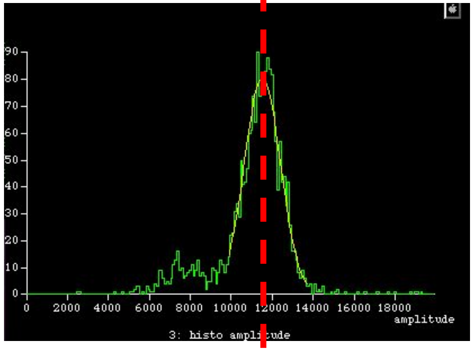

90º

Rise time vs Amplitude

Amplitude

^{55}Fe source position

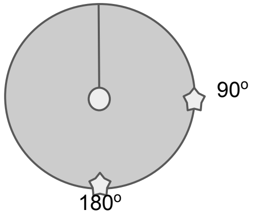

The difference in gain between the two positions is close to the statistical error

Performance of the resistives umbrellas - B

Stability

Pulse Height (ADU)

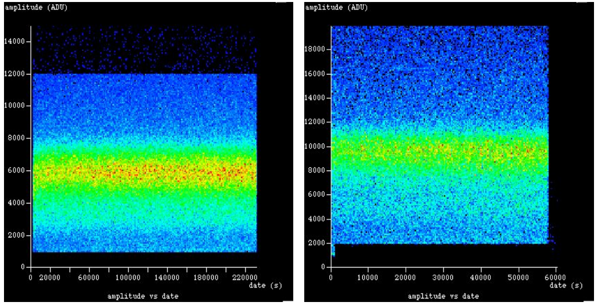

Time (s)

Ball: Φ2 mm steel
Gas: He+30%Ar+7%CH4
P = 715 mbar
HV1 = 1830 V
HV2 = 0 V

Ball: Φ2 mm steel
Gas:
He+10%Ar+2.5%CH4
P = 1880 mbar
HV1 = 2300 V
HV2 = 0 V

Resolution

Rise time (µs)

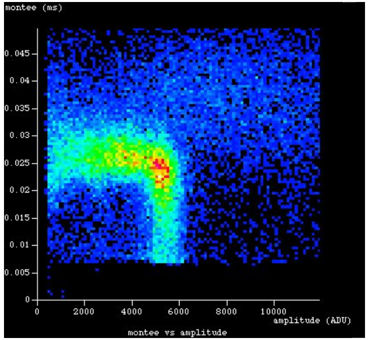

Pulse Height (ADU)

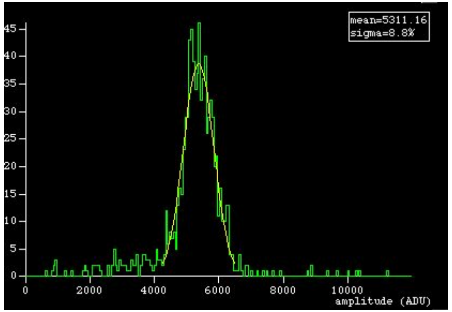

Iron fluorescence (~6.4 keV)

Ball: Φ3 mm steel
Gas: He+30%Ar+3%CH4
P = 1000 mbar
HV1 = 2300 V
HV2 = 0 V

Evolution of the sensor “umbrellas”

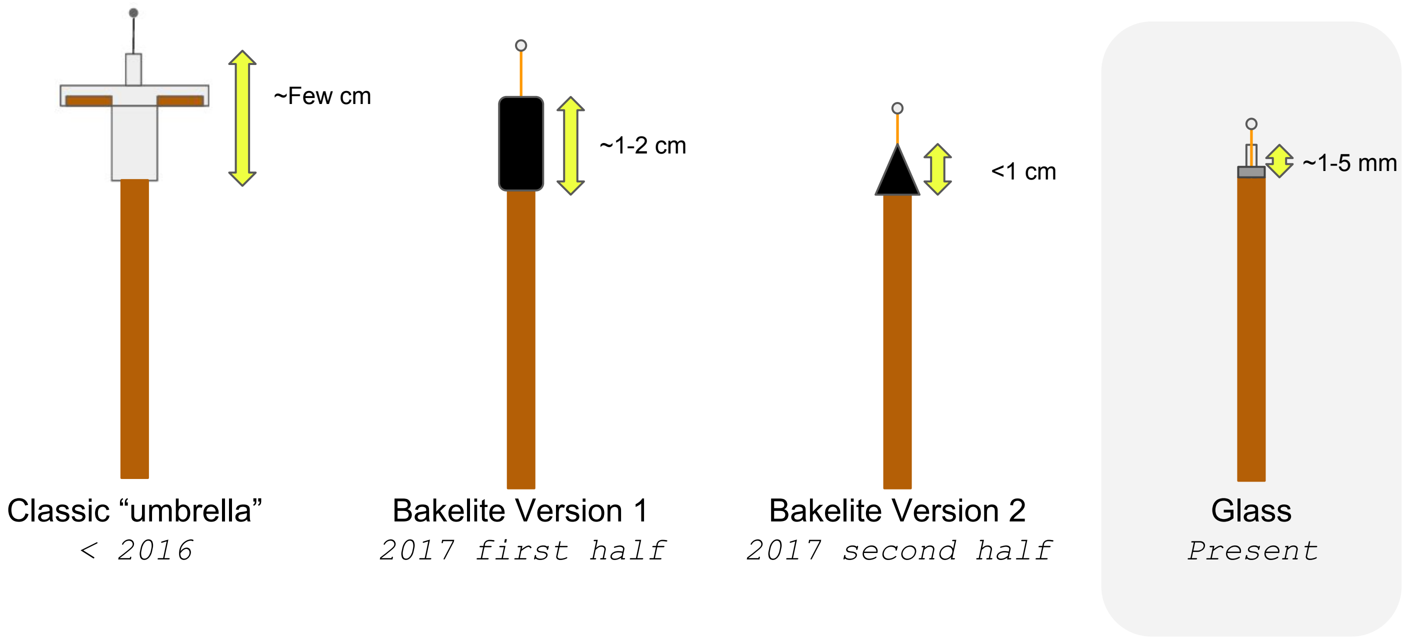

Evolution targets:

- Precision
- Easy construction
- Low mass
- Detector stability
- Homogeneous response
- Low radioactivity

The multiball sensor - ACHINOS

Dealing with the low electric field magnitude (~1 V/cm) at large detectors

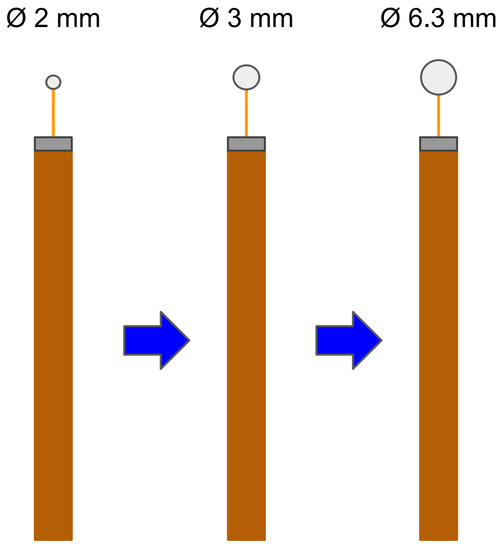

The idea: Use multiple balls placed in the same potential instead

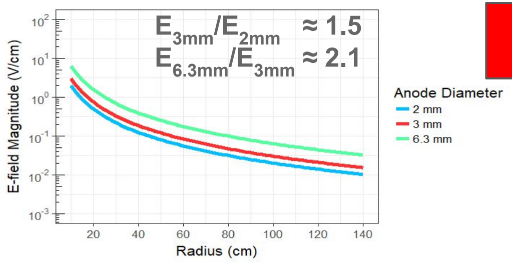

Comparison of E-field strength for anode of different radii vs the radius

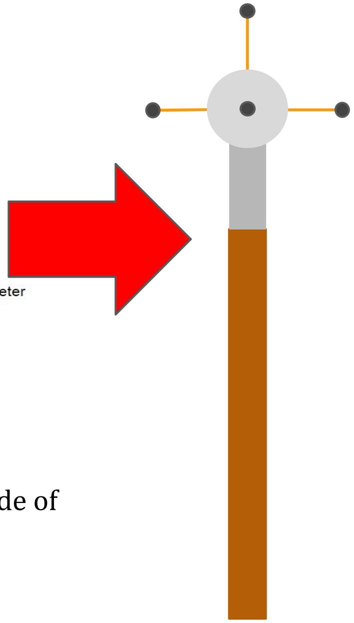

$$E(r) = \frac{V_0}{r^2} r_1$$ *Electric field dependence on the radius*

AIM:

1. Operation in high pressure
2. Build larger volume detectors

Conundrum:

Both Gain and Drift time are a function of E/P

$$lnM = \int_{E(r1)}^{E(r2)} a(E/P) \frac{dr}{dE} dE$$

$$v_{drift} = \mu \frac{E}{P}$$

The elegant solution – ACHINOS

- Decoupling Gain -Drift
- Tunes Volume electric field
- Anodes can be read out individually

Study of the Electric field using FEM software

Field lines close close to the central structure

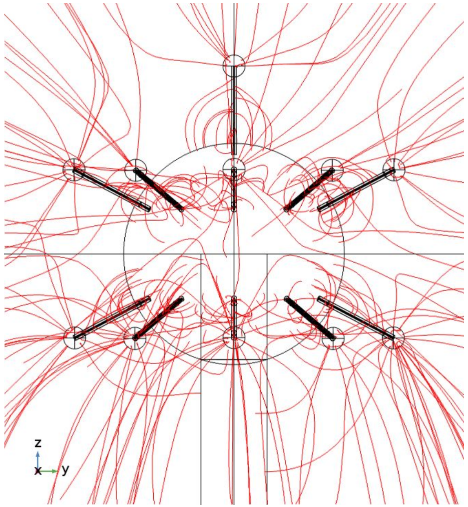

Creation of collective iso-potentials

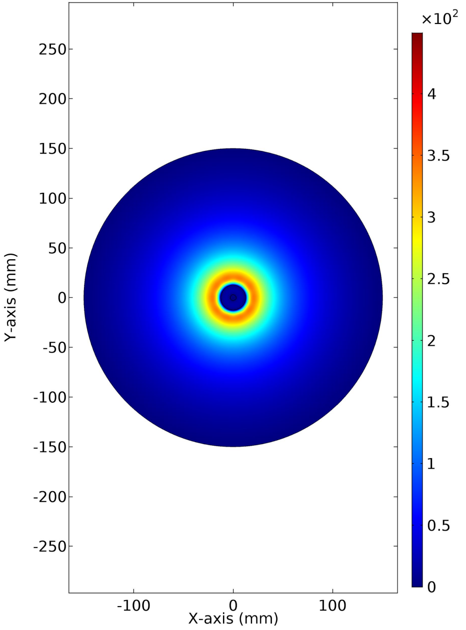

Electric field magnitude with ACHINOS

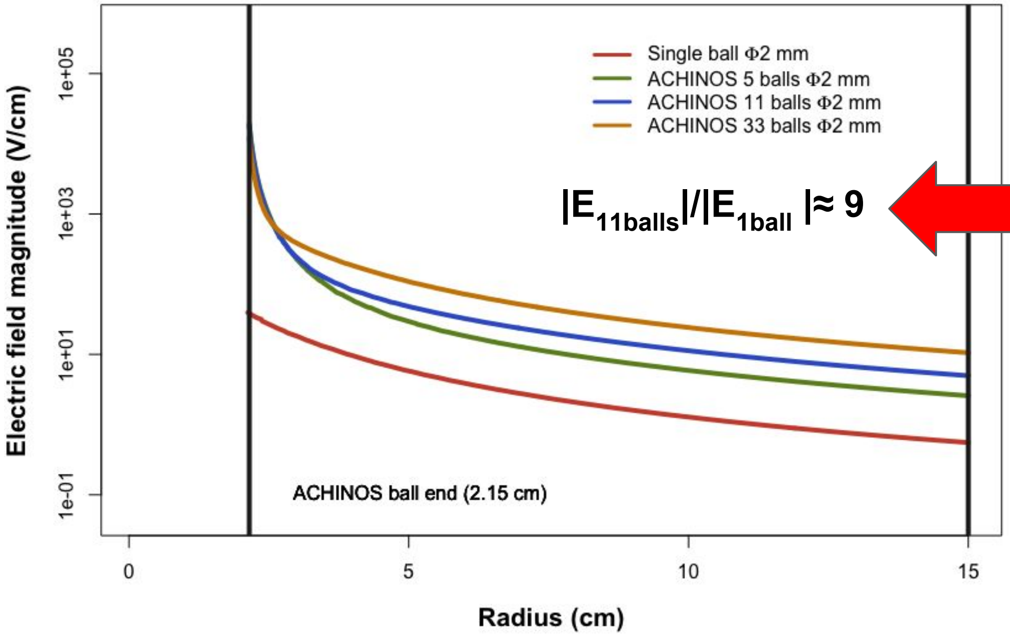

$|E_{11balls}|/|E_{1ball}| \approx 9$

The first ACHINOS prototypes

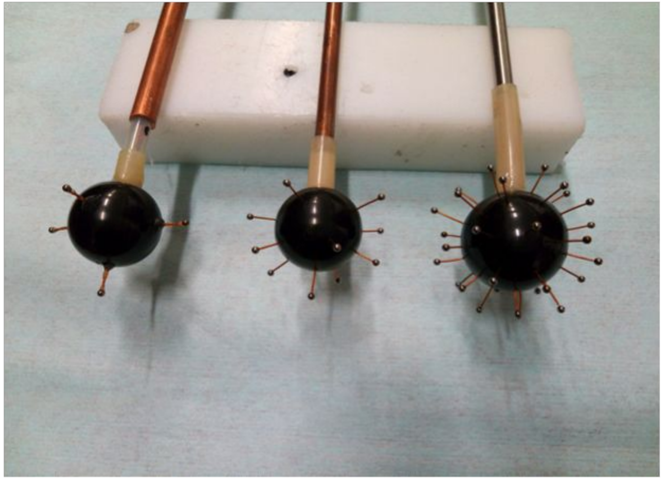

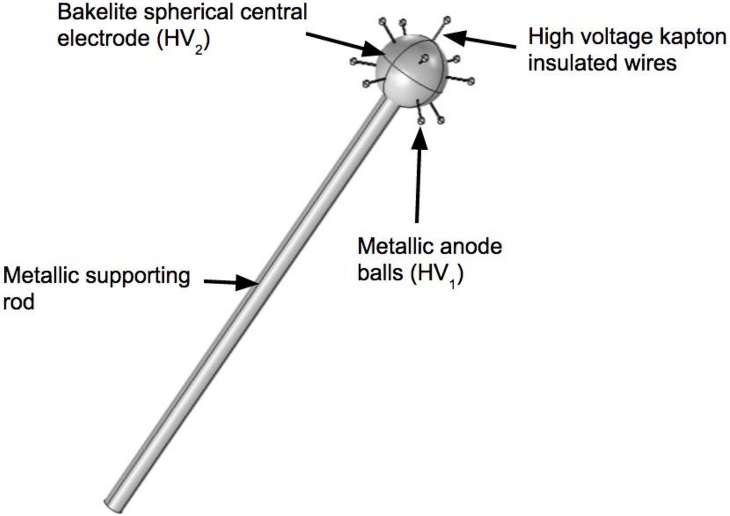

<u>Composition:</u>

- 5, 11, or 33 balls
- Anode Ø 2 mm
- Placed in a virtual spherical surface
- Set in the same HV1
- Bias electrode made of bakelite (resistive) HV2

Positive results with the first prototypes

Stability in terms of sparking

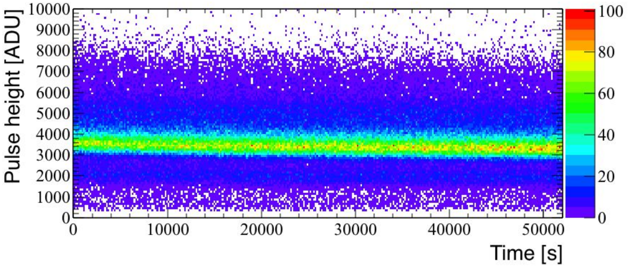

Measurement of the 5.9 keV line

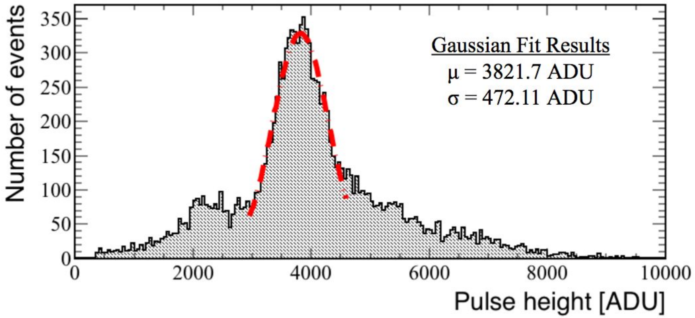

Rise time vs Pulse height
Single ball

Rise time vs Pulse height
11-balls

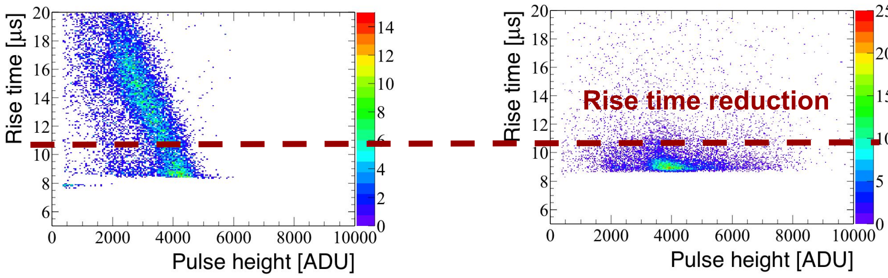

<u>Conditions:</u>

- Gas Mixture: He:Ar:CH4 (80:11:9)
- Pressure: 640 mbar
- HV1 = 2015 V, HV2 = -200 V

Preliminary results with the 2nd gen prototypes

On going study of the 2nd gen prototypes

Measurement of the 5.9 keV ^{55}Fe X-ray line

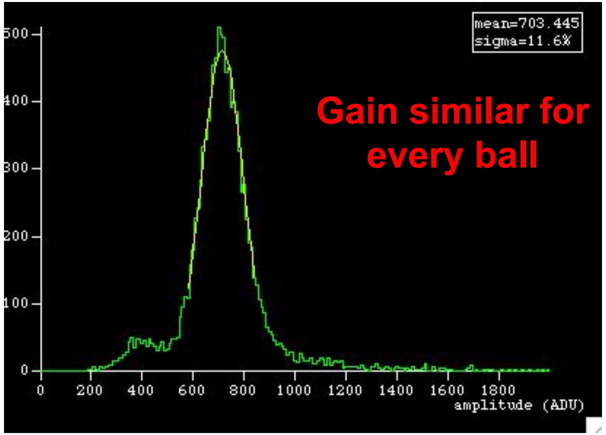

Conditions:

- *Gas Mixture: He:Ar:CH4 (56:37:7)*
- *Pressure: 455 mbar*
- *HV1 = 1100 V, HV2 = -100 V*

Prospects

- Alternate coatings such as copper power/glue
- More compact design of the 3D printed support structure
- Anode balls of Ø1 mm
- Operation in higher pressure
- Operation in high gain

Why such a weird name

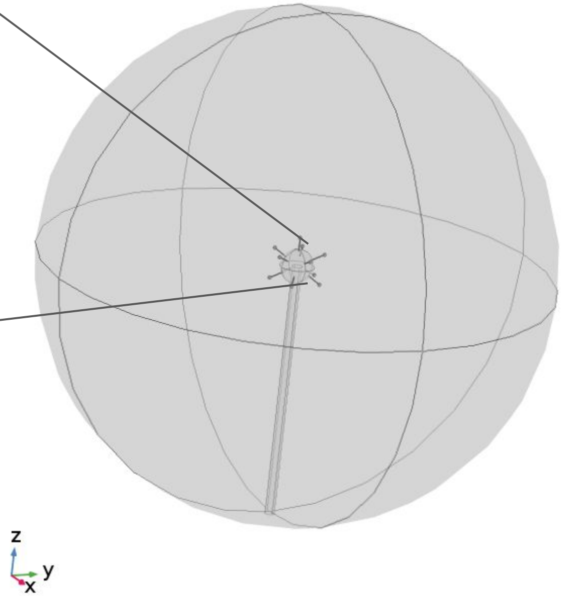

ACHINOS = Sea urchin = Αχινός

Development of detailed simulation methods to model the detector response

The power of combining state-of-the art software

Software for the simulation of particle passage through matter

- Build geometry
- Transport of particles
- Particle interaction
- Generation-Transport of secondaries
- …
- Energy deposition in the ROI

Geant4

Software for the simulation of gaseous detectors

- Drift of charges
- Diffusion
- Avalanche
- Signal Induction
- Electronics

Garfield
Garfield++

Software based on FEM

- Electric Field
- Magnetic Field
- Particle tracks

COMSOL

ANSYS®

Simulated detector response

Examples of simulated pulses treated with the same analysis algorithm as real pulses

Surface e- extracted by a 5.9 keV X-ray

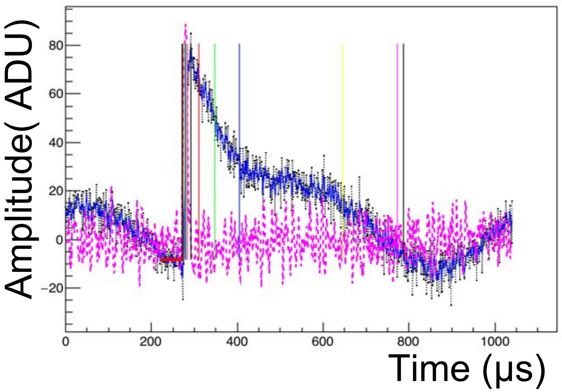

Atmospheric Muon

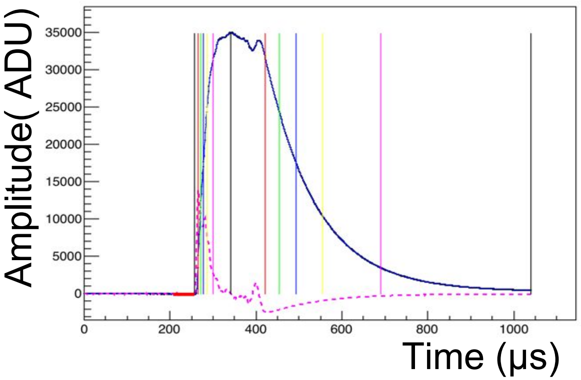

No pulse - only noise

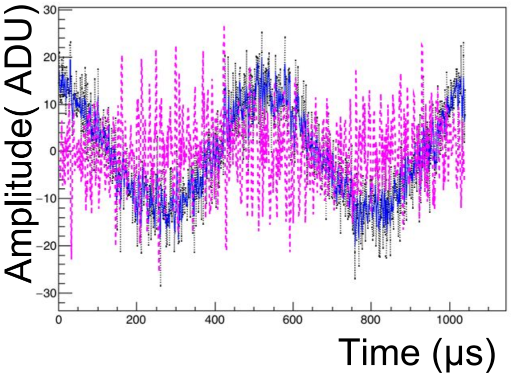

He+10%CH4 @ 1 bar
Irradiation of the volume with an 5.9 keV ^{55}Fe source

An illustration of the method

Assumed an τ=100 μs for our preamp with g=0.45mV/fC and 50 ADU/mV 2800 V applied on Φ 3mm anode

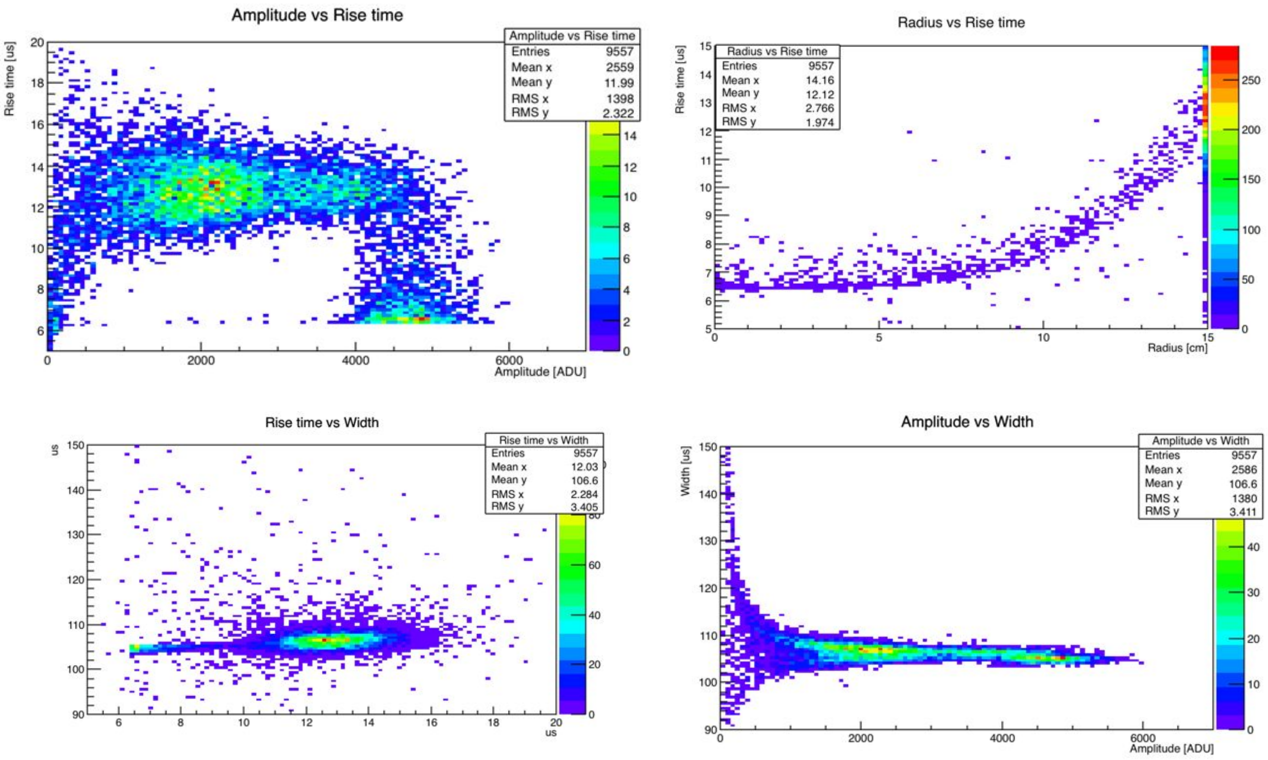

From the initial interaction to the detector response

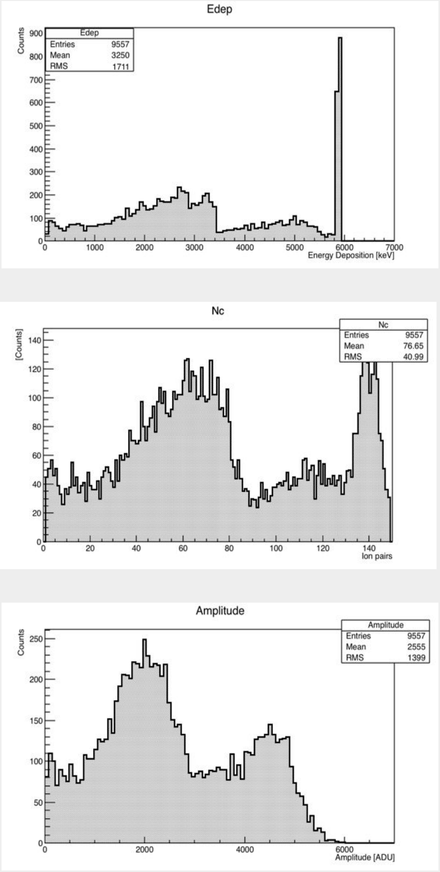

A qualitative comparison with the experiment

Simulation

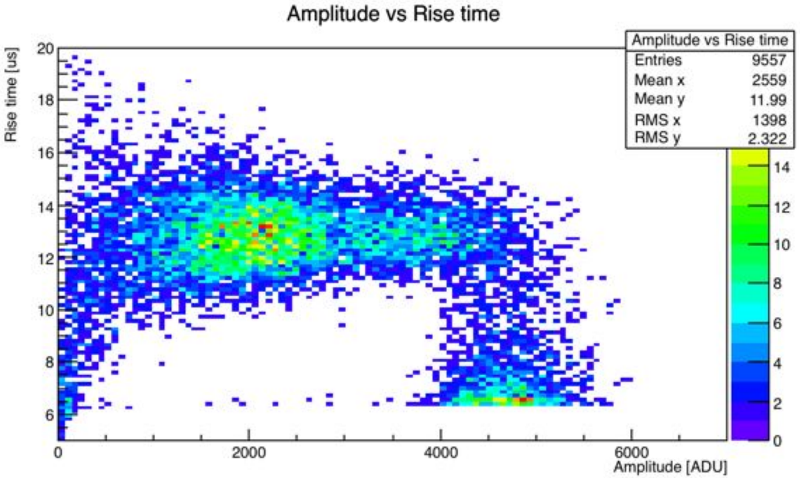

Experiment

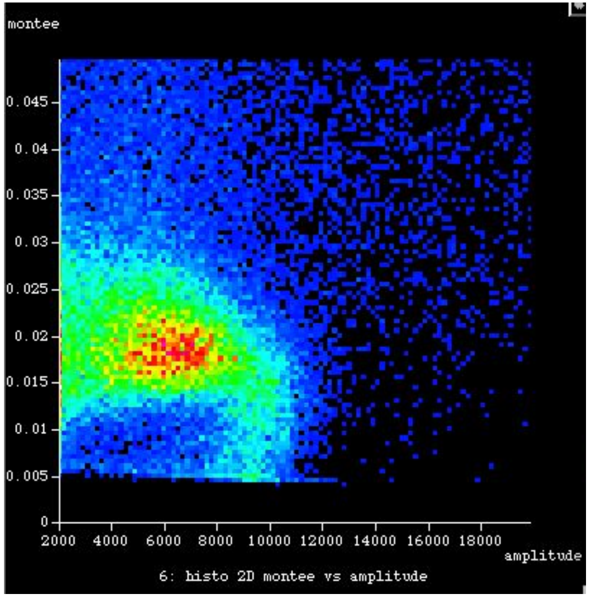

Detector: Spherical Proportional Counter (SPC)
Source: 55Fe X-ray (5.9 keV)
Gas: He/CH4 at 500 mbar

Quenching factor measurements at LPSC Grenoble

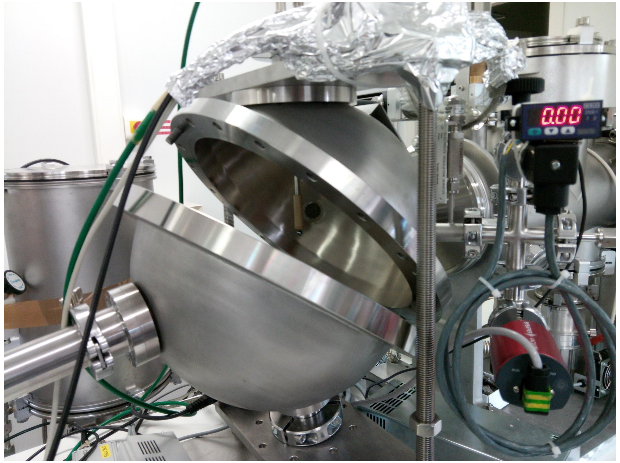

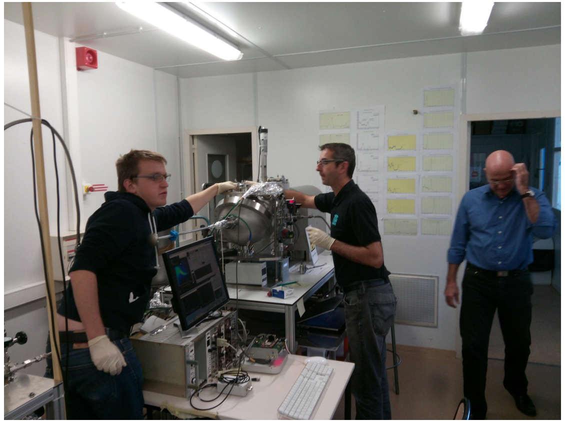

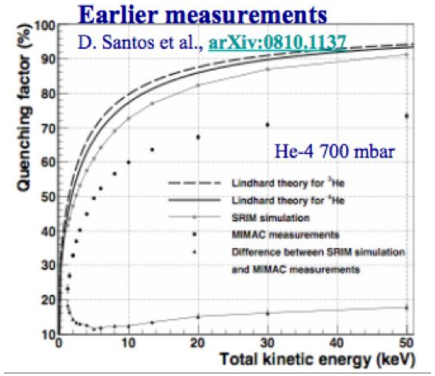

Electrons and ions are passing <u>through a 1μm in diameter hole</u> to enter in the gaseous volume of the SPC !!!

- "High" flux environment (~10^{10} $cm^{-2}s^{-1}$)
- Very low energy threshold (<100 eV)

LAST BUT NOT LEAST!!!

NEWS-G at SNOLAB

The underground laboratory in the Sudbury, Canada

Deeper underground
0.25 μ/m²/day
~8x lower μ flux than LSM

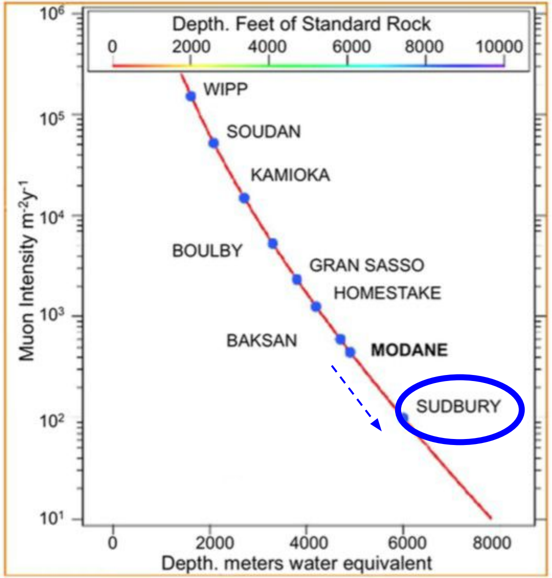

Practically, at 2 km is the deepest clean room in the world

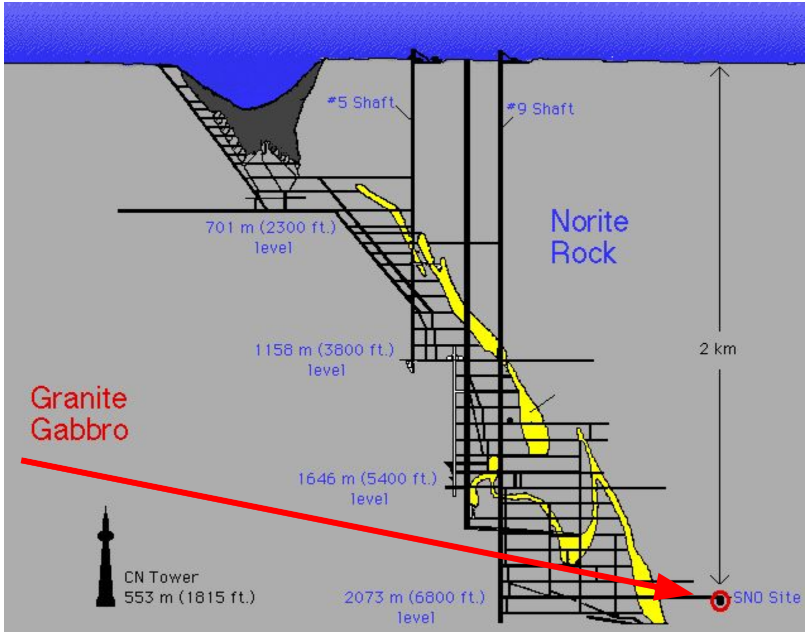

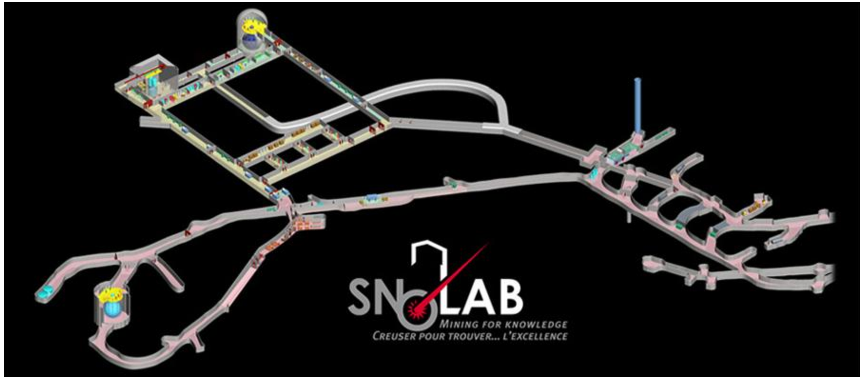

NEWS-G at SNOLAB

The new and improved setup

Copper vessel (140 cm ⌀, 12 mm thick)

- Low activity copper (C10100)
  - 7 to 25 μBq/kg Th
  - 1 to 5 μBq/kg of U
- Electropolishing & Electroplating

Upgraded compact shielding (35t)

- 40 cm PE + Boron sheet
- 22 cm VLA Pb (1 Bq/kg ^{210}Pb)
- 3 cm archaeological lead
- Airtight envelope to flush pure N (against Rn)

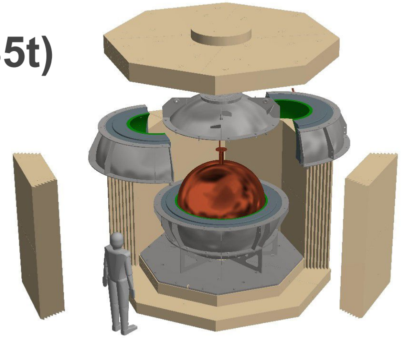

Hemispheres built in France, stored at LSM before welding

Glove box for Radon free rod installation

Estimated background

Simulation done with 12mm thick 140cm diam copper sphere full with 99% Ne 1%CH4, 11.43 kg of gas

Source Position	Mass (kg) or Surface (cn	Source	evts/kg/day/[(µBq/kg) or (nBq/cm2)]	contamination	units	evts/kg/day < 1ke
CopperSphere	627.83 kg	Co60	0.0018	30	µBq/kg	0.054
CopperSphere	627.83 kg	U238	0.0036	3	µBq/kg	0.011
CopperSphere	627.83 kg	Th232	0.0049	12.9	µBq/kg	0.063
InnerSurface	57255 cm^2	Pb210	0.012	0.16	nBq/cm2	0.002
ArchLead	2108.95 kg	U238	0.001	61.8	µBq/kg	0.062
ArchLead	2108.95 kg	Th232	0.0011	9.13	µBq/kg	0.010
Rod	0.0931721 kg	Co60	2.95E-007	30	µBq/kg	0.000
Rod	0.0931721 kg	U238	1.81E-006	3	µBq/kg	0.000
Rod	0.0931721 kg	Th232	2.11E-006	12.9	µBq/kg	0.000
Wire	2.66005e-05 kg	Co60	1.48E-010	31000	µBq/kg	0.000
Wire	2.66005e-05 kg	U238	2.12E-009	300000	µBq/kg	0.001
Wire	2.66005e-05 kg	Th232	1.42E-009	50000	µBq/kg	0.000
Wire	2.66005e-05 kg	K40	5.41E-010	1660000	µBq/kg	0.001
LabArea		Tl208/K40				0.076

Total	**0.279**

Copper

Internal surface

Lead shield

External BG with SNO Flux

NEWS-G at SNOLAB

Projected sensitivity

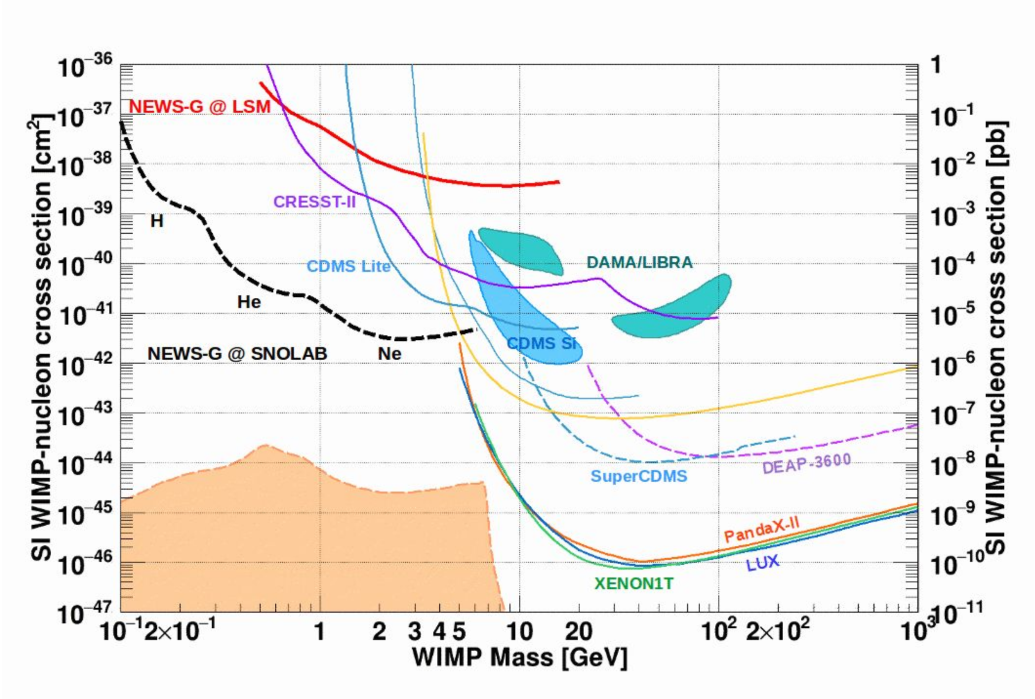

100 kg.days, 200eVee ROI above threshold at 1 electron.
(Not accounting for sensitivity improvement from resolution effects and RT cuts)

The NEWS-G collaboration

- **Queen's University Kingston –** G Gerbier, P di Stefano, R Martin, G Giroux, T Noble, D Durnford, S Crawford, M Vidal, A Brossard, F Vazquez de Sola, Q Arnaud, K Dering, J Mc Donald, M Clark, M Chapellier, A Ronceray, P Gros, J Morrison, C Neyron
  - Copper vessel and gas set-up specifications, calibration, project management
  - Gas characterization, laser calibration, on smaller scale prototype
  - Simulations/Data analysis
- **IRFU** (Institut de Recherches sur les Lois fondamentales de l'Univers)**/CEA Saclay** -I Giomataris, M Gros, C Nones, I Katsioulas, T Papaevangelou, JP Bard, JP Mols, XF Navick,
  - Sensor/rod (low activity, optimization with 2 electrodes)
  - Electronics (low noise preamps, digitization, stream mode)
  - DAQ/soft
- **LSM** (Laboratoire Souterrain de **Modane**), IN2P3, U of Chambéry **-** F Piquemal, M Zampaolo, A DastgheibiFard
  - Low activity archeological lead
  - Coordination for lead/PE shielding and copper sphere
- **Thessaloniki University –** I Savvidis, A Leisos, S Tzamarias
  - Simulations, neutron calibration
  - Studies on sensor
- **LPSC (**Laboratoire de Physique Subatomique et Cosmologie) **Grenoble** - D Santos, JF Muraz, O Guillaudin
  - Quenching factor measurements at low energy with ion beams
- **Pacific National Northwest Lab–** E Hoppe, DM Asner
  - Low activity measurements, Copper electroforming
- **RMCC (**Royal Military College Canada**) Kingston –** D Kelly, E Corcoran
  - 37 Ar source production, sample analysis
- **SNOLAB –Sudbury –** P Gorel
  - Calibration system/slow control
- **University of Birmingham –** K Nikolopoulos, P Knight
  - Simulations, analysis, R&D

Associated lab : TRIUMF - F Retiere
- Future R&D on light detection, sensor

Thessaloniki, Greece 2018

Thank you very much for your attention

Additional material

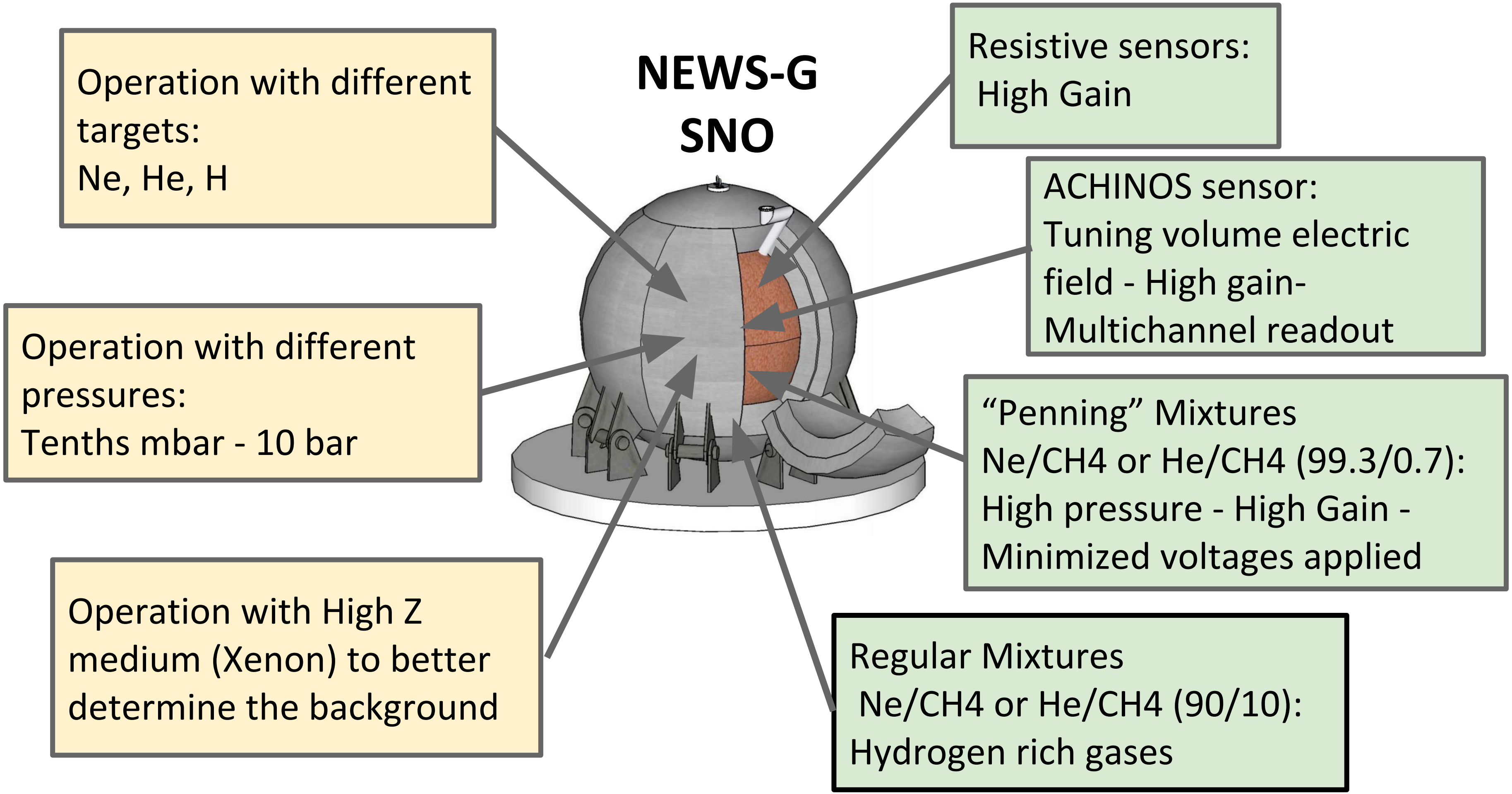

NEWS-G
SNO
Operation with different targets:
Ne, He, H
Operation with different pressures:
Tenths mbar - 10 bar
Operation with High Z medium (Xenon) to better determine the background
Resistive sensors:
High Gain
ACHINOS sensor:
Tuning volume electric field - High gain- Multichannel readout
“Penning” Mixtures
Ne/CH4 or He/CH4 (99.3/0.7):
High pressure - High Gain - Minimized voltages applied
Regular Mixtures
Ne/CH4 or He/CH4 (90/10):
Hydrogen rich gases

Illustration of the basic analysis principle

^{109}Cd source
Irradiation through 200µm Al window
P = 100 mb, Ar-CH4 (2%)

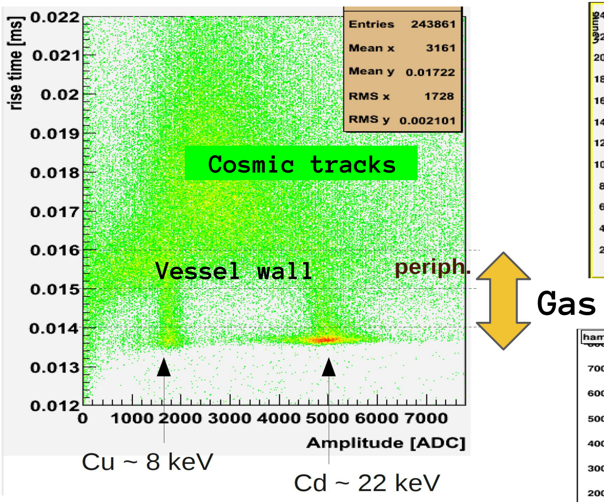

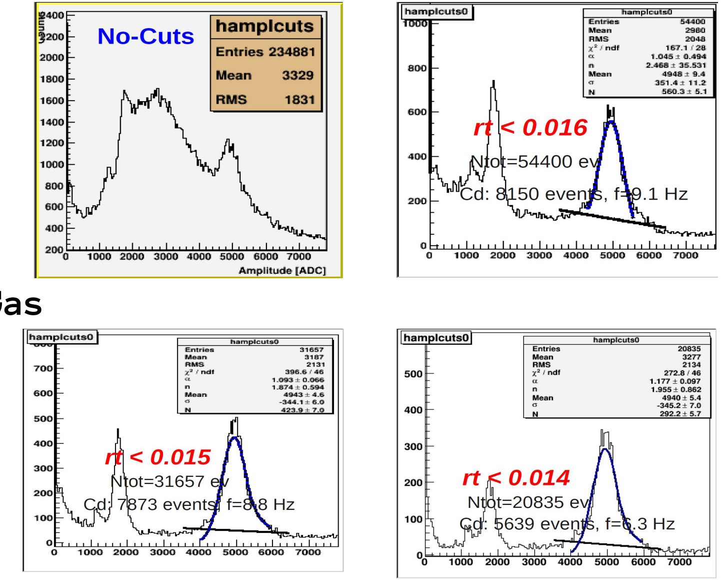

Efficiency of the cut in rt → ~ 70% signal (Cd line)
Significant background reduction

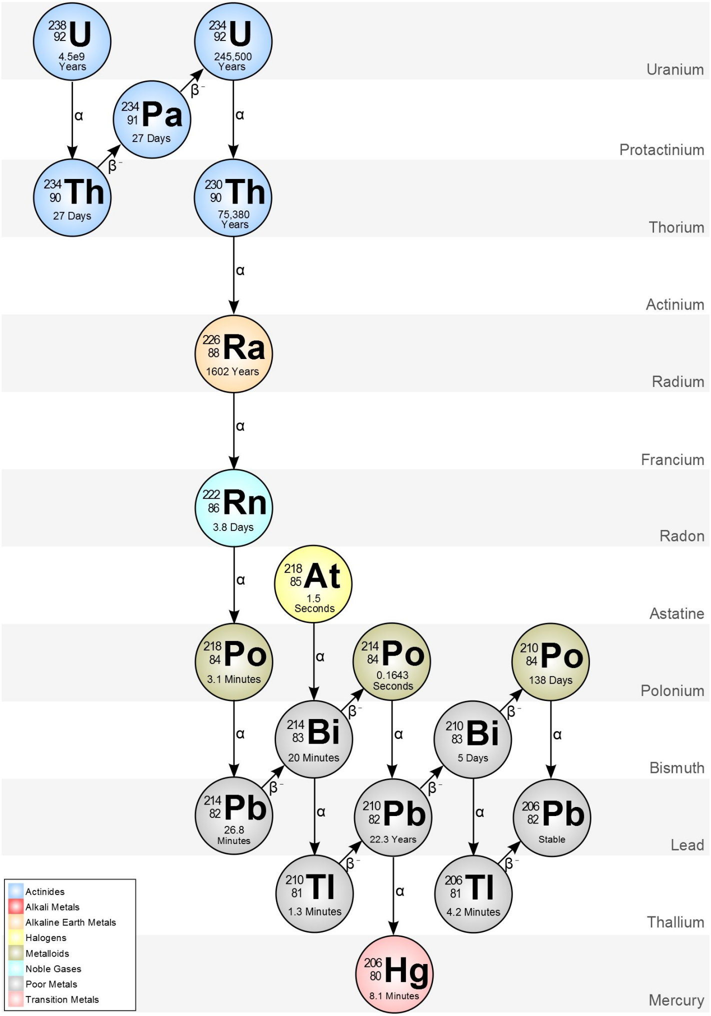

238 92 U 4.5e9 Years
234 92 U 245,500 Years
Uranium
234 91 Pa 27 Days
Protactinium
234 90 Th 27 Days
230 90 Th 75,380 Years
Thorium
Actinium
226 88 Ra 1602 Years
Radium
Francium
222 86 Rn 3.8 Days
Radon
218 85 At 1.5 Seconds
Astatine
218 84 Po 3.1 Minutes
214 84 Po 0.1643 Seconds
210 84 Po 138 Days
Polonium
214 83 Bi 20 Minutes
210 83 Bi 5 Days
Bismuth
214 82 Pb 26.8 Minutes
210 82 Pb 22.3 Years
206 82 Pb Stable
Lead
210 81 Tl 1.3 Minutes
206 81 Tl 4.2 Minutes
Thallium
206 80 Hg 8.1 Minutes
Mercury
α
β⁻
Actinides
Alkali Metals
Alkaline Earth Metals
Halogens
Metalloids
Noble Gases
Poor Metals
Transition Metals

Table 1. Radiocarbon results. Material codes and protocols are described in Crann et al. (2017).

Lab ID	Submitter ID	Material	Mat. Code[a]	^{14}C yr BP	±	$F^{14}C$	±	A (Bq/kg)	±
UOC-6176	Bakelite_NewsG	Bakelite	D	9334	35	0.3129	0.0014	69.52	0.47

	^{14}C	^{14}C
Bakalite	69,52 Bq/kg	69,52 mBq

Bq/kg

	BN_Graphite_Like		BN Spray_1		BN Spray_2		BN powder		BN_Diamant_Like	Bakaleite	
226Ra	**2,22E+00**	±7,47E-02	**5,19E+00**	±8,65E-01	**1,34E+00**	±1,90E-01	**5,65E-02**	±4,23E-02	**<1,97E-01**	**2,78E+00**	±0,120300
228Th	**1,48E-01**	±1,95E-02	**1,20E+01**	±9,54E-01	**3,23E+00**	±1,45E-01	**7,79E-03**	±1,74E-02	**<1,10E-01**	**4,31E+00**	±0,114112
210Pb	**1,04E+00**	±1,42E-01	**1,73E+01**	±3,53E+00	**7,13E+00**	±6,74E-01	**6,72E-02**	±3,56E-02	**<6,23E-01**		
238U	**9,20E-01**	±1,19E-01	**2,04E+01**	±3,46E+00	**3,17E-02**	±4,86E-03	**1,31E-01**	±9,76E-02	**<4,20E-01**		
137Cs	**<0,02140**		**<9,77E-01**		**<2,92E-03**		**<6,89E-02**		**<1,39E-01**		
40K	**<0,433558**		**<6,01E+00**		**4,61E-01**	±7,34E-02	**<6,58E-01**		**<1,49E+00**	**1,36E+02**	±2,448022
228Ra	**<0,144085**		**1,49E+01**	±2,66E+00	**3,31E+00**	±3,62E-01	**3,31E+00**	±0,362473831	**<4,76E-01**	**4,99E+00**	±0,3117708

Glass tube					Bakalite
	Bq/kg		**Bq/m**	**Bq/tube**	**Bq/umbrella**
226Ra	4,06	± 0,223	1,70E-04	**1,54E-03**	**2,78 E-03**
228Th	1,46	± 0,081	6,11E-05	**5,55E-04**	**4,31 E-03**
210Pb	3,28	± 0,467	1,38E-04	**1,25E-03**	
238U	3,02	± 0,371	1,27E-04	**1,15E-03**	
40K	1,3	± 0,410	5,48E-05	**4,94E-04**	**1,36 E-01**
228Ra	1,36	± 0,225	5,70E-05	**5,17E-04**	**4,39 E-03**

Glass tube dimension :

High : 100 mm

$Radius_{ext}$: 2mm

Thickness : 0.5 mm

Weight : 0.38g

Bakalite conic umbrella :

Weight : ≈ 1g

Illustration of particle identification – Background rejection

Run with Ar/CH_4 + 3g ^3He @ 200 mb SPC 130cm Ø @ LSM

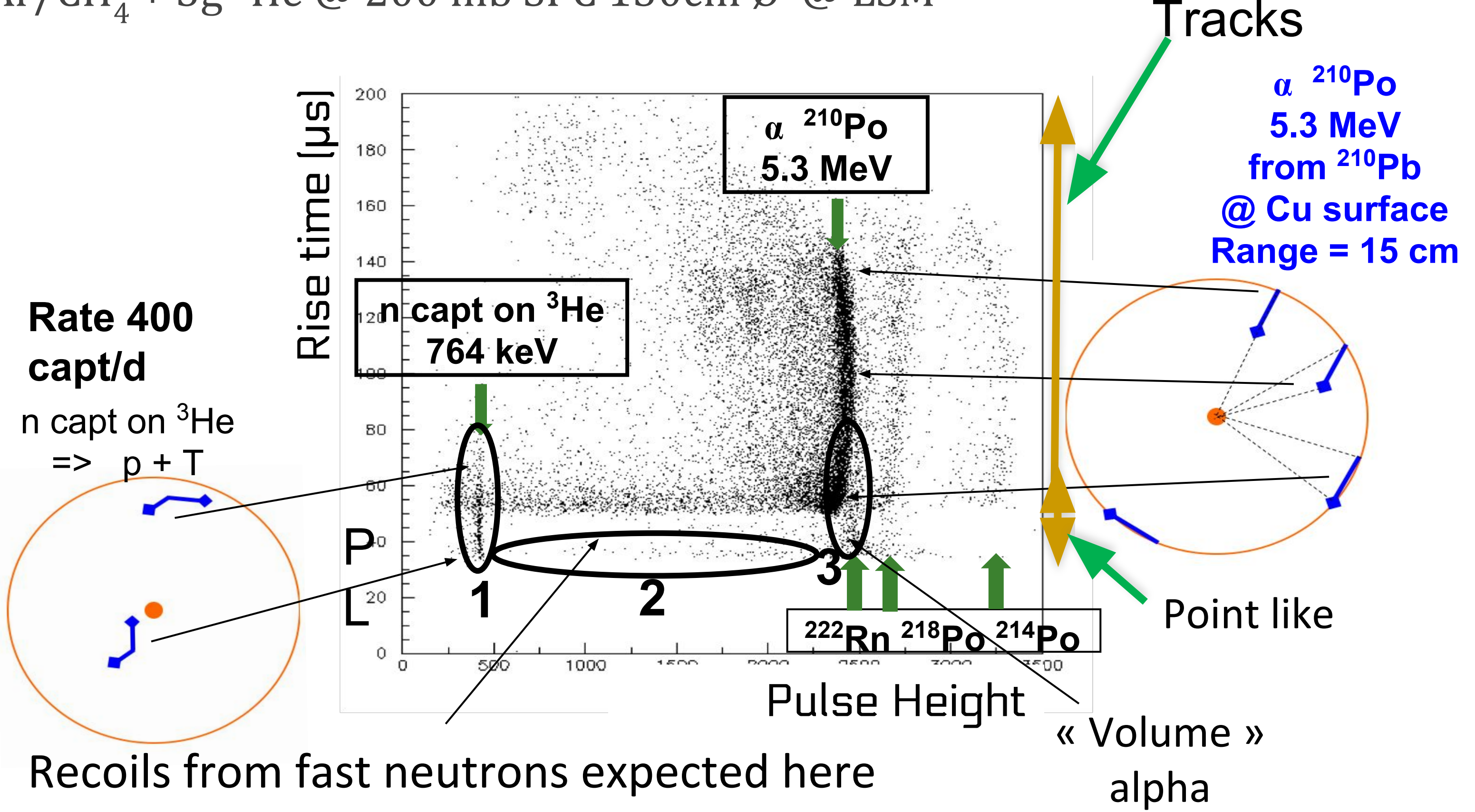

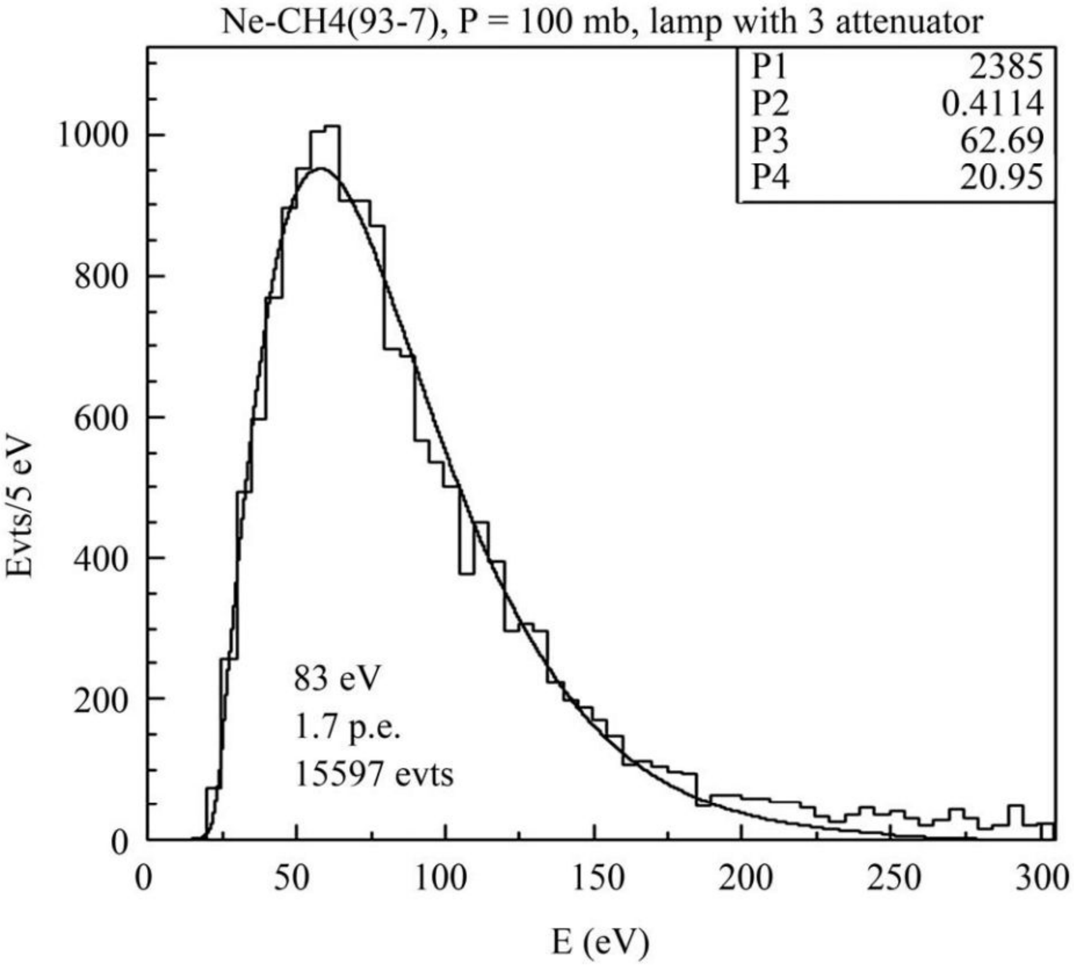

Ne-CH4(93-7), P = 100 mb, lamp with 3 attenuator
P1 2385
P2 0.4114
P3 62.69
P4 20.95
83 eV
1.7 p.e.
15597 evts
Evts/5 eV
E (eV)
0
200
400
600
800
1000
50
100
150
200
250
300

The umbrella

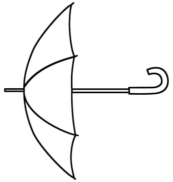

Material used: Copper, Brass, Steel, Iron, PE, PEEK, Teflon, Kapton, Plexiglass, Si, Araldite

Introduction of a secondary correction electrode

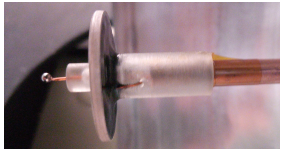

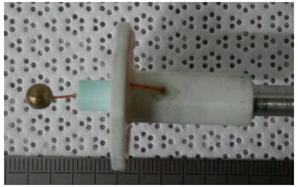

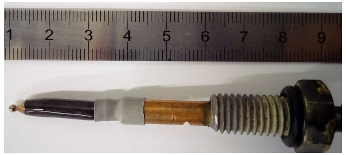

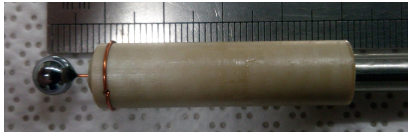

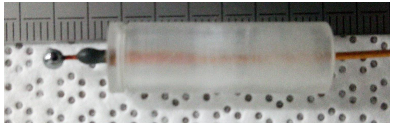

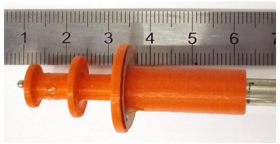

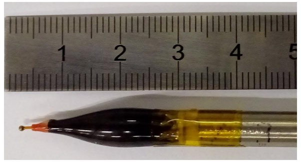

Goals:

- Homogeneous field
- limited discharges
- operation in high pressure
- stability

Coaxial cable umbrella

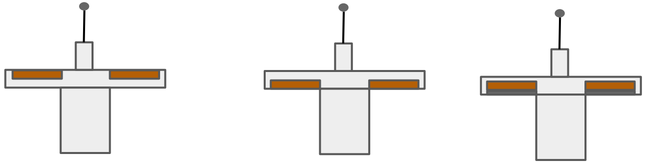

“Classical” umbrella

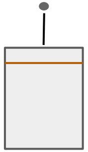

Kapton wire umbrella

The resistive umbrella

<u>*Bakelite*</u>
Chemical Formula:
$(C_6\text{-}H_6\text{-}O.C\text{-}H_2\text{-}O)x$

Thermosetting phenol formaldehyde resin, formed from a condensation reaction of phenol with formaldehyde.

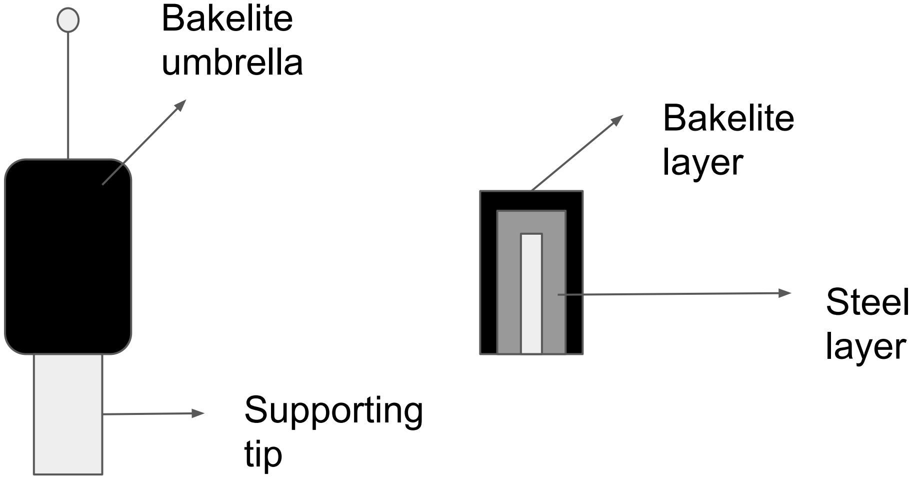

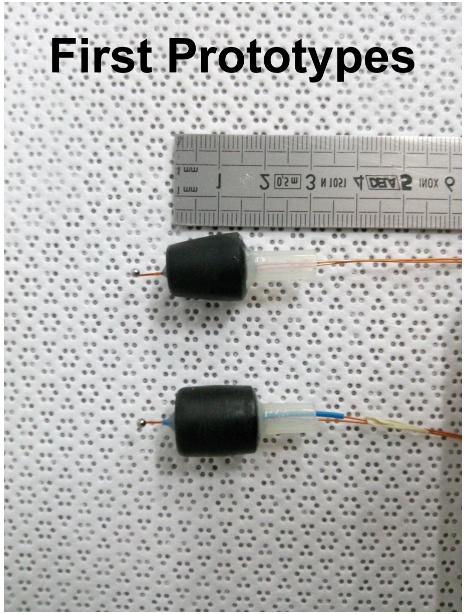

Advantages:

- Bakelite resistivity ~ $10^{12}\ \Omega\cdot\text{cm}$
- Compact and homogeneous material
- Very good conduct between the steel (conducting) layer and the bakelite layer
- Minimized insulating surface

“Glass” sensor prototype performance

Stability

Pulse Height (ADU)

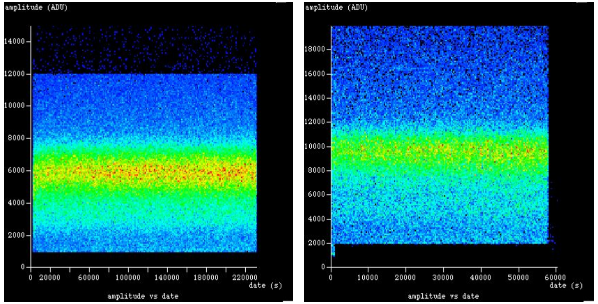

Time (s)

Ball: Φ2 mm steel
Gas: He+30%Ar+7%CH4
P = 715 mbar
HV1 = 1830 V
HV2 = 0 V

Ball: Φ2 mm steel
Gas:
He+10%Ar+2.5%CH4
P = 1880 mbar
HV1 = 2300 V
HV2 = 0 V

Resolution

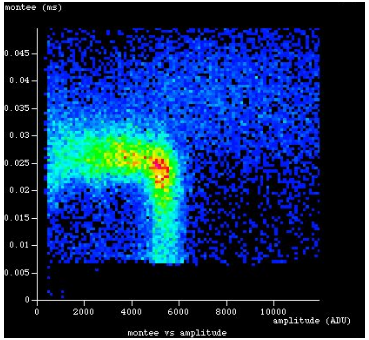

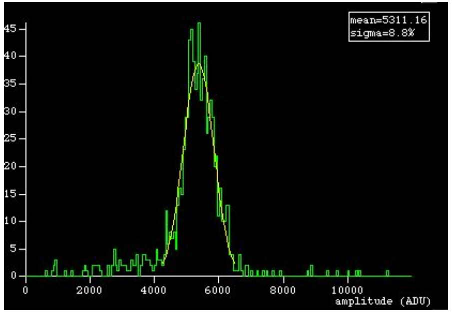

Ball: Φ3 mm steel
Gas: He+30%Ar+3%CH4
P = 1000 mbar
HV1 = 2300 V
HV2 = 0 V

Iron fluorescence (~6.4 keV)

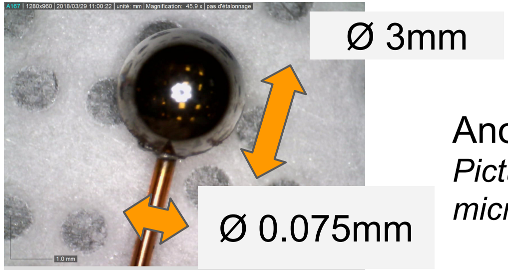

Anode micro-soldering
Picture from digital microscope (x 45.9)

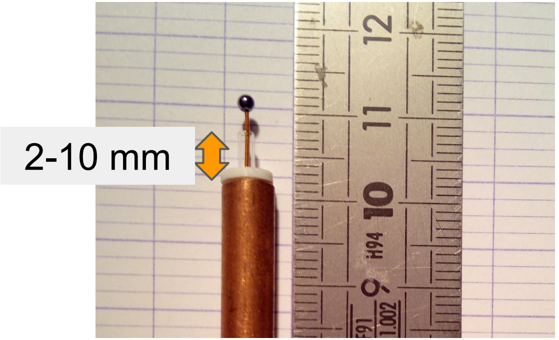

The μ-soldered ball

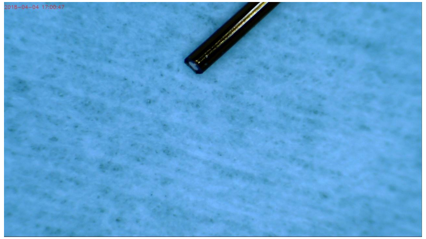

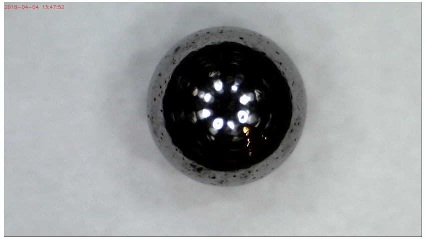

Motivation

- Better sphericity
- Avoidance of ball deformations
- Field homogeneity

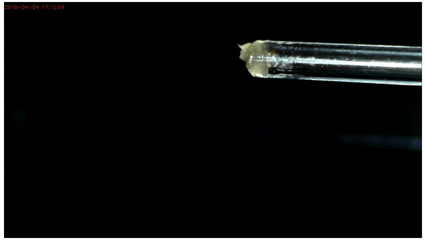

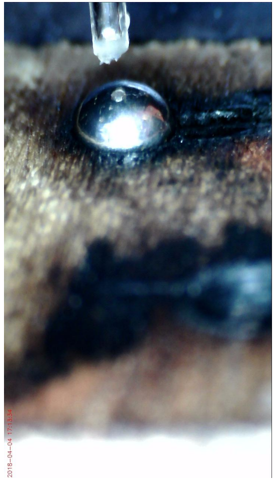

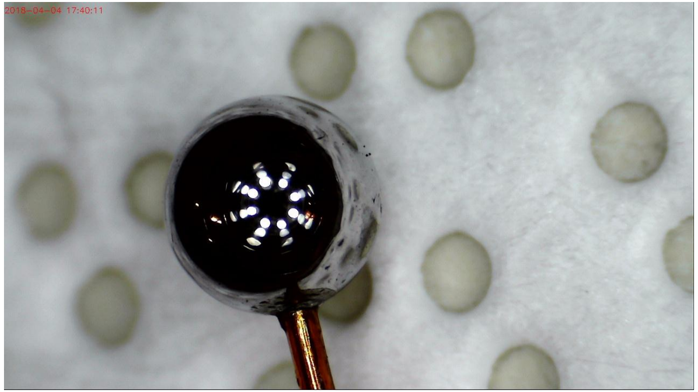

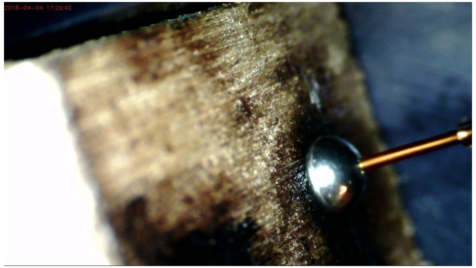

Control of ball quality

Checking diameter and surface smoothness

2 mm Inox ball

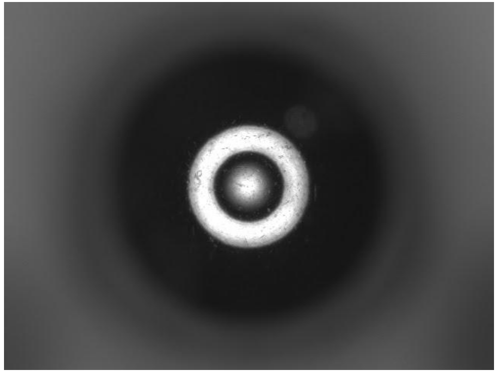

3 mm steel ball

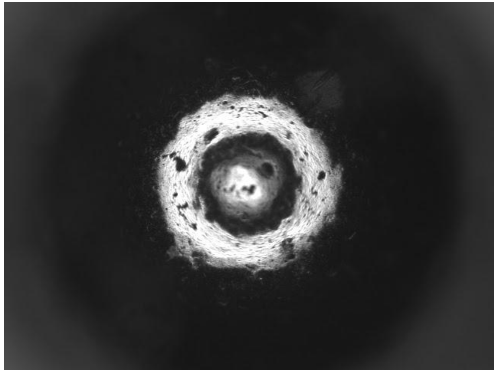

A closer look on a 3 mm ball

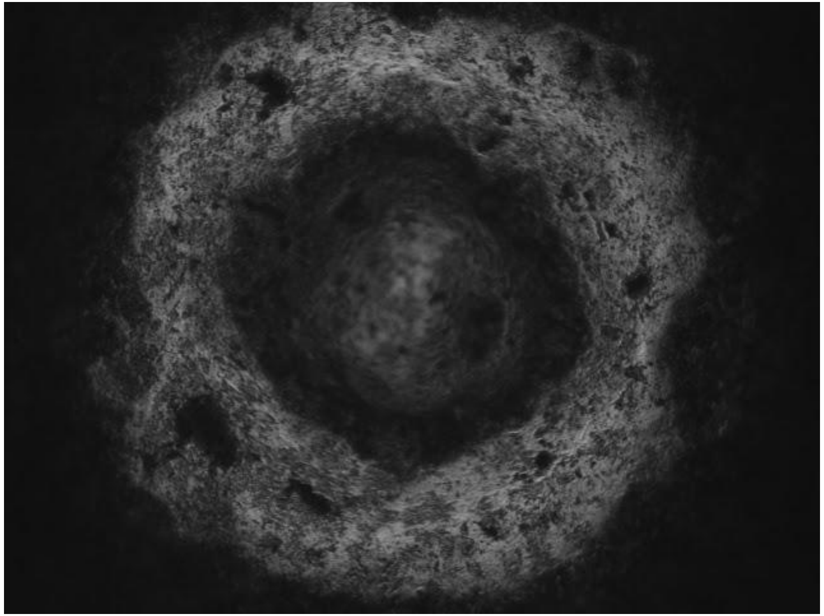

Metallized glass umbrella

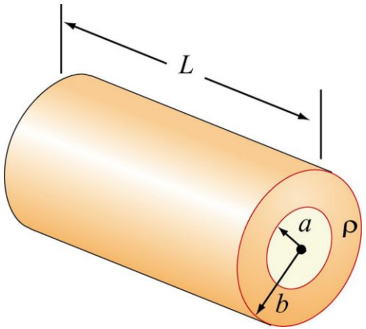

Hollow resistive cylinder

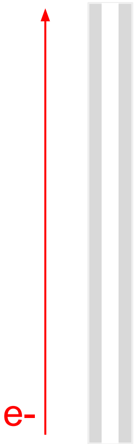

$$R = \frac{\rho L}{\pi(b^2 - a^2)}$$

Resistive cylinder with metallized inner surface

$$R = \frac{\rho}{2\pi L} ln(\frac{b}{a})$$

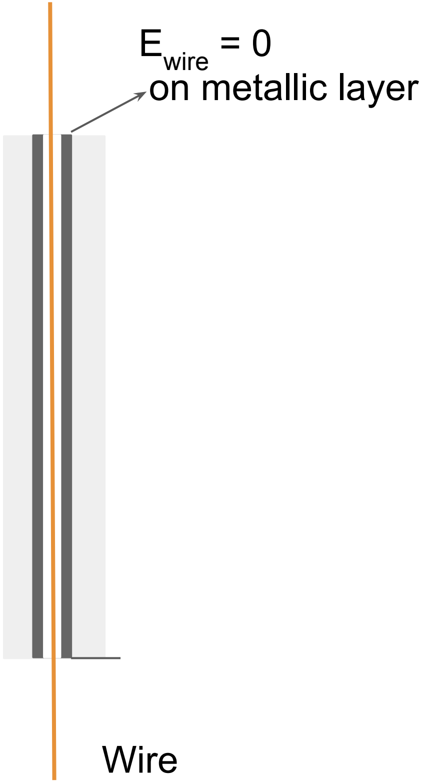

Properties of “Soda”-glass

Resistivity - Activity - Density

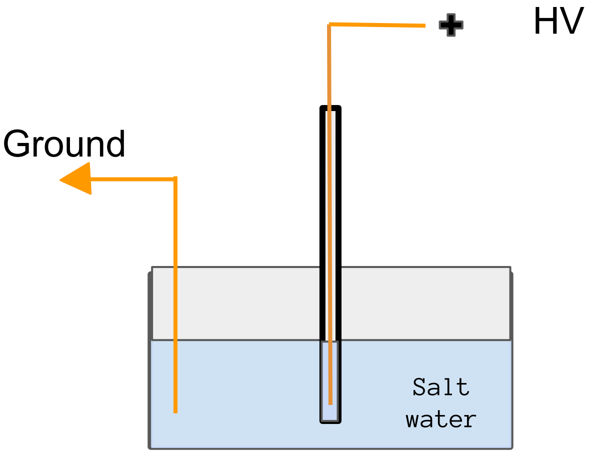

Schematic

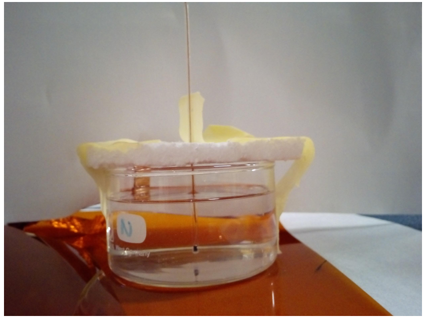

Real structure

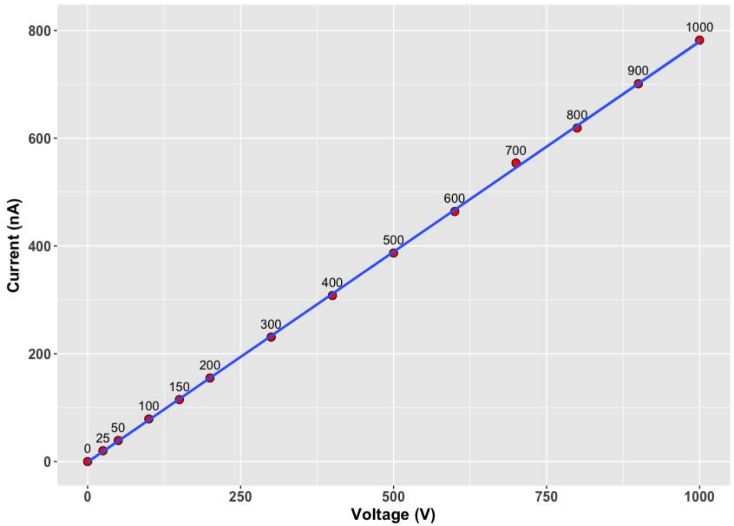

Activity: 14.48 mBq/g

Density: 2.1-2.25 g/cm^3

<u>Measurement result</u>

$\varrho = 5.05\times10^{10}\ \Omega\cdot\mathrm{cm} \pm 26.6\%$

Second generation of prototypes under investigation

The new 11-ball ACHINOS modules based on 3D-printed supporting structures, coated with graphite-glue layer (resistivities in the 10^6 Ω·cm-10^{12} Ω·cm) and glass tubes to extend the bias electrodes

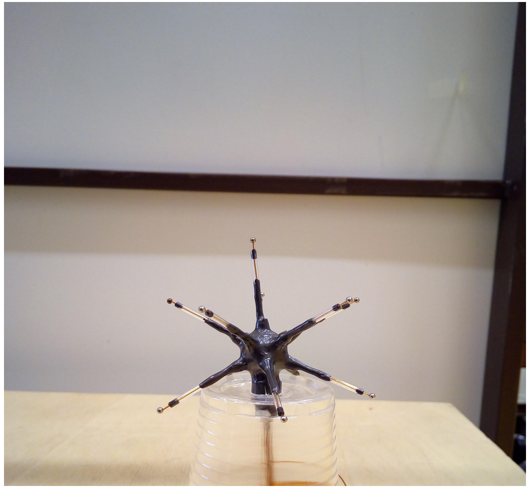

A new idea

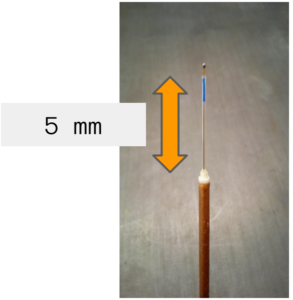

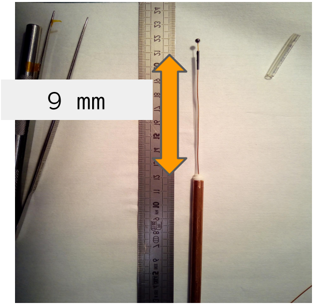

Improvement of the electric field in the far region of the detector

Degrader

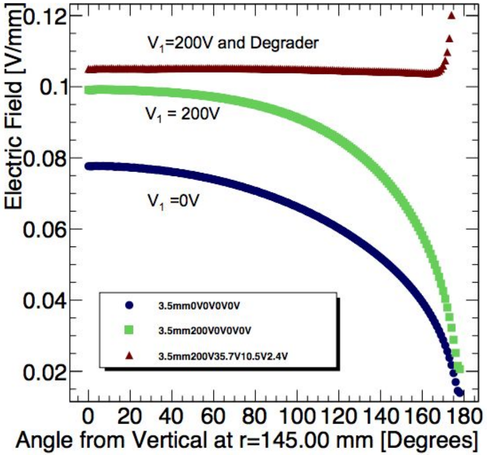

Mini-Degrader

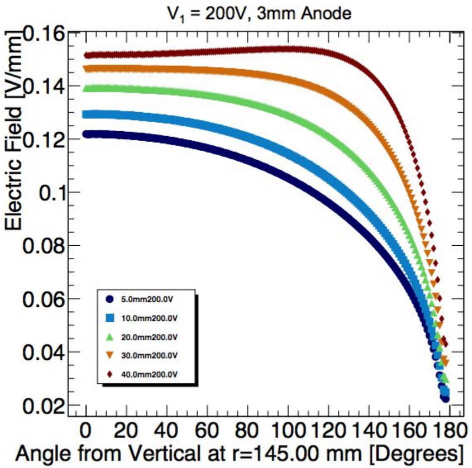

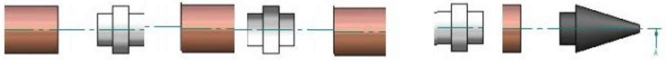

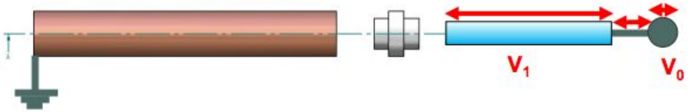

Figures from P.Knights recent presentation at IOP

A sensor upgrade

Sensor development - ACHINOS

If instead of one ball we use a number of them placed at equal distance on a sphere you can have the same gain but increased field at the outer region of the detector

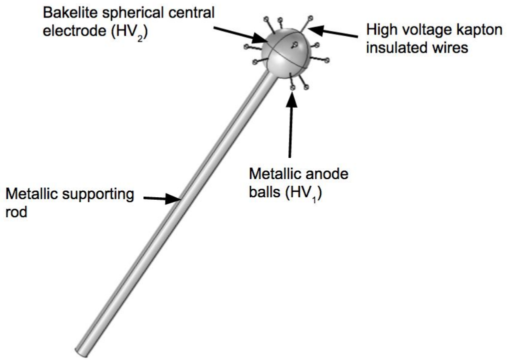

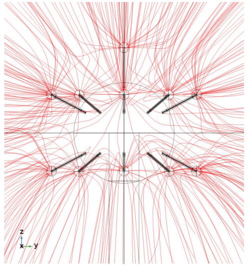

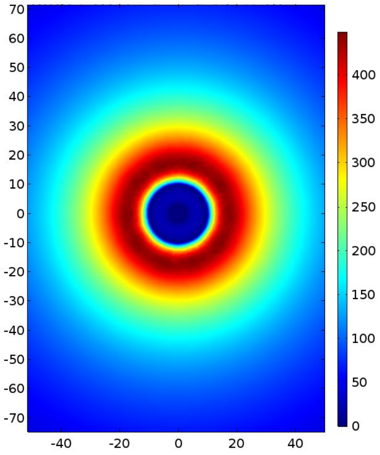

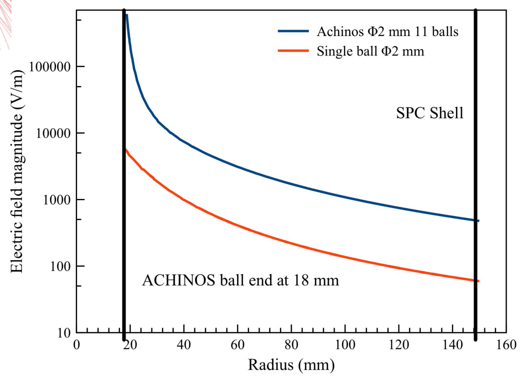

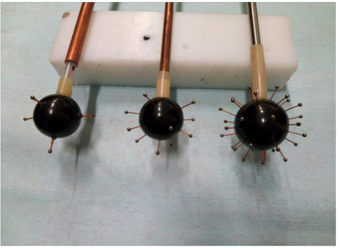

AIM:

1. Operation in high pressure
2. Build larger volume detectors

Conundrum:
Both Gain and Drift time are a function of E/P

$$\ln M = \int_{E(r1)}^{E(r2)} a(E/P)\frac{dr}{dE}dE$$

$$v_{drift} = \mu \frac{E}{P}$$

The elegant solution – ACHINOS

- Decoupling Gain -Drift
- Tunes Volume electric field
- Anodes can be read out individually

Possible improvements

- Construction method
- Testing of different geometries
  - Simulations
  - Prototypes
- Looking for the optimal number of anodes
  - Performance
  - Complexity
  - Noise
- Material for the bias electrode
  - Resistive coating
  - Bakelite
  - Thin layer of deposited carbon (<50 nm)

Glass bias electrodes

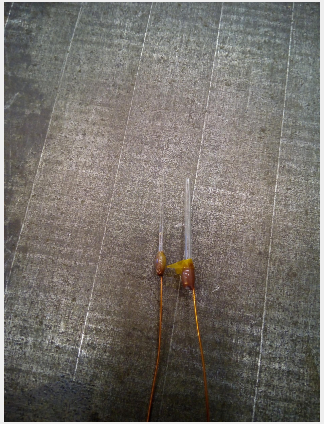

3D printed designs

Increased number of anodes

Resistive coatings

WIMP Recoil Spectrum

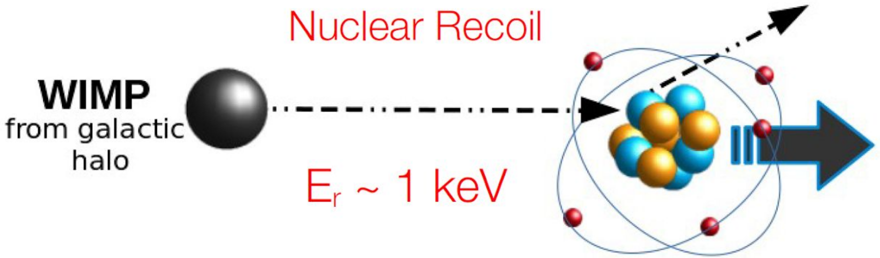

Neon, 1 kg.year, 1pb, 1 GeV WIMP

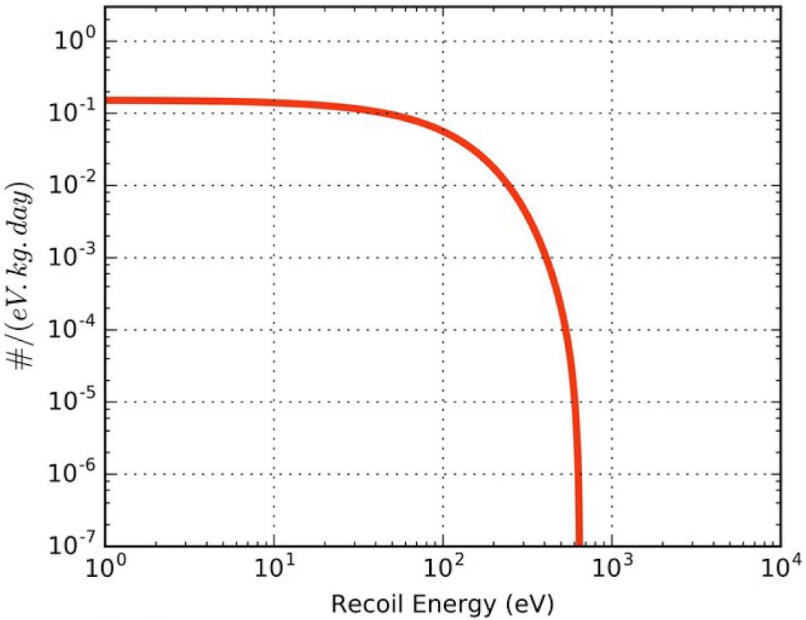

$$\frac{dR}{dE_r} = M_T \frac{\rho_0 \sigma_0}{2 m_\chi m_r^2} F^2(E_r) \int_{v_{min}} \frac{f(\vec{v})}{v} d^3 v$$

Schnee, R. W. (2009). Introduction to Dark Matter Experiments. In Theoretical Advanced Study Institute in Elementary Particle Physics. Boulder, Colorado, USA.

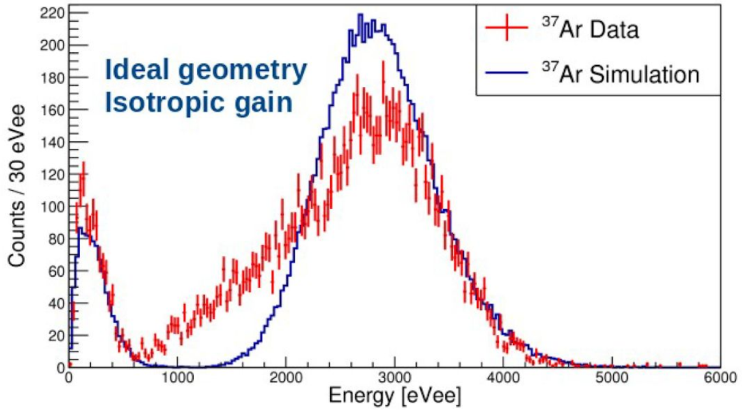

Ideal geometry
Isotropic gain
^{37}Ar Data
^{37}Ar Simulation
Counts / 30 eVee
Energy [eVee]

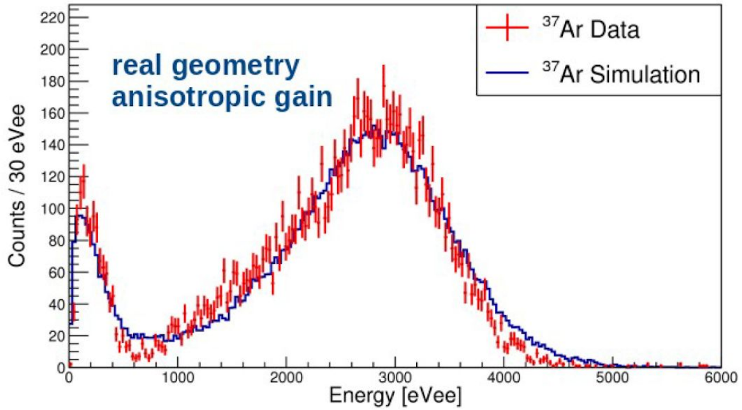

real geometry
anisotropic gain
^{37}Ar Data
^{37}Ar Simulation
Counts / 30 eVee
Energy [eVee]

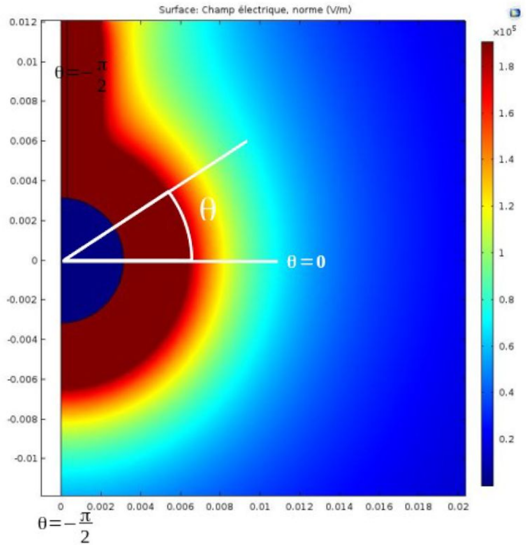

Surface: Champ électrique, norme (V/m)
θ
θ = 0

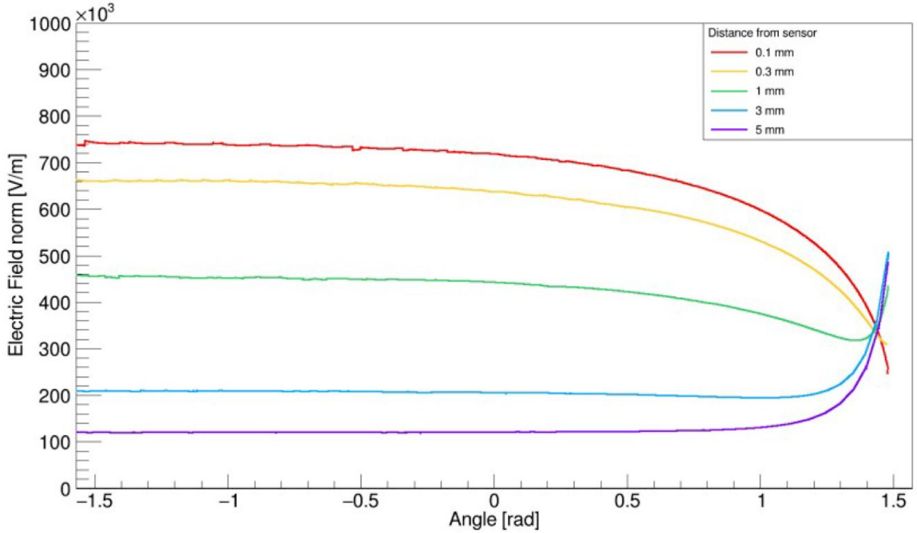

Distance from sensor
0.1 mm
0.3 mm
1 mm
3 mm
5 mm
Electric Field norm [V/m]
Angle [rad]

Avalanche process

<Gain> ~ 7000 secondary ions / primary electron

large statistical fluctuations

W_{Ne}=36eV

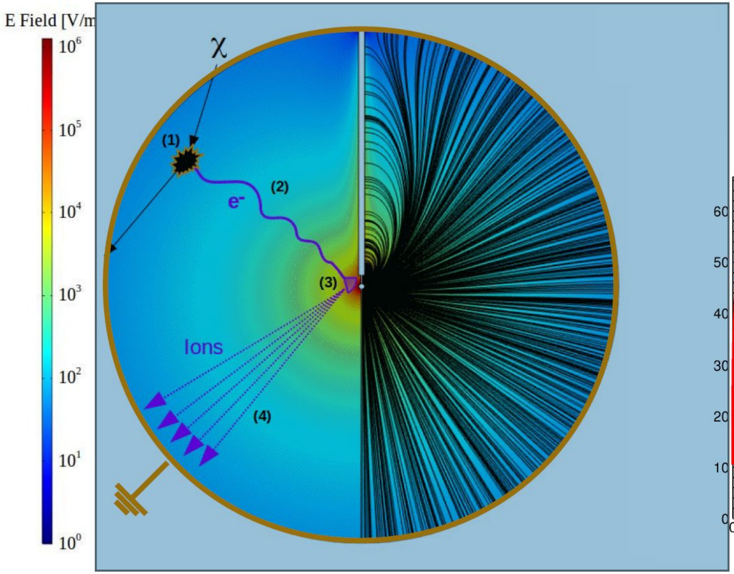

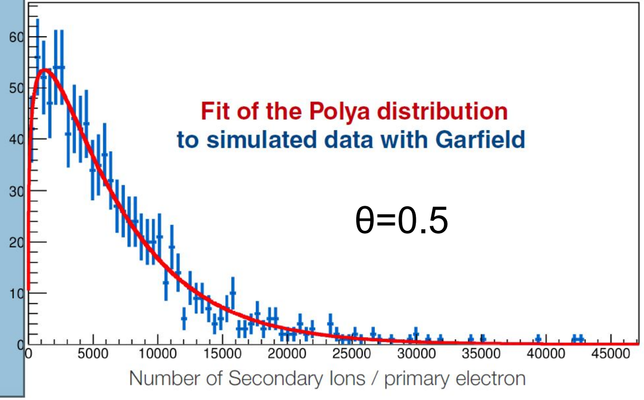

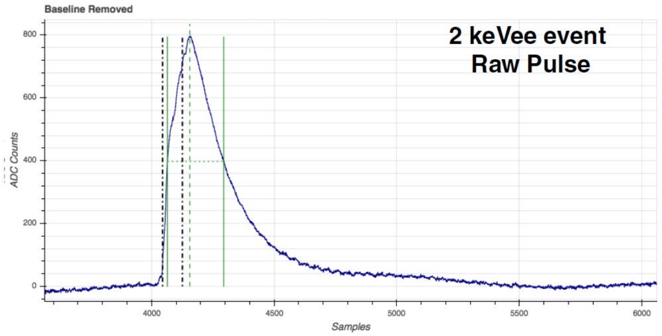

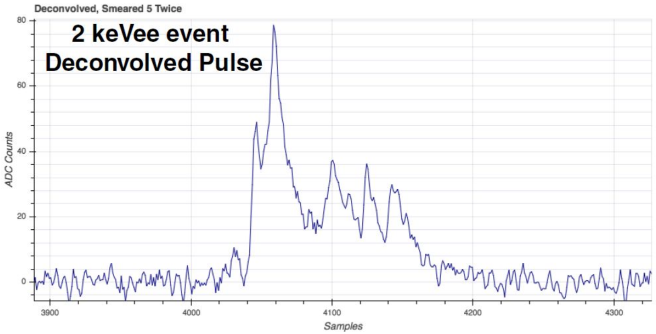

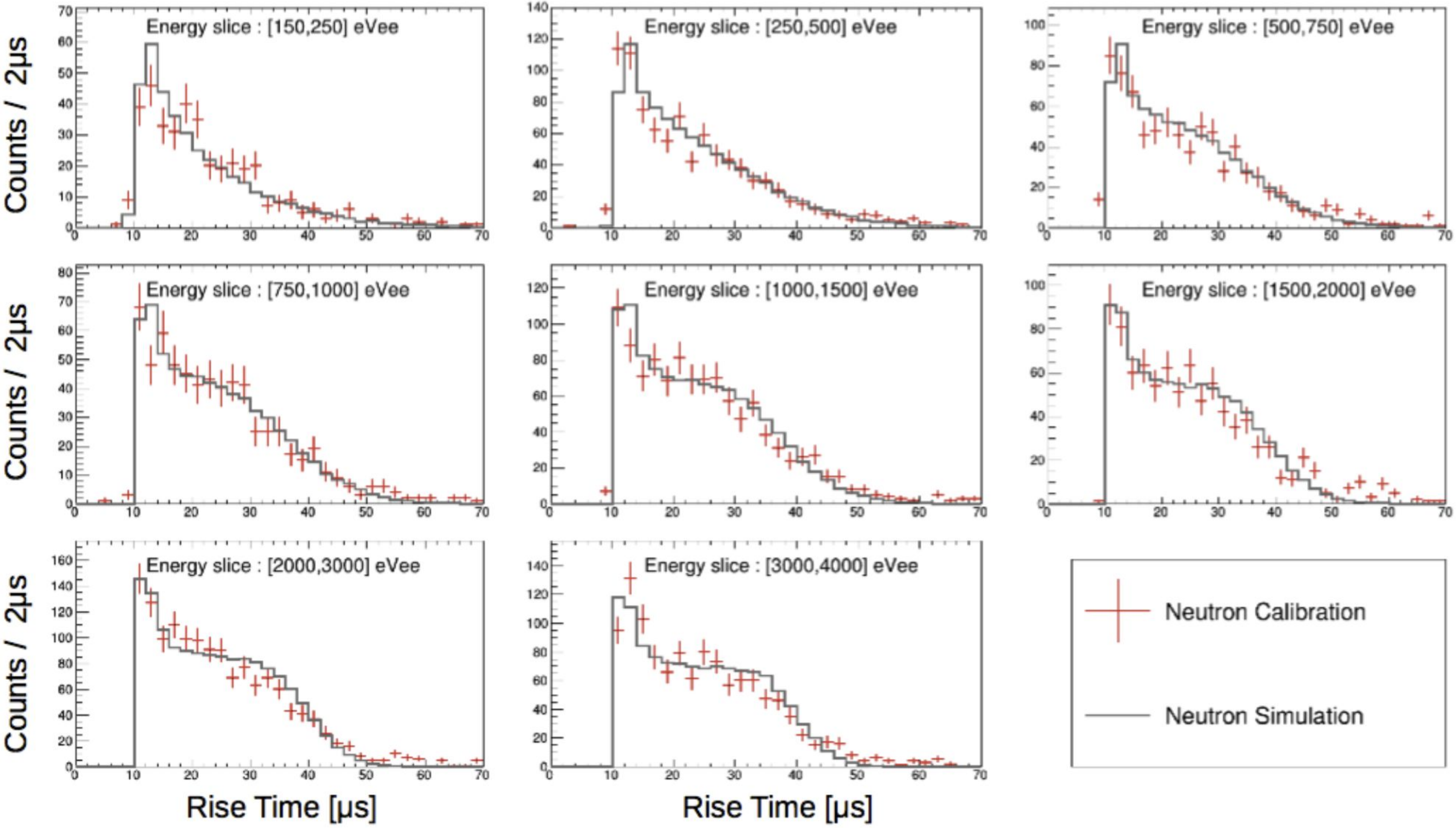

Energy slice : [150,250] eVee
Energy slice : [250,500] eVee
Energy slice : [500,750] eVee
Energy slice : [750,1000] eVee
Energy slice : [1000,1500] eVee
Energy slice : [1500,2000] eVee
Energy slice : [2000,3000] eVee
Energy slice : [3000,4000] eVee
Counts / 2μs
Rise Time [μs]
Neutron Calibration
Neutron Simulation

Simulation

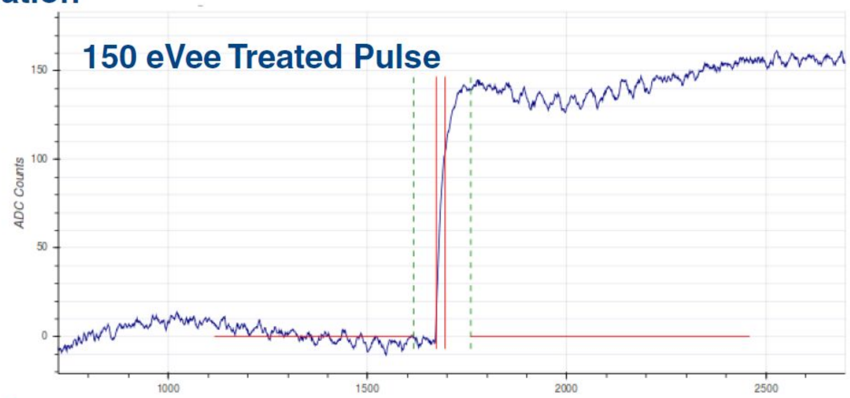

Data

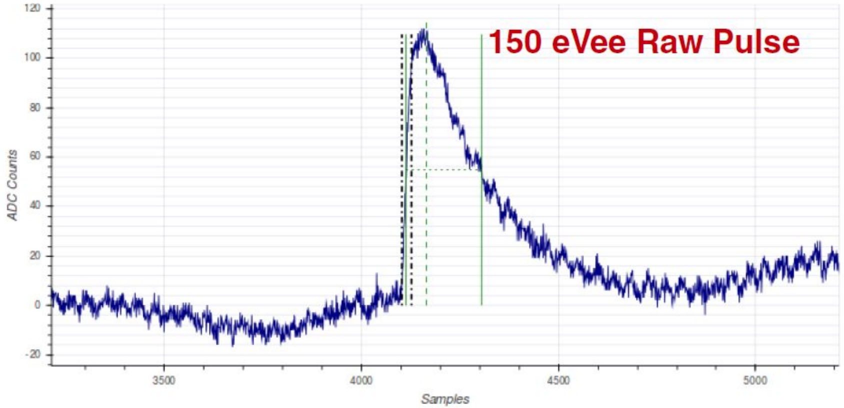

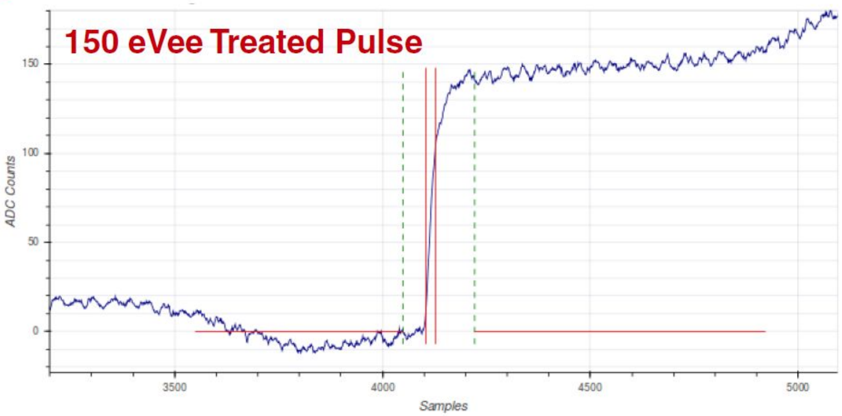

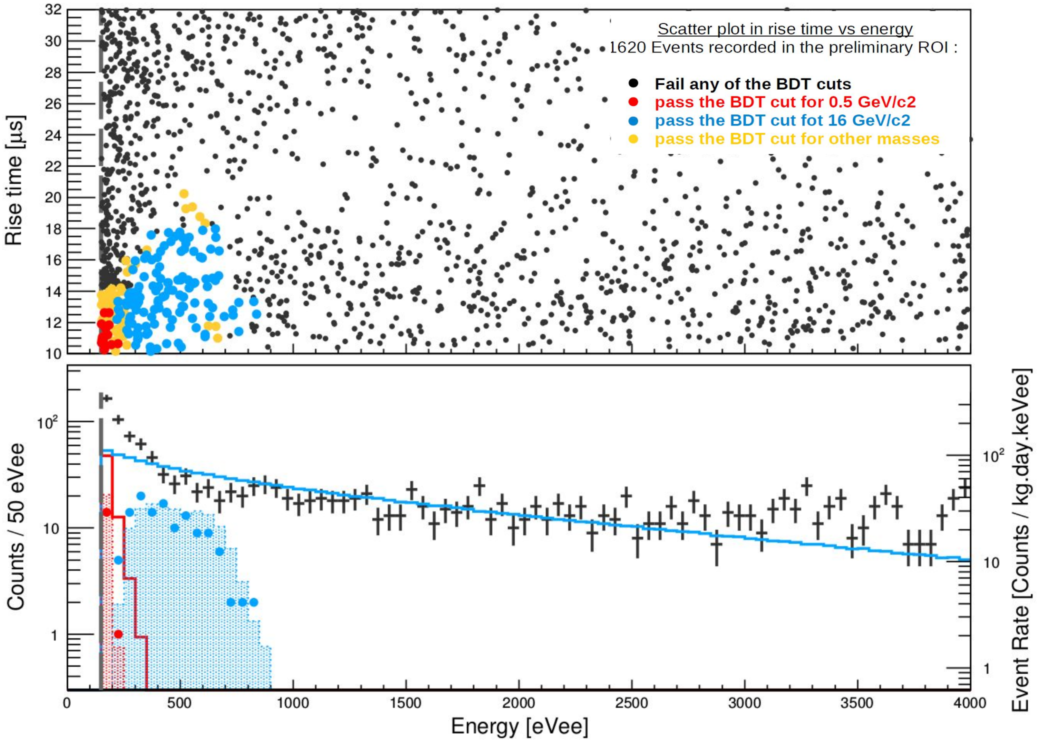

Top panel: distribution of the 1620 events recorded during the physics run in the preliminary ROI. Events that fail (resp. pass) the BDT cut for any of the WIMP masses are shown in black (resp. colour) dots. Events accepted as candidates for 0.5 GeV/c2 and 16 GeV/c2 WIMP masses are shown in red and blue, respectively, while for intermediate WIMP masses, candidates are shown in yellow.

Bottom panel: the energy spectrum of events recorded during the physics run in the preliminary ROI is indicated by the black markers. Energy spectra of 0.5 GeV/c2 and 16 GeV/c2 WIMP candidates are shown in red and blue dots. The energy spectra before and after the BDT cut of simulated 0.5 GeV/c2(resp. 16 GeV/c2) WIMPs of cross section $\sigma_{excl}=4.4\times10^{-37}cm^2$ (resp. $\sigma_{excl}=4.4\times10^{-39}cm^2$) excluded at 90% (C.L.) are shown in unshaded and shaded red (resp. blue) histograms, respectively.

Proportion of simulated WIMPs that pass a successive set of cuts vs the WIMP mass

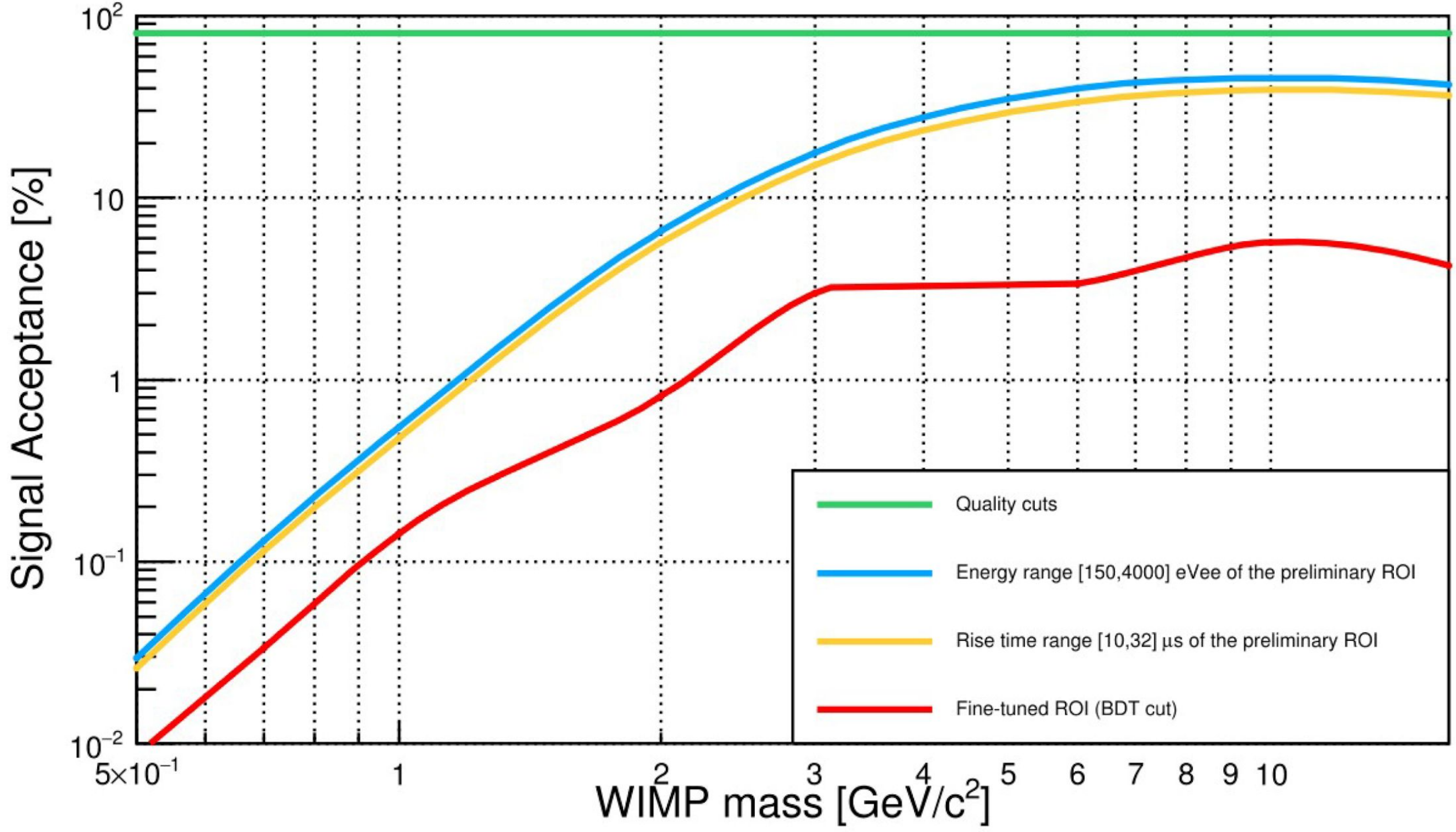

Analysis threshold set @ 150 eVee far above the trigger threshold of ~35 eVee (100% trigger efficiency @ 150 eVee)

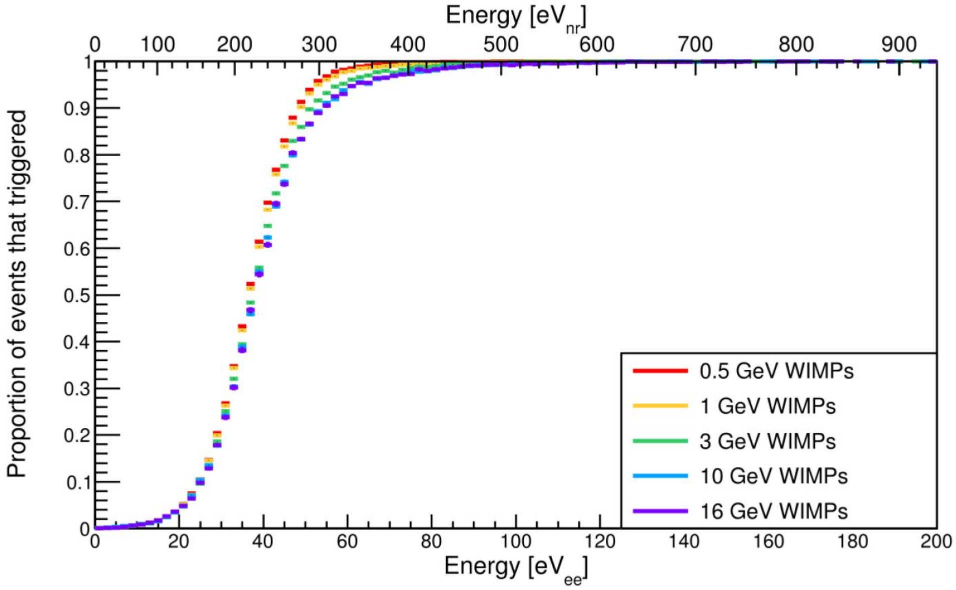

Proportion of events that trigger when pulses are added on top of a baseline vs the energy of the pulse alone

Trigger efficiency derived from simulated WIMP events of various masses to point out its dependence with the WIMP mass.

The trigger algorithm performs slighlty better for single PE events

For 0.5 GeV WIMPs : mostly single PE events VS For higher WIMP masses : single & multiple PE events

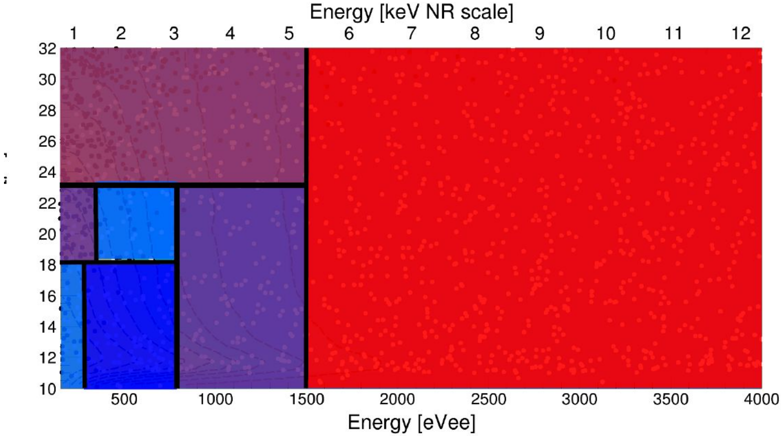

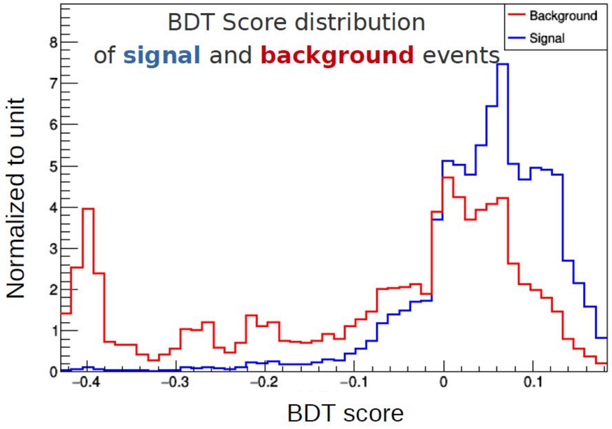

Background like
low BDT Score

Signal like
high BDT Score

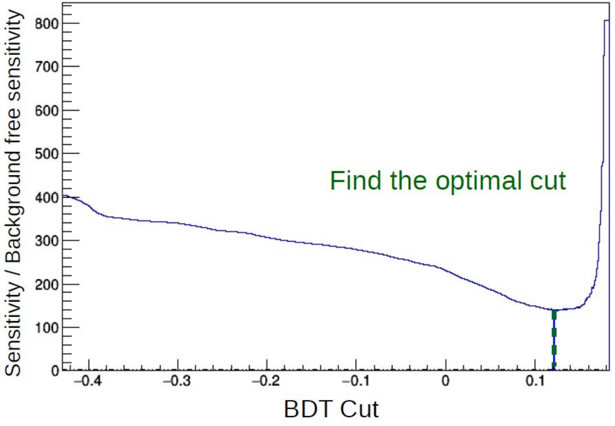

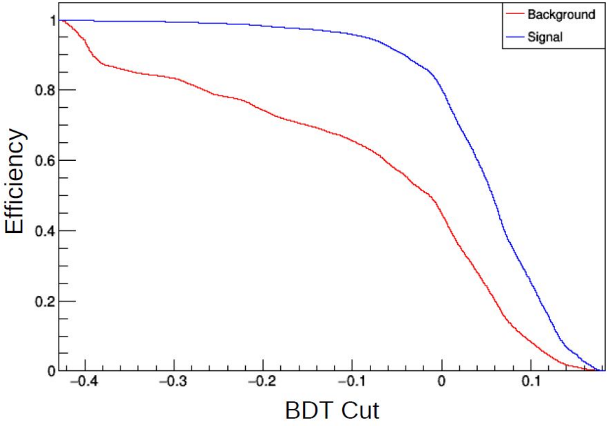

The weak electric field

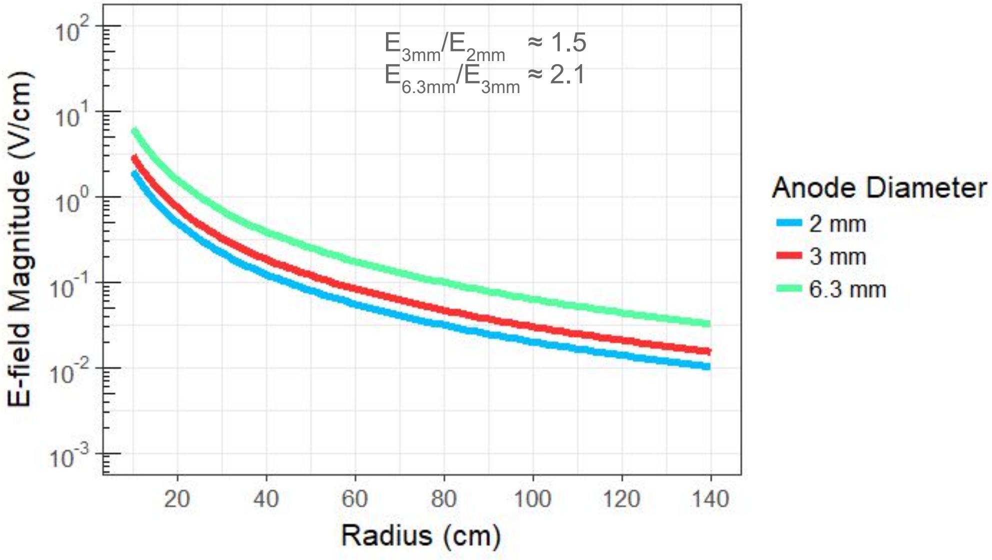

Comparison of E-field magnitude for different anode diameters (HV=2000 V)

AIM:

1. Operation in high pressure
2. Build larger volume detectors

Conundrum:
Both Gain and Drift time are a function of E/P

$$lnM = \int_{E(r1)}^{E(r2)} a(E/P)\frac{dr}{dE}dE$$

$$v_{drift} = \mu\frac{E}{P}$$

Quenching factor measurements at TUNL

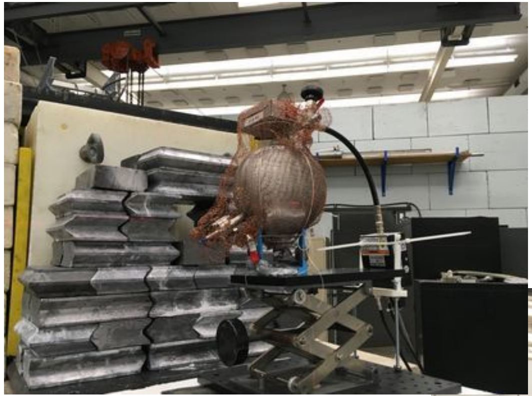

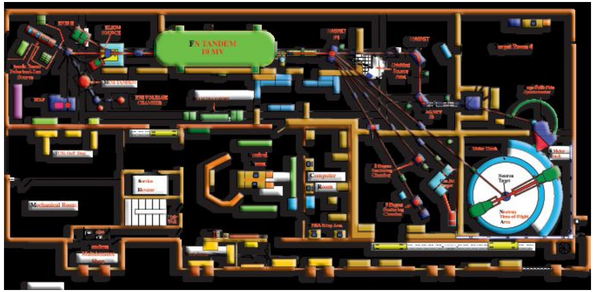

Why a spherical detector ?

Answer:

- **It is a geometry that permits the construction of robust, large volume detectors that can sustain high pressure with minimal material.**
- **The simplicity of the design permit a construction solely by radiopure materials**
- **The configuration of the electric field provide a handle for background rejection, through event discrimination and volume fiducialization**
- **The low capacitance even for large volumes provides single electron detection threshold**

An illustration of the method

The Geant4 simulation

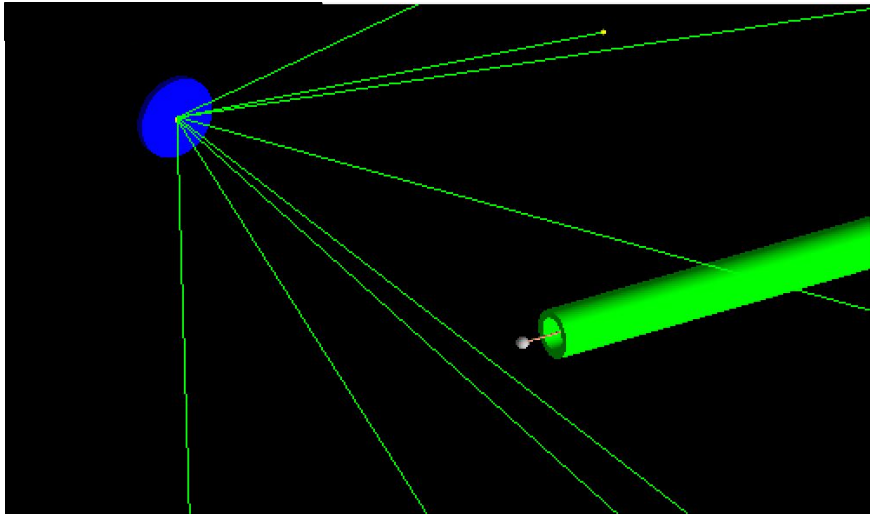

The setup

- SPC Φ 30cm
- Anode Φ 3 mm
- Gas Mixture He+10%CH_4 at 1 bar
- Copper rod include along with the wire
- **Fe55 X-ray source inside the detector (shielded)**

Low energy electromagnetic interactions enabled along with fluorescence models

Metallized glass umbrella

He + 29.7% Ar + 2.% CH4 700 mbar
HV1=1650 V, HV2= 0 V

First results - Stability in high gain - Grounded umbrella

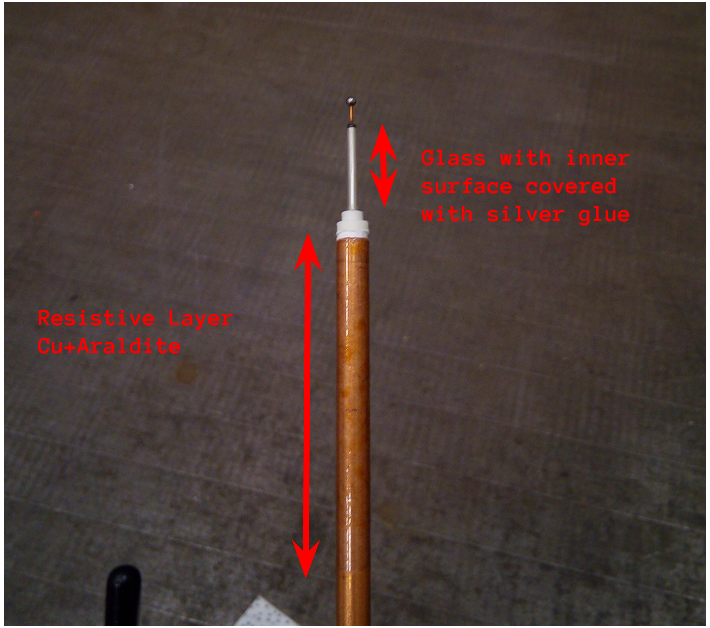

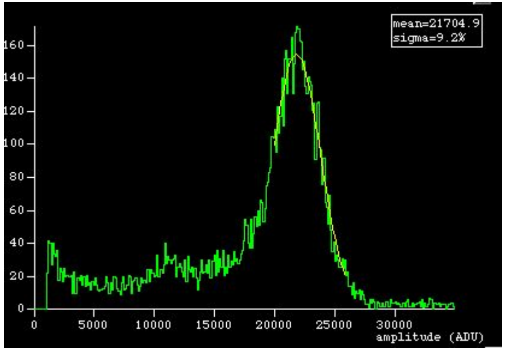

An illustration of the method

Assumed an τ=100 μs for our preamp with g=0.45mV/fC and 50 ADU/mV 2800 V applied on Φ 3mm anode

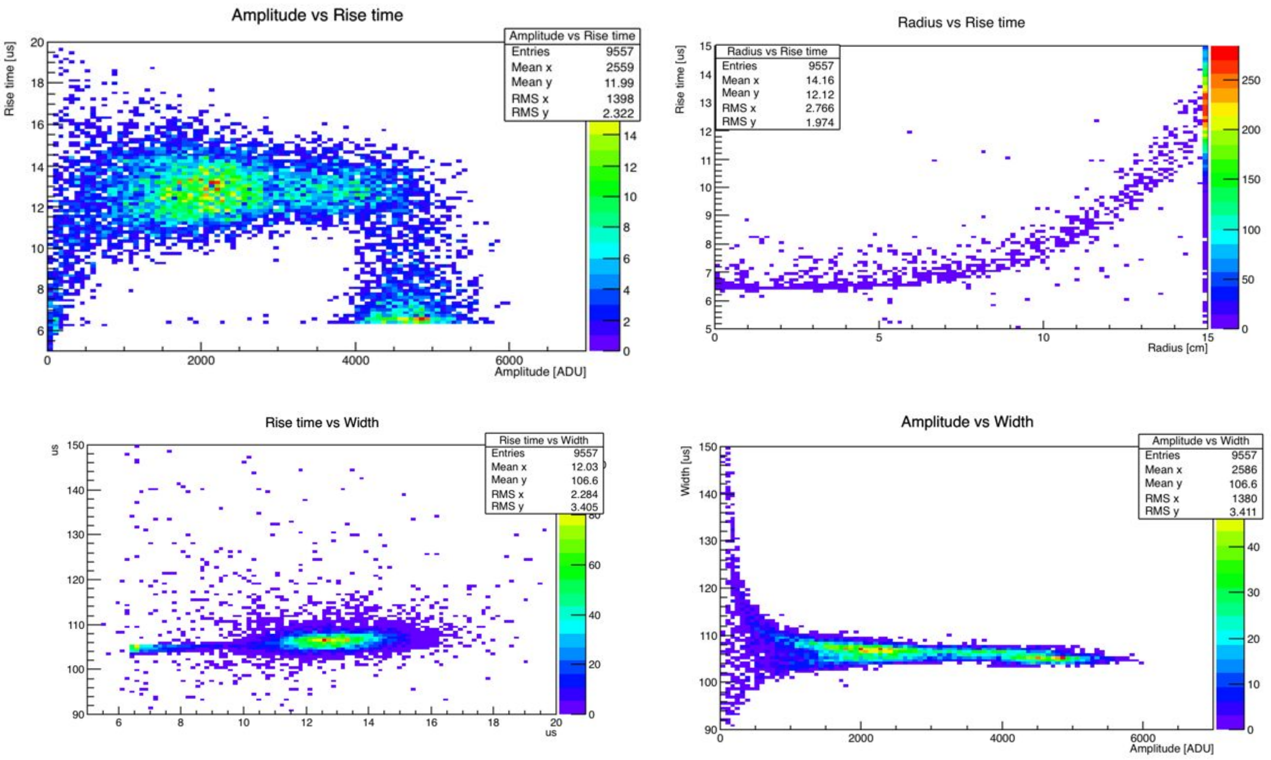

From the initial interaction to the detector response

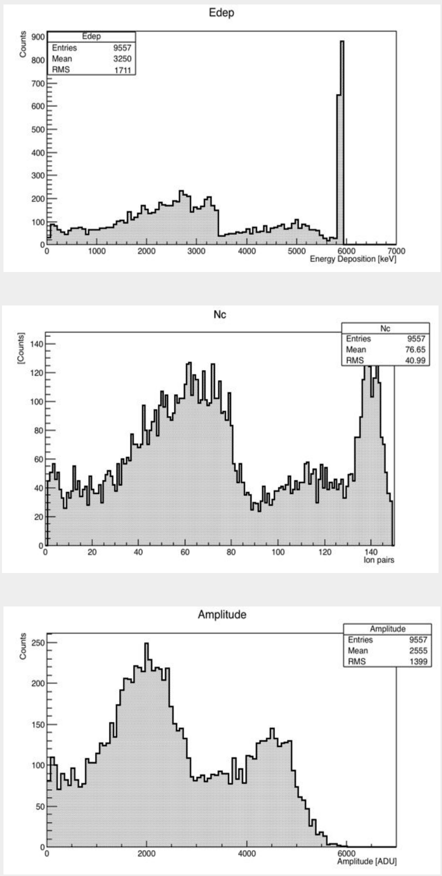

Background rejection capabilities-A

Fiducialization

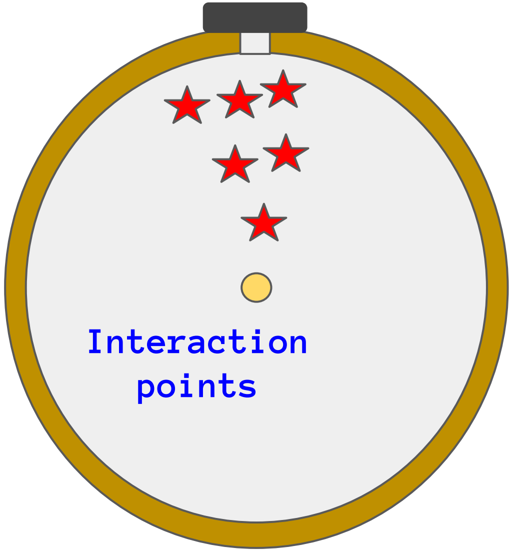

Primary e- drift time dispersion

$$\sigma(r) \propto (r/r_{sphere})^3$$

5.9 keV X-rays line

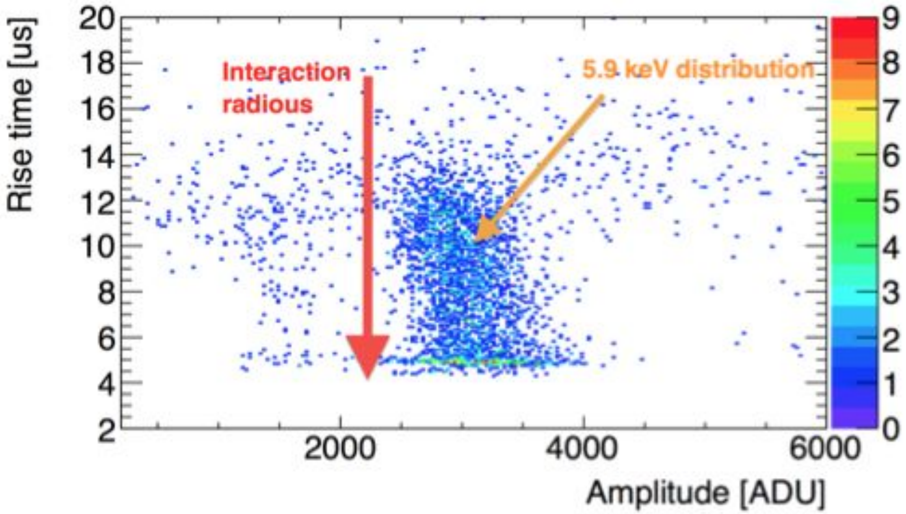

Rise time → Δt between 90% - 10% of pulse height